Parametric Study for Minimization of Spring back of Carbon Fiber Reinforced Polymer (CFRP) Reflector

By

LAV KAUSHIK

(14MMED04)

NIRMA UNIVERSITY
INSTITUTE OF TECHNOLOGY
NAAC ACCREDITED 'A' GRADE

DEPARTMENT OF MECHANICAL ENGINEERING
INSTITUTE OF TECHNOLOGY
NIRMA UNIVERSITY
AHMEDABAD-382481

May 2016

Parametric Study for Minimization of Spring back of Carbon Fiber Reinforced Polymer (CFRP) Reflector

Major Project Report

Submitted in partial fulfillment of the requirements

For the Degree of

Master of Technology in Mechanical Engineering

(Design Engineering)

By

LAV KAUSHIK

(14MMED04)

Guided By

Prof. S.J. Joshi

Prof. D.B. Shah

DEPARTMENT OF MECHANICAL ENGINEERING
INSTITUTE OF TECHNOLOGY
NIRMA UNIVERSITY
AHMEDABAD-382481

May 2016

Declaration

This is to certify that

- The thesis comprises of my original work towards the degree of Master of Technology in Mechanical Engineering (Design Engineering) at Nirma University and has not been submitted elsewhere for a degree.
- Due acknowledgment has been made in the text to all other material used.

LAV KAUSHIK

14MMED04

Undertaking for Originality of the Work

I, **Lav Kaushik**, Roll. No. **14MMED04**, gives undertaking that the Major Project entitled "**Parametric Study for Minimization of Spring back in Carbon Fiber Reinforced Polymer (CFRP) Reflector** " submitted by me, towards the partial fulfillment of the requirements for the degree of Master of Technology in Mechanical Engineering (Design Engineering) of Nirma University, Ahmedabad, is the original work carried out by me and I give assurance that no attempt of plagiarism has been made. I understand that in the event of any similarity found subsequently with any published work or any dissertation work elsewhere; it will result in severe disciplinary action.

Signature of Student

Endorsed by

(Signature of Guide)

Date:

Place: Ahmedabad

Certificate

This is to certify that the Major Project Report entitled "**Parametric Study for Minimization of Spring back in Carbon Fiber Reinforced Polymer (CFRP) Reflector** " submitted by **Mr. Lav Kaushik (14MMED04)**, towards the partial fulfillment of the requirements for the award of the Degree of Master of Technology in Mechanical Engineering (Design Engineering) of Institute of Technology, Nirma University, Ahmedabad is the record of work carried out by him under our supervision and guidance. In our opinion, the submitted work has reached a level required for been accepted for examination. The result embodied in this major project, to the best of our knowledge, has not been submitted to any other University or Institution for award of any degree.

Prof. S. J. Joshi
Guide and Associate Professor,
Department of Mechanical Engineering,
Institute of Technology,
Nirma University,
Ahmedabad.

Prof. D. B. Shah
Co-Guide and Assistant Professor,
Department of Mechanical Engineering,
Institute of Technology,
Nirma University,
Ahmedabad.

Dr. R N Patel
Professor and Head,
Department of Mechanical Engineering,
Institute of Technology,
Nirma University,
Ahmedabad

Dr. P N Tekwani
Director,
Institute of Technology,
Nirma University,
Ahmedabad

Acknowledgements

I want to show my gratitude to those who have helped me throughout my project work and presentations. First of all, I would like to thank my internal project Guide and PG coordinator Prof. S. J. Joshi & Head of Department Dr. R. N. Patel, Director Dr. P N Tekwani for providing valuable guidance. I am grateful for patience and interest they have shown from me. Without his guidance, this project would see the light of the day.

Then I express my sincere gratitude towards the project co-guide 'Prof. Dhaval B. Shah' who always stretch my limitations and made me capable enough to work on the project.

The blessings of God and support of my parents encouraged me which led to a successful project work for which I am very much grateful to them.

I am also thankful to all my dear friends for their motivation and every possible help.

-Lav Kaushik

Abstract

The Carbon Fiber Reinforced Polymer (CFRP) is extensively used for space application due to their good specific properties over conventional metals and alloys. Autoclave processing is used for manufacturing of composite part for space and aerospace applications. During processing in autoclave the manufactured composite part contains dimensional inaccuracy such as spring back and warpage. The spring back and warpage can be affected by different processing parameters such as cure cycles, tool geometry, composite ply layup sequence, tool material, tool surface condition, thickness of laminate and type of prepreg .

The work presented aims to determine the effect of various parameters on spring back of the reflector. The parameters considered are tool material, cure cycles, thickness of laminate, layup sequence. Two methods are planned for this study a) Numerical and b) Experimental. COMPRO, a customized software for simulating the curing process of composite material along with Abaqus is used for numerical simulation. Initially curing process simulation of L-shaped laminate is conducted using compro software to validate the results with available literature for verifying the methodology used. The results of the study are in good agreement with the available literature results. Selection of the mould material, consolidation material and prepreg is perfomed for conducting experiments. Manufacturing of mould is carried out on VMC as per the CAD model of the mould. The experiment for manufacturing of reflector is conducted using hot air oven, the steel mould material is used during the experiments. The coordinates of the manufactured reflector and mould are measured at fourty different locations using Coordinate Measuring Machine (CMM). Spring back of the reflector is obtained by taking the difference of reflector coordinates and mould coordinates. Study of the curing process on the dimensional stability of L-shape CFRP components is carried out. In the study rectangular cross section aluminium mould is used, on two faces of the mould laser engraving is done. During the experiments, portion of mould surfaces was treated with release agent and other with release film. The effect of laser engraving and mould surface condition is observed after demoulding of the L-shape CFRP parts. All engraved holes on the face of mould have their impressions on the manufactured composite parts and composite parts have better surface finish with the use of a release agent. Simulation of the curing process of reflector is carried out using Abaqus and Compro by considering different parameters, i.e., type of curing cycle, layup sequence and thickness of the laminate. Simulation is conducted for eight different layups of prepreg. Layup having prepreg layers with four different orientation experiences least springback magnitude. In addition to this, as the layup thickness increases springback magnitude decreases.

Contents

List of Figures

List of Tables

Abbreviation

CFRP	Carbon Fibre Reinforced Polymer
VMC	Vertical Machining Center
CMM	Coordinate Measuring Machine
RTM	Resin Transfer Moulding
PTFE	Polytetrafluoroethylene
CTE	Coefficient of Thermal Expansion
SS	Stainless Steel
CI	Cast Iron
FEA	Finite Element Analysis
CCA	Compro Component Architecture

Chapter 1

Introduction

1.1 Composite Material

A composite material is made by combining two or more materials to give a unique combination of properties. In composites constituent materials are different at the molecular level and are mechanically separable. In this the constituent materials work together but remain in their original form. The ultimate property of the composite which we get is much better than its constituent material properties. Typically, composite material is formed by reinforcing fibers in a matrix resin. The reinforcements can be fibers, particulates, or whiskers, and the matrix materials can be metals, plastics, or ceramics. Polymers, ceramics, and metals. The fibers can be continuous, long, or short. Composites made with a polymer matrix have become more common and are widely used for various applications. Matrix material can be classified into thermoset and thermoplast polymers. And majorly used fibers are carbon fibers and glass fibers. The reinforcing fabric provides strength and stiffness to the composite, whereas the matrix gives rigidity and protection from the environment. Typically composite are formed by combining fiber and matrix materials as shown in Figure 1.1

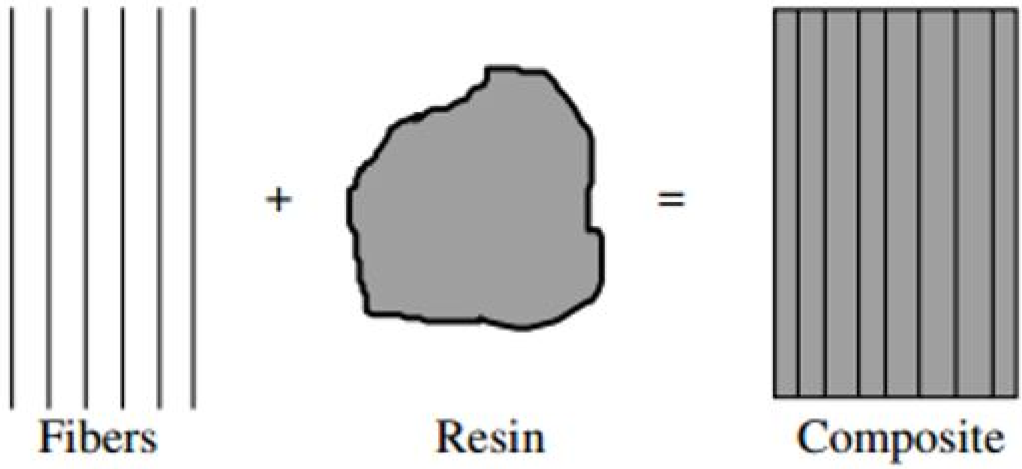

Figure 1.1: Formation of Composite Material Using Fibers and Resin. [1]

1.2 Functions of Matrix material and Fibers in the Composite Material

Fiber in the composite carry the load upto 70 to 90% of the load acting. Fibers provide stiffness, strength, thermal stability in the composite. Matrix material binds the fibers together and transfers the load to the fibers. It provides desired shape to the composite. It slows down the crack propagation in the fibers by transferring the load to adjacent fibers. The matrix also provide protection against corrosion and other chemical effects propagated due to environmental effects. Ductile matrix material increases the toughness of the composite.

1.3 Advantages of Composites Over Other Conventional Materials

Composite materials provide capabilities for part integration. Several metallic components can be replaced by a single composite component. These materials have high specific strength and stiffness which makes them lighter and more efficient structures in terms of fuel consumption, along with these fatigue strength and impact properties of composites are much better.

1.4 Drawbacks of Composites

The material cost of composite materials is very high compared to that of steel and aluminum. It is almost 5 to 20 times more than aluminum and steel on a weight basis. Large design databases are available for metals but designing parts with composites lacks such books because of the lack of a database which limits knowledge of composite technology. Dimesional stability can be affected due to moisture absorption in composites.

1.5 Application of Composites

Composites material are widely used in aerospace industries due to its high strength to weight ratio which leads to saving in fuel consumption. Airplanes, rockets and missiles all can fly at higher speed and can cover larger distance with the composite materials. Glass, carbon and kevlar fibers are commonly used fibers in this industry. Composite material can also be used in automotive industry to deliver high quality surface finish, styling-detail and processing options. Mostly glass fibers are used as main reinforcement along with matrix material. Apart from that composite materials are also popular in sporting goods industry, marine, consumer goods and for construction and civil structures.

1.6 Types of Fiber and Matrix Materials

The most common fibers used are glass, carbon/graphite, and kevlar. Glass is the most common fiber used in polymer matrix composites. Its advantages include its high strength, low cost, high chemical resistance, and good insulating properties. The drawbacks include low elastic modulus, poor adhesion to polymers, high specific gravity, sensitivity to abrasion (reduces tensile strength), and low fatigue strength. Graphite/Carbon fibers are very common in high-modulus and high-strength applications such as aircraft components, etc. The advantages of graphite fibers include high specific strength and modulus, low coefficient of thermal expansion, and high fatigue strength. The drawbacks include high cost, low impact resistance, and high electrical conductivity.The main difference between carbon and graphite fiber is that carbon fibers have 93 to 95% carbon content, but graphite has more than 99% carbon content. Some common types of glass fibers shown in Figure 1.2.

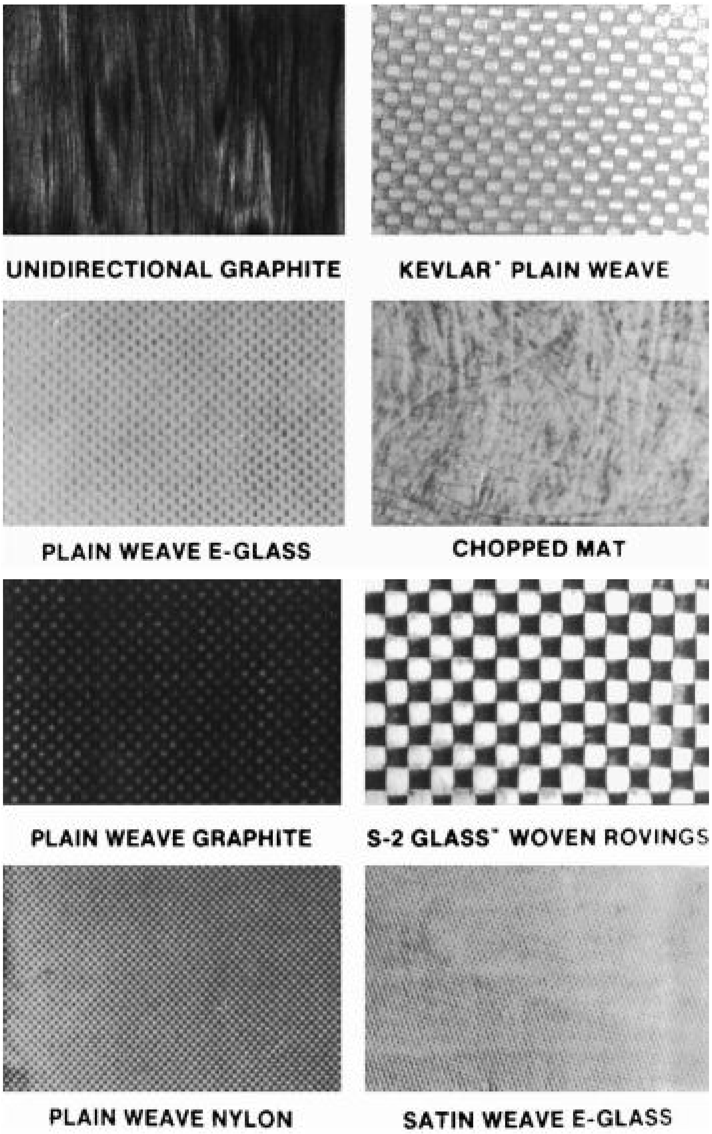

Figure 1.2: Fibers Available in Different Forms. [2]

Epoxy is a very commonly used resin system which is a thermoset polymer, Due to its versatility in nature epoxy have broad range of properties and processing capabilities. Low shrinkage is noticed in epoxies. Epoxies are the most widely used resin materials and are used in many applications, from aerospace to sporting goods. An epoxy resin is present in liquid form which also contains some epoxide such as diglycidyl ether of bisphenol A (DGEBA). During curing DGEBA molecules form crosslinks with each other as shown in Figure. These crosslinks of the polymer expands in a 3-dimension network as shown in Figure 1.3 and finally it converts into a solid epoxy resin.

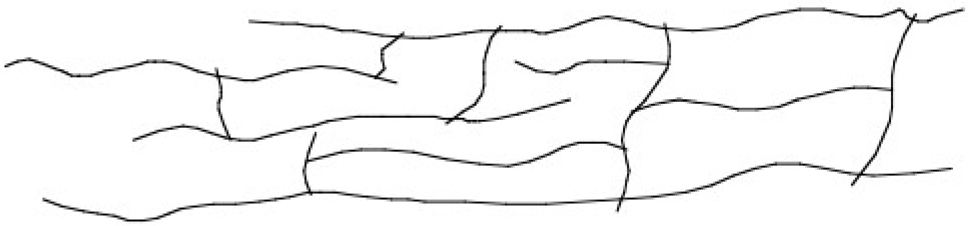

Figure 1.3: Cross-linking of Polymers [1]

Epoxy-based composites can be used for high temperature applications. Epoxies can operate well up to 400°F. For such high temperature requirements the cost of epoxy also gets increased, but at the same time they offer good chemical and corrosion resistance.

1.7 Prepreg

A prepreg is a pre-impregnated fibers with resin material. These prepregs should be stored in low temperature environment such as in low temperature refrigerator which can maintain the temperature at the range of -18^oC. Figure shows the various types of prepregs available as unidirectional tape, woven fabric tape, and roving as shown in Figure 1.4.

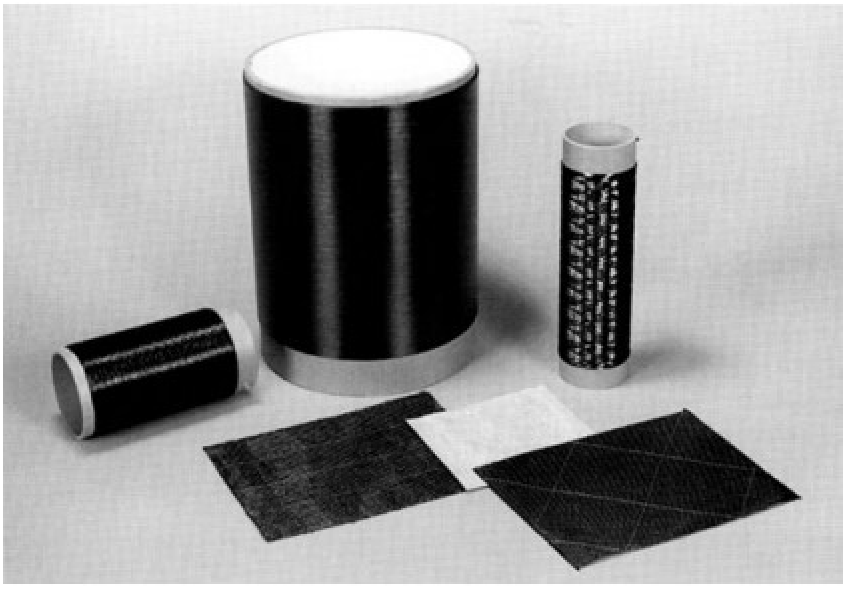

Figure 1.4: Prepreg types: unidirectional tape, woven fabric prepregs, and rovings. [1]

Using unidirectional tape one can tailor the properties of composite in desired direction. The place where maximum flexibility is required wowen fabics are used.

These prepreg can also be used along with honeycomb core to make sandwich structures. Using sandwich structures overall weight of the structure can be reduced. The prepreg thickness ranges from 0.127 to 0.254 mm. The use of prepreg enable us to eliminate the need for manual mixing of fibers and resin with perfect ratio. More controlled properties can be obtained by using prepregs.

1.8 Special Cases of Laminates

Based on angle, material, and thickness of plies, the symmetry or antisymmetry of a laminate may zero out some elements of the three stiffness matrices $[A]$, $[B]$, and $[D]$. Symmetric laminates result in no warpage in a flat panel due to temperature changes in processing.

1. Symmetric Laminate: A laminate is called as symmetric if the material, angle, and thickness of plies are the same above and below the mid plane. An Example Of Symmetric Laminate is [0/30/60/60/30/0]

2. Cross-Ply Laminates: A laminate is called a cross-ply laminate if only 0 and 90 °plies are stacked up make a laminate. An example of a cross ply laminate is a [0/90] laminate.

3. Angle Ply Laminates: A laminate is called an angle ply laminate if it has plies of the same material and thickness and only oriented at corresponding positive and negative directions and can be represented as $[+\theta, -\theta]$. An example of anangle ply laminate is $[-30/30/-30/30]$.

4. Anti-symmetric Laminates: A laminate is called anti-symmetric if the material and thickness of the plies are the same above and below the mid-plane, but the ply orientations at the same distance above and below the mid-plane are negative of each other. An example of an anti-symmetric laminate is $[60/45/-45/60]$.

5. Balanced Laminates: A laminate is balanced if their exist layers with plus and minus pairs of $+\theta$ and $-\theta$. An example of a balanced laminate can be $[20/50/-30/30/-50/-20]$.

6. Quasi-Isotropic Laminates: A laminate is called quasi-isotropic when stacking of the plies are such that the lamiante behaves same as that of isotropic material Some of the Examples of quasi isotropic laminates are $[0/\pm 60], [0/\pm 45/90]_s$, and$[0/36/72/-36/72]$.

1.9 Reflector (Antenna)

A reflector is a device that reflects electromagnetic waves. Antenna reflectors can exist as a standalone device for redirecting radio frequency (RF) energy, or can be integrated as part of an antenna assembly.

1.9.1 Parabolic Reflector

The three-dimensional shape of the reflector is called a paraboloid. These types of antenna reflectors are used in space for satellite communication. The material used to manufacture is CFRP. A typical antenna is shown in Fig. 1.5

Figure 1.5: Parabolic Reflector. [3]

Explanation of functional requirement of the parabolic profile reflector is done with the help of Fig. 1.6 [3]

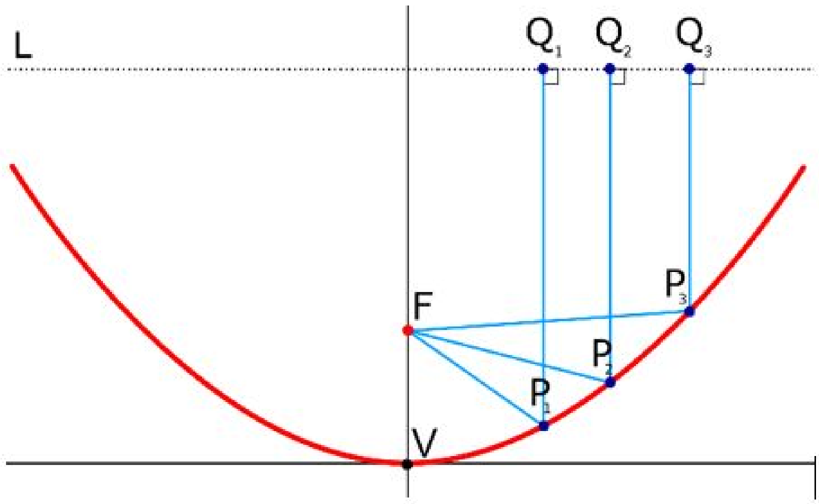

Figure 1.6: Focal Length Description [3]

The light rays reflects from the concave face of the reflector, after reflecting all rays meet at a common point is called as focal point. And distance of this point from point V on the reflector at principal axis is called focal length i.e. distance VF as shown in Fig. 1.6.

1.10 Composite Manufacturing Techniques

There are many techniques available for composite manufacturing such as resin transfer moulding process (RTM), hand lay up process, wet lay up , prepreg lay up and autoclave process. Autoclave Process is widely used for composite manufacturing of Space standard components.

1.10.1 Autoclave Processing

In auotoclave, curing of the uncured stack of prepreg which is called as laminate takes place. In the process uncured laminate is laid on the tool such that flexible uncured prepreg takes the shape of mould. Over the prepreg some additional layers of peel ply, breather, bleeder etc. are kept. These additional layers are added for proper curing of laminate in autoclave during the process. Then the whole assembly is vacuum bagged and placed inside an autoclave. In the autoclave machine as shown in Fig. 1.7 assembly is passed through a curing cycle. Once the cycle gets completed, assembly is taken out of the autoclave and laminate is demoulded from the tool. The autoclave process is widely used for aerospace industry for making tougher and good quality composite parts.

Figure 1.7: Curing process in Autoclave Machine [4]

Consolidation

This step involves creating intimate contact between each layer of prepreg or lamina. This step ensures that all the entrapped air is removed between layers during processing. Consolidation is a very important step in obtaining a good quality part. Both resin and fibers share the applied pressure during consolidation process. There are different layers as shown in Fig. 1.8 over the prepreg, this assembly is then enclosed in vacuum bag.

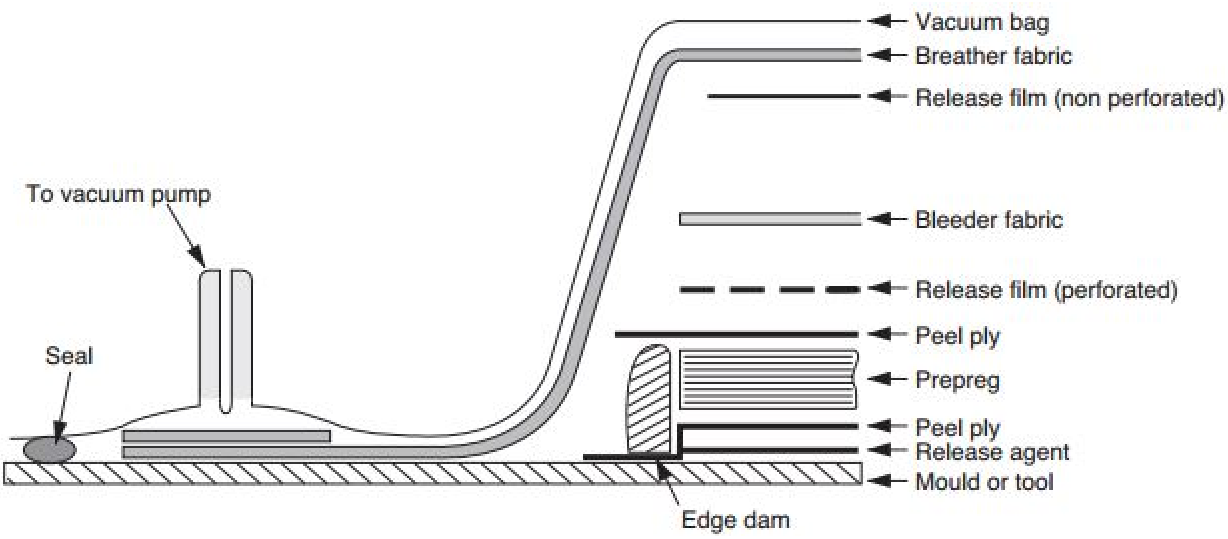

Figure 1.8: Vacuum bag lay-up [5]

Each layer has its own function which are explained as follows:

- Release agent - It helps in decresing the friction coefficient between tool and part so that part can easily slide over the tool.
- Peel ply - It can be used to provide bondable surface of the composite after curing process completes.
- Bleeder fabric - It helps in absorbing excess matrix material and helps in adjusting the fiber volume fraction. It is mainly used in resin transfer moulding process where the resin quatity is larger with
- Peel ply - It can be used to provide bondable surface of the composite after curing process completes.
- Bleeder fabric - It helps in absorbing excess matrix material and helps in adjusting the fiber volume fraction. It is mainly used in resin transfer moulding process where the resin quatity is larger within the system.
- Release film - It is a thin PTFE based film used to prevent adhession of pregpreg layup with tool. This is a substitute to release agent.
- Breather fabric - It helps by providing way to apply vaccum pressure and also hepls in air and volatile removal from entire assebly. It also helps in distributing equal autoclave pressure in assembly.
- Vacuum bag - It seal the entire assembly and provide passage for removing air and volatiles from the assembly.

Autoclave Curing Cycle

A Curing cycle is a representation of combination of pressure and temperature which is applied on the vacuum bagged assembly during the processing inside the autoclave. A typical curing cycle is shown in Figure 1.9. The objective of this 'process cycle' is to cure the resin and promote resin flow such that an optimum resin content and a void free part are obtained. At the same time, the dimensions of the produced structure must not vary beyond pre-set tolerance limits.

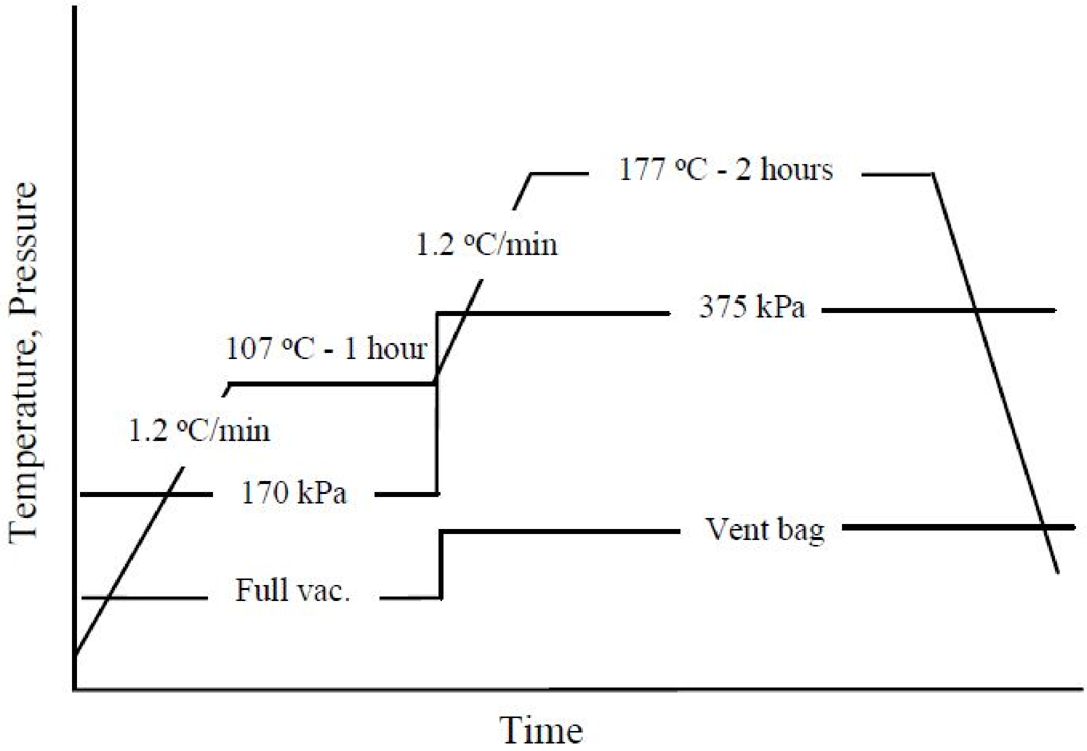

Figure 1.9: A Typical Curing Cycle [12]

1.11 Resin Transfer Moulding Process

The resin transfer molding (RTM) process shown in Fig. 1.9 is also known as a liquid transfer molding process. In this process there are two moulds upper half and lower half and inbetween them there is cavity in which preform can be kept. A pressurized resin mixed with catalyst, colour etc. is pumped inside the mould via ports available in the mould. After curing process completes the part can be recovered by opening the moulds. Using this manufacturing process components for automobile, aerospace and sports industry can be manufactured.

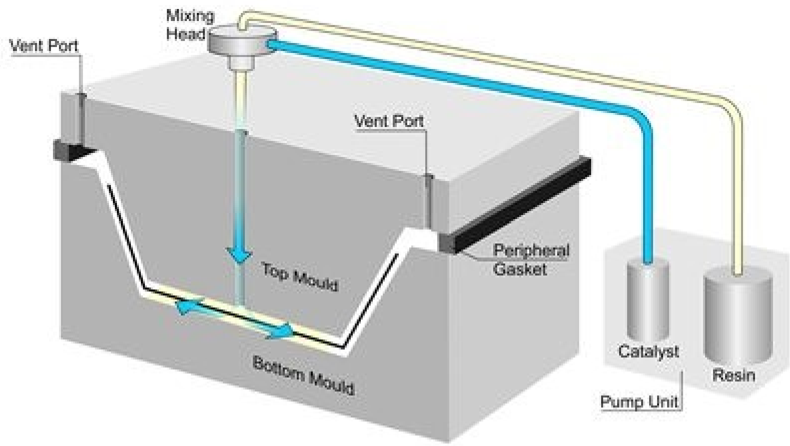

Figure 1.10: Resin Transfer Molding [6]

1.12 Defects in Manufactured Composite Laminate

Springback

Springback is defined as the decrease of the enclosed angle of a corner section, which occurs even when the through thickness stress distribution is uniform. Typically for CFRP composites, the change of the enclosed angle of a 90° corner section is of the order of 1° to 3°. Spring–forward is primarily caused by the combination of anisotropic material behaviour and the geometry of the corner.

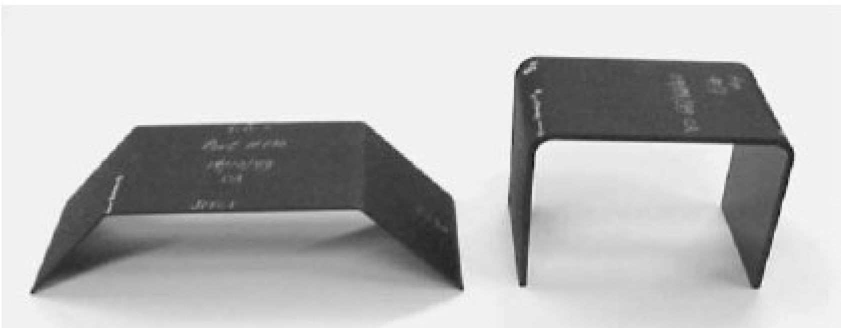

Figure 1.11: Spring Back in Angled Laminates [8]

Warpage

Warpage is defined as the curvature and twist of initially flat parts, and is mainly the result of a non–balanced stress distribution through the thickness of the composite laminate. Mechanism of warpage is shown in Fig. 1.12

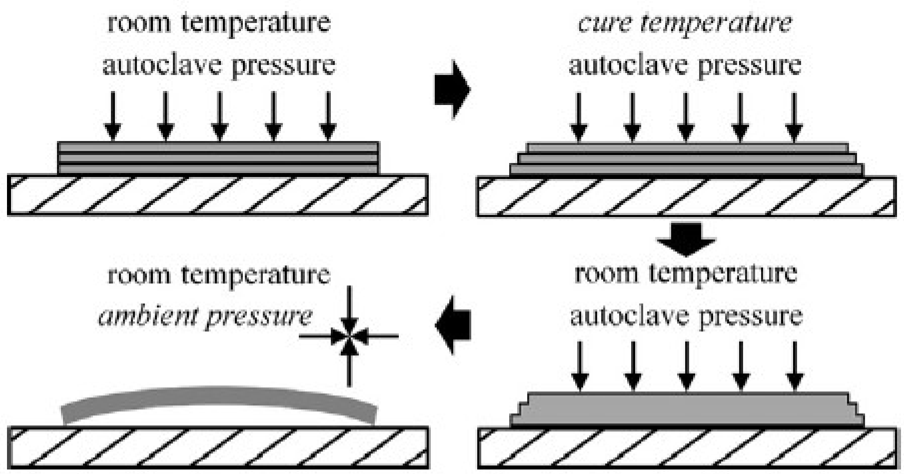

Figure 1.12: Warpage in flat laminate[8]

1.13 Project Objectives

1. To determine the springback of CFRP reflectors using experimental and numerical techniques.
2. To determine the values of process parameters which results in the least springback deformation.
3. To study the effect of surface finish on manufactured L-shape composite part.

1.14 Methodology

1.14.1 Experimental Approach

1. Selection of suitable mould materials and grade of prepreg.
2. Manufacturing of mould using Vertical Machining Center (VMC).
3. To arrive at the plan of experiiments.
4. Procurement of consolidation material such as peel ply, breather cloth, release film etc.
5. Vacuum bagging of mould and prepreg using vacuum pump and valve.
6. Curing of prepregs in Hot air oven and demoulding of cured component from mould.
7. Measurement of coordinates of mould using Coordinate Measuring Machine (CMM).

1.14.2 Numerical Approach

1. Create/Import composite part and mould geometry in Abaqus
2. Mesh the composte and mould parts with 3D stress hex elements.
3. Add materials using COMPRO and assign them to respective parts.
4. Assemble the mould and composite parts and assign interaction property to the interface.
5. Assign initial temperature and displacement boundary condition to assembly.
6. In the thermochemical module, specify curing cycle and heat transfer coefficient to composite and tool surfaces.
7. Obtain temperature and degree of cure plot from thermochemical analysis.
8. Using the results from thermo-chemical, run stress deformation analysis to obtain the deformed shape of the composite part.

Chapter 2

Literature Review

2.1 Literature Review

Residual Stresses and deformation is an unavoidable phenomenon in Carbon Fiber Reinforced Polymer (CFRP) processing.To overcome this problem extensive studies has been conducted from very long time on the parameters effecting the residual stresses and deformation. Complexity of the problem which involves several parallel mechanisms taking place at a time makes its study more complicated.

During curing some stresses got developed which varies with respect to temperature development. A method based on total-strain-temperature relation is formulated and applied to determine the curing stresses in boron/epoxy composite laminate [9]. Quality of manufactured composite part depends on process parameters which are time, temperature and pressure. The important choice of three parameters produces composites which are fully cured, compacted and of high quality. A slight deviation of these recommended processing parameters can results in unaccepted product quality. Residual stresses induced while curing in autoclave or hot press is one of the most significant cause of deviation of the quality of a product. Process induced residual stresses can be of a great extend which can results into cracking of resin matrix before mechanical loading. For the prediction of residual stresses during curing process a model has been developed. In the model mechanical properties are the function of degree of cure and transverse compliance. Based on this predictions study has been carried out for composite system IM6/3100 graphite/bismaleimide prepreg. Thermal strains were shown to increase during cure cycle due to increase in matrix strength and stiffness development. A good agreement is obtained between model prediction and experimental warpage data. The manufacturer recommended curing cycle is varied at some of the intermittent cure points [10][11].

Warpage and spring-in are caused after demoulding of laminate from the tool due to relaxation of residual stresses from the interacting surface of composite laminate.

Hence the part manufactured is distorted and unacceptable. If the behaviour of deformation while manufacturing of layered composite laminate is well known in advance so that can be used for compensating the tool. For prediction of these deformations traditional experimental techniques were adopted but they are very hard to practice due to its high cost and unsuitable for larger components. So there is a critical need to supplement the current techniques with a science-based manufacturing approach. A 2-D finite element model for prediction of process-induced deformation has been developed. A virtual environment of autoclave has been introduced to predict structure boundary conditions during processing. Models are developed to describe the composite material behaviour during processing [12]. It is a plane strain model for prediction of process induced deformations of complex shaped composite structures. We know that composite is the combination of matrix and fiber material. Out of these two, resin material solidifies during its manufacturing which is called as curing process. To represent the mechanical behaviour of composite matrix resin "cure hardening-instantaneously linear elastic" model is employed. For determining the mechanical properties of the ply macro-mechanics of lamina is used. From the experiments conducted it is observed that tool-part interaction also plays important role in inducing warpage, to represent this tool-part interaction layer (elastic shear layer) is introduced. Using these module one can develop software and can simulate some general 2-D cross section laminates. These codes limits us to simulate the 2-D cross-section of laminate only. [13]

The main reasons for generation of residual stresses in polymer is resin cure shrinkage and anisotropic nature of fiber-reinforced polymer matrix composite material. To know the cause of the above mentioned phenomena different parameters of autoclave process such as prepreg material, cure cycle, tool surface, geometry and layup are studied. The effect of these parameters have been studied on dimensional stability of composite parts manufactured using autoclave process. Using above parameters, Design of experiments were conducted. This enable us to perform least no. of experiments to study the behavior of the parameters on final manufactured part. Experiments were conducted and along with that with the same input data numerical analysis was also conducted using Compro software. The study shows that FEA results are in good agreement with the experimental results. From the study it is observed that tool surface condition and cure cycles are major contributor of spring-in in laminate. With single hold cycle tool with no release agent, L-shape laminate shows lesser spring-in than tool with release agent and subsequently with double hold cycle the behavior is vice-versa i.e., when release agent is applied on tool, the L-shape laminate showed lesser spring-in. [14][15]

Parameters can be classified into design and process parameters which can have significant contribution for inducing warpage. To get the effect of these parameters more number of experiments has to be performed. These parameters include laminate angle, component thickness, stacking sequence, laminate flange length, mould material, tool surface condition, and cure cycle applied for cuirng in auclave. From the previous research it is confirmed that the cause of spring-in is difference of CTE between tool and composite. Tool has more CTE than composite, due to which while curing process residual stress get developed in composite part which results into spring-in after tool removal. Some analytical formulations are also carried for angled parts such as for L-shaped and C-shaped parts. C-shaped parts shows larger spring-in as compared to L-shaped parts. Larger thickness part shows less spring. Warpage in the flange portion can also effect spring-in of angled laminate. Various parameters were found that affects the warpage of the component, which includes composite laminate thickness, composite flange length, cure cycle, the tool material, and mould surface condition. To decrease the magnitude of induced deformations it is better to use the tool material which is having lower CTE [16][7]

For detailed analysis of tool part interaction experments were conducted. This analysis includes quantification of tool-part shear interaction during composite processing. For the study of compaction and flow of laminates, a scanning electron microscope was used to observe the tool-part interfacial region of the laminate during the curing process. Strain gauge rosette are mounted on tool in longitudinal and transverse direction to obtain the strain magnitude. Sticking and sliding friction conditions are studied. From the experiment a conclusion can be drawns that before gel point there was no significant mechanical interaction between mould and prepreg regardless of mould surface condition. It can be justified by the results of strain calculated at tool-part interface that strain was approximately same due to free expansion of tool. But after composite reached the gel point, there is change in strains which is a function of temperature. This strains represents the longitudinal and transverse coefficient of thermal expansion of CFRP component rather than that of tool. At high degree of cure Shear stress during sliding friction condition is much greater for higher autoclave pressure. [17]

Some experiments were conducted on samples of flat laminates to by considering various parameters which are part aspect ratio, process conditions for a given material and layup. These parametrs are studied on tool-part interaction inducing warpage. These experimental results are used to develop an empirical relation for the prediction of warpage in flat laminates. And along with that a numerical model (FE model) is also developed and verified with analytical results. From the experiments it is concluded that part aspect ratio has greater effect on warpage than autoclave pressure. The empirical formula implies that maximum warpage is directly proportional to the part length and inversely proportional to the thickness of the laminate. Using tool with lower C.T.E. induces lesser warpage in composite part. [18][19]

Most of the aerospace part are sandwich composite laminates. Honeycomb nomex as core material is sandwich between composite prepregs(skins). By using these sandwich composite structures overall weight of the component can be reduced. While manufacturing of angled laminates, spring-in is observed in component. For the prediction of spring-in of angled composite sandwich panel analytical models were developed. This analytical model is validated with finite element model. Some assumptions are made to simplify the analytical models. [20, 21]

An analytical equation of effective coefficient of thermal expansion is derived, and that equation is used for predicting the spring-in in angled laminate.[22] This approach is also validated with the Finite element results. For validation purpose L-shaped laminate made up of prepreg system T300 carbon fiber/CYCOM934 is used. It is analysed for different stacking sequence such as cross ply and unidirectional ply.

Experimental work has been performed for determining the effects of pressure, degree of cure, ramp up rate on coefficient of friction between tool and composite part. Tests were conducted on Cytec Fiberite's MXB7701-7781-B3 glass/epoxy fabric prepreg. In all experiments single layer of prepreg is used. As the degree of cure increases with ramp rate 1.7 degcel/min static coefficient of friction first decreases and then increases and again it decreases. [23]Results of this study are used by zeng et al [24] along with 3-D process model and contact element. This 3-D model is successful in predicting the warpage of an aeroplane composite curved part.

Experimental work is conducted by Stefniak et al. [8] to quantify the different mechanisms (such as Property gradient mechanism, stress gradient mechanisms) with respect to their relative contribution to composite part distortions. A new model is developed based on theory of frozen matrix strains induced during tool-part interaction. Design of experiments is conducted by taking the parameters as configuration of specimen, prepreg system, length of composite part, number of prepreg layers, surface roughness of tool, tool surface condition. Two prepreg systems are used, one is M21/268/T800 and other is AS4/8552/194. The results of the experiments are consistent with the new model.

2.2 Literature Review Summary

In the literature, extensive study has been conducted and various parameters are identified which plays important role in inducing warpage and spring back in laminate. Different methodologies are adopted for capturing the exact behaviour of the curing process. It is observed that uptill now major study has been carried out on flat and angle laminates and various conclusions have also been drawn to reduce the warpage in those laminates. It feels that more study is required to be conducted on Curved Profile Laminates such as for paraboloid shape and predict the more accurate behaviour of these laminates during its curing process.

Chapter 3

Selection and Procurement of Mould, Prepreg and Consolidation material for Experimental Work

Different materials and consumables will be required for carrying out the experiments. These materials includes mould materials, consumable technical fabrics and vacuum bag, vacuum valve and hose pipe connections etc.

3.1 Mould Materials Selection Process

Mould and composite part interaction is the key factor for process induced deformation of the composite parts. To reduce the post cure deformation of composite parts one must select the mould material which is having least coefficient of thermal expansion (CTE) values. Due to comparable CTE values of composite and mould, residual stresses induced in the composite part can be reduced and hence reduces the process induced deformation of part after demoulding. For the purpose three different mould materials are selected which are as follows,

1. Graphite
2. Stainless Steel
3. Grey Cast Iron

3.1.1 Selection of Graphite Material

Selection of the graphite as one of the mould material is due to its lesser CTE values. Properties of different grades of graphite are shown in Table 3.1.

Table 3.1: Various Grades of Graphite

Grade	GLM	EDM	FE679	GP1-IA	ICS-844	IC-6002	IC-6003
Specific Gravity(g/cc)	1.7	1.86	1.92	1.85	1.83-1.87	1.74	1.81
Grain Size	0.04	0.02	0.02	0.02	0.02	0.075	0.04
C.T.E($/^0C$) [$\times 10^{-6}$]	4.8	4.4	5.5	4.3	5.4	5.3	4.0
Thermal Conductivity(W/mK)	108	139	128	_	80	_	_
Shore Hardness	46	54	68	60	70-85	60	70
Flexture Strength (MPa)	39.2	53.9	63.7	45.11	50-65	23-25	35-45
Surface Finish	low	high	high	low	high	low	low

The selection of material is on the basis of CTE and surface finish. By comparing all above grades of graphite, EDM is selected because it has lowest CTE and high surface finish from which one can obtain mirror surface finish after lapping process. Graphite block of size 300*300*70 mm is procured which is shown in Figure 3.1.

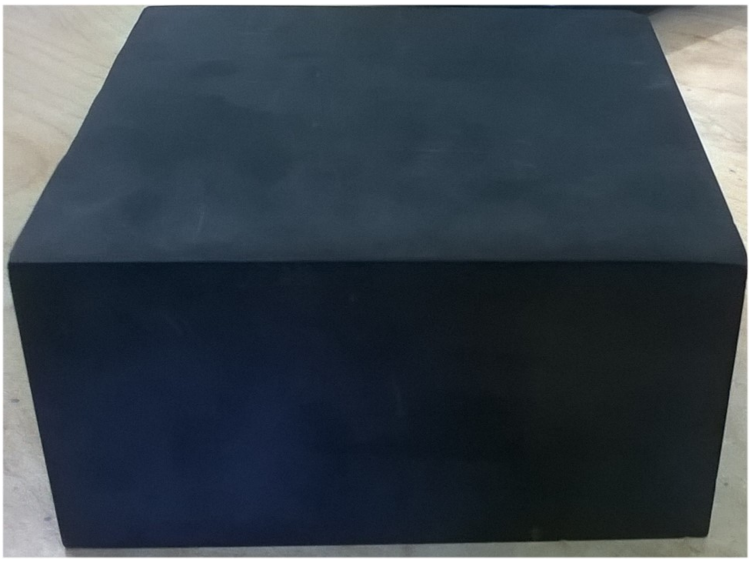

Figure 3.1: Graphite Block

3.1.2 Selection of Stainless Steel

Stainless Steel (SS) is widely used due its corrosion resistant property, high strength and ease of availability. Some of the grades are selected which are shown in Table

3.2 having least coefficient of thermal expansion.

Table 3.2: Various Grades of Stainless Steel

Grade (AISI)	202	304	316	301	310	410	430
Specific Gravity (g/cc)	7.62	7.9	8	8	8	7.8	7.8
C.T.E ($/^0C$) [$\times 10^{-6}$]	17.3	16.9	16.4	16.8	15.9	11	10.2
Thermal Conductivity (W/mk)	15	16.2	14.6	16	14.2	30	25
Max.Yield Tensile Strength (MPa)	540	820	820	1050	310	660	280
Youngs Modulus (Gpa)	200	200	200	200	200	210	210

From the above different grades of stainless steel material, AISI 430 grade is selected due to its lowest coefficient of thermal expansion as compared to other grades and also have required good thermal conductivity. It is a ferritic grade of SS. SS of size 300*300*70 mm is procured as shown in Figure 3.2.

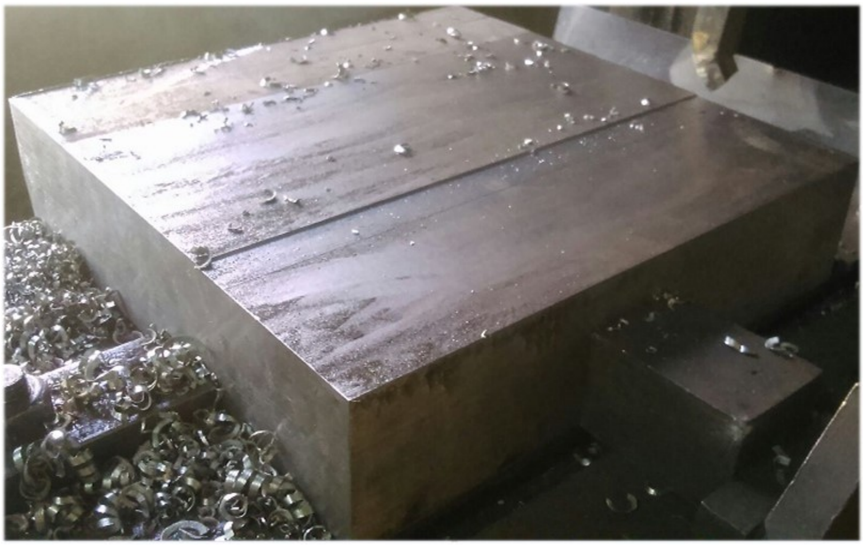

Figure 3.2: SS Mould Material

3.1.3 Selection of Grey Cast Iron

Almost all the grades of cast iron (C.I.) have similar CTE values. In an autoclave upto 7 bar pressure can be applied during curing process. Such grade of Grey Cast Iron should be selected which do not deform due to autoclave pressure while processing. If it deforms then there exists a inherent spring back due change in geometry of the tool. Some of the grades are selected which are shown in table 3.3.

Table 3.3: Various Grades of Grey Cast Iron

Grade (ISO)	20 (150)	30(200)	35(250)	40(300)	50(350)
Specific Gravity (g/cc)	7.2	7.2	7.2	7.2	7.2
C.T.E($/^0C$) [$\times 10^{-6}$]	10.5	10.5	10.5	10.5	10.5
Thermal Conductivity (W/mk)	46	46	46	46	46
Max.Yield Tensile Strength (MPa)	150	180	250	270	410
Max.Compressive Strength (MPa)	570	670	750	860	1130

It is observed that, in the above properties that as the grade succeeds from 20 to 60 strength of compressive strength increases. For this purpose, criteria for selection is deformation and stress generated in the mould under 7 bar autoclave pressure. Finite element static structural analysis is carried on grey cast iron mould. Cast Iron Grade 30 is selected because it shows negligible deformation than grade 20. Grade 30 is selected as one of the mould material.

3.2 Selection of CFRP Prepreg

Prepreg system having carbon fibers and epoxy resin as its constituents is selected. For space application carbon fiber are used because of their good specific strength and stiffness properties. Epoxy resin material is used because of its capability of sustaining temperature upto 200^{0}C. Hinpreg HCU 200 / A45 which is a unidirectional prepreg system is selected. Hinpreg A45 is an advanced epoxy prepreg developed to enable economic manufacturing of various high performance composite applications. It has a versatile curing cycle, from 100^{0}C to as high as 150^{0}C. It is been specially formulated to achieve excellent through-cure and mechanical performance as it can be combined with glass, carbon as well as aramid. Mechanical properties of fiber and epoxy is shown in Table 3.4.

Table 3.4: Mechanical Propreties of Fiber and Epoxy

HCU 200 - Fibre	
Density (g/cm^3)	1.8
Filament Diameter ($10^{-6}m$)	7
Tensile Strength (MPa)	3450
Tensile Modulus (GPa)	230
Elongation Percentage (%)	1.5
Filaments	12K
GSM	200

A45 - Epoxy	
Tensile Strength (MPa)	48
Tensile Modulus (GPa)	2915
Elongation Percentage(%)	1.6

Some of the advantages of Hinpreg A45 prepreg are excellent surface finish, wide choice of application process (vacuum bagging, autoclave, heated mould etc) suitable for wide range of curing temperature and excellent mechanical properties.

For curing of prepreg two type of curing cycles can be used,

a) Single hold curing cycle

b) Double hold curing cycle as shown in Figure 3.3.

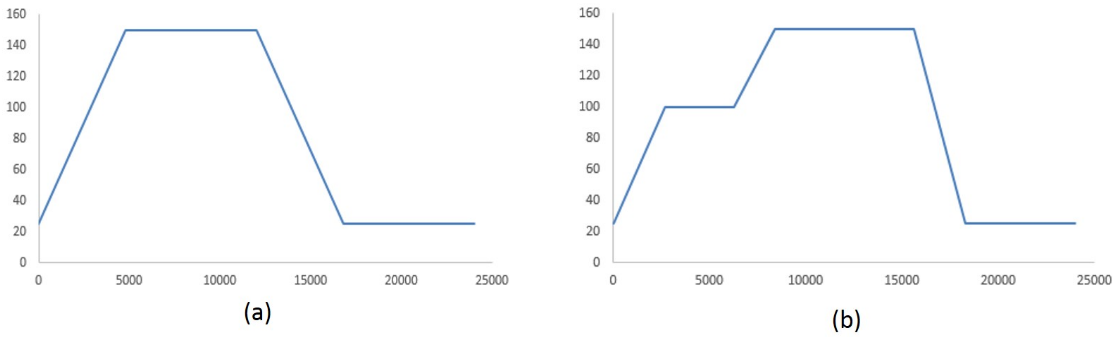

Figure 3.3: Curing Cycle used for Curing of CFRP Prepreg

Hinpreg A45 should be stored as received, at -18^{0}C in deep freezer, in sealed condition. A sample of Prepreg roll is shown in Figure 3.4.

Figure 3.4: Unidirectional Fibre Prepreg Roll [35]

3.3 Consolidation Materials

Consolidation materials are the essential component which are needed during manufacturing of composite parts using autoclave or hot air oven. These materials contains consumable fabrics and bagging materials. Following consolidation materials are used during curing process of CFRP reflector. The function of respective material is explained in detail which is as follows,

- Release agent - It allows release of the cured prepreg component from the tool.
- Peel ply - It allows free passage of volatiles and excess matrix during the cure. Can be removed easily after cure to provide a bondable or paintable surface.

- Release Tape - It is used to prevent the adhesion of composite layup with the tool during curing process.

- Release Agent - This is liquid agent which is applied on the mould to prevent the adhesion of composite layup with the tool during curing process.

- Breather fabric - Provides the means to apply the vacuum and assists removal of air and volatiles from the whole assembly. Thicker breathers are needed when high autoclave pressures are used.

- Vacuum bag and sealant tape - Provides a sealed bag to allow removal of air to form the vacuum bag.

All these consolidation materials are selected such that they can sustain temperature upto 200^oC. Consolidation material are shown in Figure 3.5.

Figure 3.5: Consolidation Materials

Chapter 4

Manufacturing of Moulds

Moulds with paraboloid profile are used during curing process of CFRP reflectors.

4.1 Dimensional Calculation of Paraboloid Profile

Actual dimension of reflector used in space is of range 2.4 m diameter. Too many experiments on such a large diameter reflector are not feasible due to economic constraints . It is decided to consider only 10% of the actual diameter. The prototype of diameter 240 mm is selected. A paraboloid can be obtained by rotating a parabolic curve with respect to its central axis. The general equation of a parabola in cartesian coordinates with its vertex at the origin and its axis of symmetry along the y-axis, so the parabola opens upward, its equation is

$$4fy = x^2 \tag{4.1}$$

where "f" is focal length . Correspondingly, the dimensions of a symmetrical parabolic dish are related by equation

$$4FD = R^2 \tag{4.2}$$

where "F" is the focal length, "D" is the depth of the dish (measured along the axis of symmetry from the vertex to the plane of the rim), and "R" is the radius of the rim as shown in Figure 4.1..

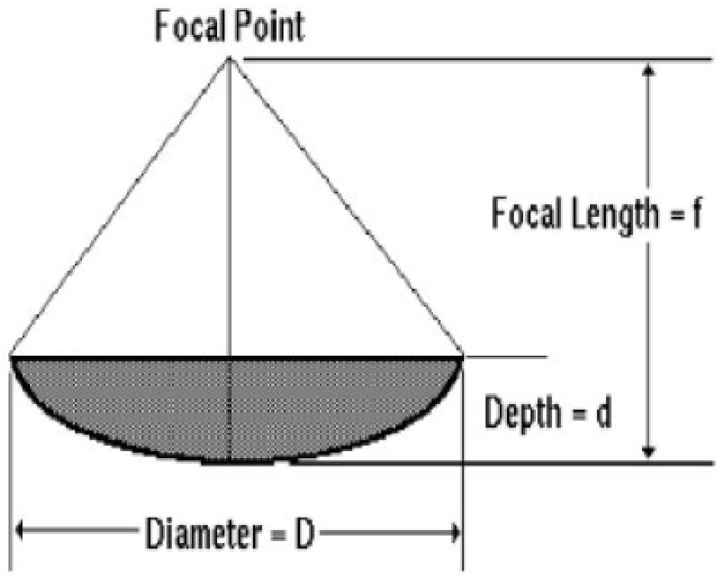

Figure 4.1: Parameter of Parabolic Profile Reflector

Here the diameter of reflector is decided to be 250 mm and depth as 50 mm. From Equation (4.2), focal length of the reflector comes out to be 78.125 mm. After putting the value of f in Equation (4.1), the equation of parabolic profile can be written as

$$312.5y = x^2 \tag{4.3}$$

Using Equation (3.1) a CAD model of the mould can be a made as shown Figure 4.2.

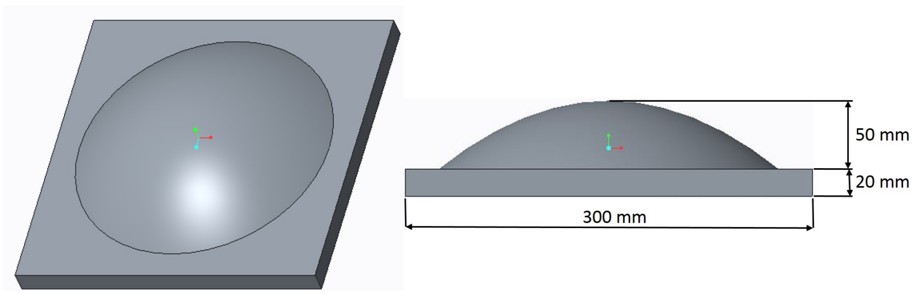

Figure 4.2: 3D CAD Model of Reflector Mould

4.2 Manufacturing of Reflector Mould

All the mould materials i.e., stainless steel, graphite and cast Iron are machined on vertical milling center (VMC). All the blocks are of 300*300*70 mm size. These are machined on the basis of CAD model shown in Figure 4.1. The machined mould are shown in Figure 4.2 (a), (b) and (c).

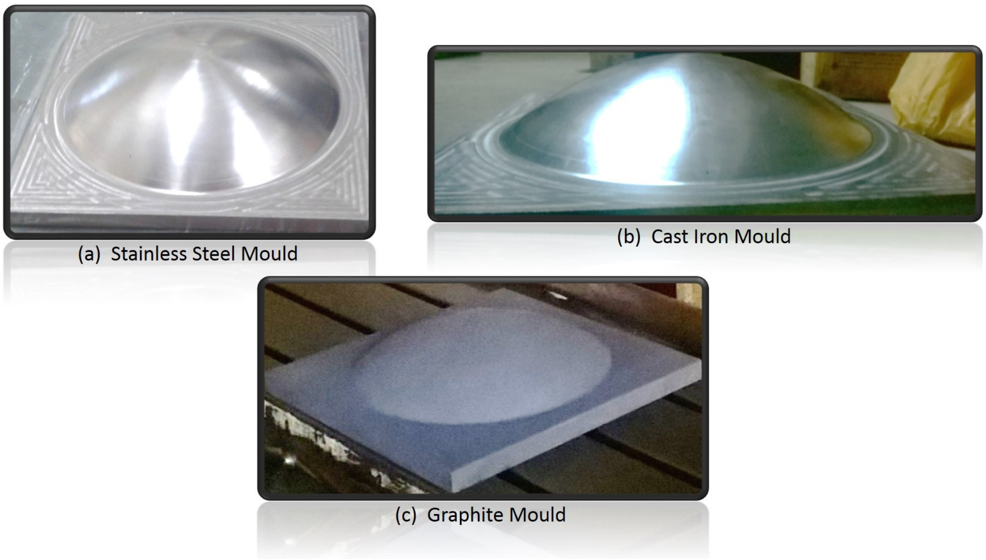

(a) Stainless Steel Mould

(b) Cast Iron Mould

(c) Graphite Mould

Figure 4.3: Manufactured Mould

Chapter 5

Experimental Work for Manufacturing of Paraboloid Reflector

An experiment is conducted for manufacturing of CFRP Paraboloid reflector. From this experimental work a methodology can be decided for carrying out the actual experiments. In this sample experiment Stainless Steel mould is used. The procedure followed is explained in subsequent section.

5.1 Methodology for Conducting a Sample Experiment

5.1.1 Setup Preparation for Curing Process of Reflector

Stainless Steel (SS) grade AISI 430 is used as a mould during the experiment. Four layers of prepreg are cut into the circular shape of diameter 300 mm. Mould and prepregs are shown in Figure 5.1. Release tape and peel ply is used during experimental work. Teflon coated release film and peel ply are used which can sustain tempreature upto 200 ^{o}C. Marking has been done on peel ply and relase film with the marker for accurate cutting. Teflon coated release film is laid on mould as shown in Figure 5.3. Teflon coated release tape is used for to prevent adhesion of prepreg with mould material during curing process. Release film is cut into 8 different parts and then arranged on mould to avoid wrinkling of the film. After arrangement of release film, four layer of layer of prepregs are laid on the mould one by one. The layup is of four prepreg layers as shown in Figure 5.4. After arrangement of prepreg layup, selant tape is applied over the four corner of mould material as shown in Figure 5.5. Peel ply and Breather cloth is also laid on the setup as shown in Figure

5.6 (a) and (b) respectively. Whole setup is vacuum bagged using a film as shown in Figure 5.7 (a). In the center of the bag, a hole is made to accomodate the vacuum valve. One end of vacuum hose is connected to valve and other at vacuum pump outlet. Using this configuration, whole air entrapped inside the bag is taken out as shown in Figure 5.7 (b). For curing of CFRP reflector, this whole setup is kept in hot air oven as shown in Figure 5.8. During the curing of reflector in oven, vacuum pressure is maintained to ensure no air inside the bag.

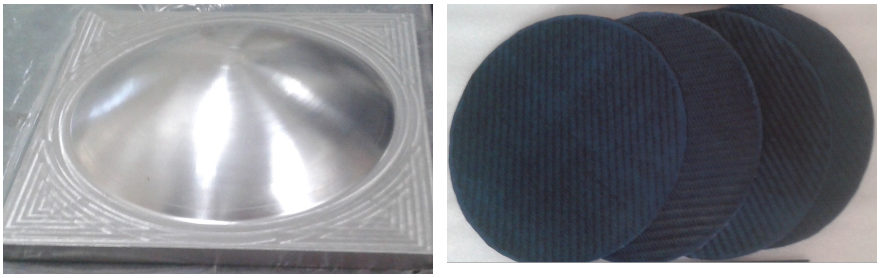

Figure 5.1: SS Mould and Prepreg

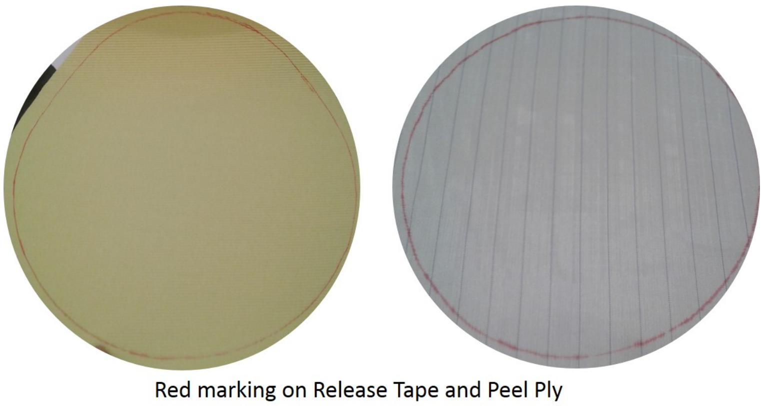

Figure 5.2: Marking on Release Film and Peel ply

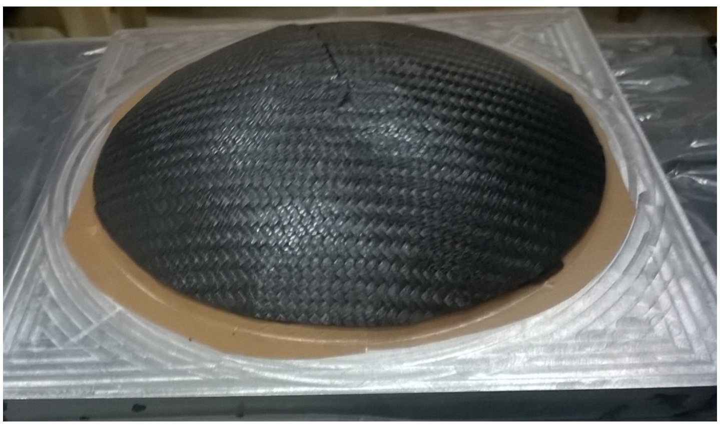

Figure 5.3: Prepreg Layup on Mould

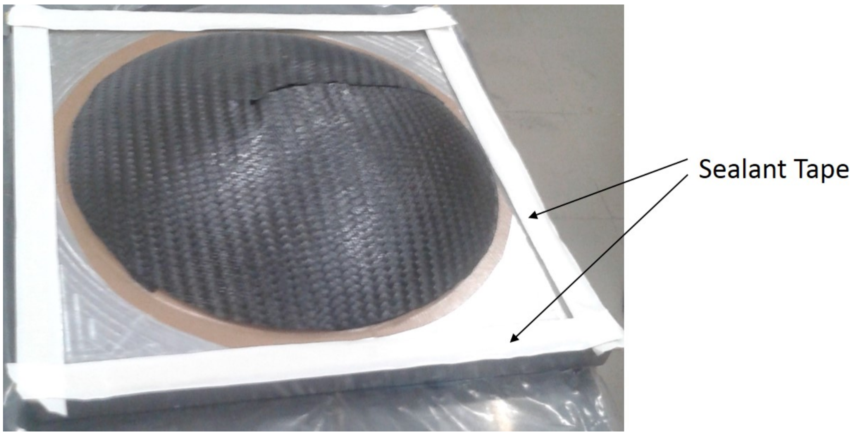

Figure 5.4: Setup of Sealant Tape

Figure 5.5: Peel ply and Breather Cloth on Setup

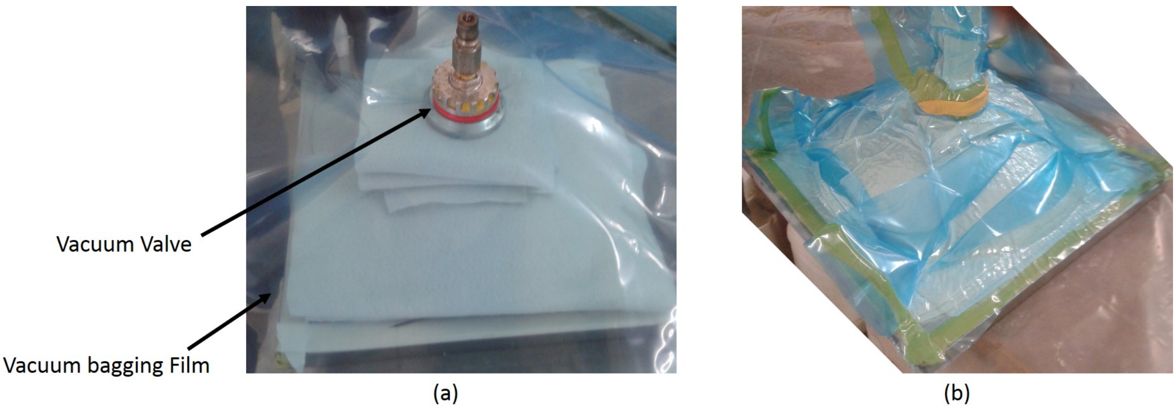

Figure 5.6: Vacuum bagging and Air Suction Process

Figure 5.7: Hot Air Oven

5.1.2 Demolding Process

Whole assembly is taken out from the hot air oven. Let the assembly cool down upto room temperature before removing the consolidation material. After it gets cool down, consolidation materials are removed from mould. And after that Composite reflector is demoulded. The sequence of process is shown in Figure 5.9.

Figure 5.8: Assembly taken out from the Oven

The demoulded cured reflector is shown in Figure 5.10

Figure 5.9: CFRP Reflector

5.2 Measurement

After getting the final product, measurement of the coordinates on specified points on mould and reflector is performed using Coordinate Measuring Machine (CMM).

5.2.1 Coordinate Measurement of Points on Mould

Measurement of specified points are performed to ensure the accuracy of the parabolic profile achieved after maching of the mould. This is accomplished by comparing the CAD and CMM data. First of all in the CAD model of mould some points have been defined on the parabloid surface and coordinates of those points are measured. The points defined are shown in Figure 5.10.

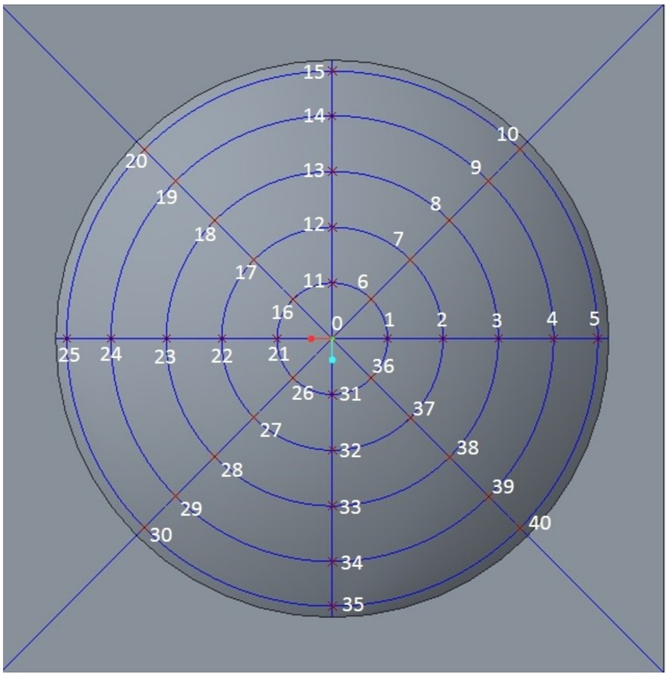

Figure 5.10: Points Defined on Mould

These points are obtained by projecting circles of diameter 50, 100, 150, 200 and 240 mm on paraboloid surface of reflector. Total 41 points are obtained. The coordinates of these points are measured which are are shown in Table 5.1.

Table 5.1: Coordinates of Points Defined on CAD Model (mm)

Point No.	x	y	z
0	0	0	0
1	25	0	48
2	50	0	42
3	75	0	32
4	100	0	18
5	120	0	3.92
6	17.6777	17.6777	48
7	35.3553	35.3553	42
8	53.033	53.033	32
9	70.7107	70.7107	18
10	84.8528	84.8528	3.92
11	0	25	48
12	0	50	42
13	0	75	32
14	0	100	18
15	0	120	3.92
16	-17.6777	17.6777	48
17	-35.3553	35.3553	42
18	-53.033	53.033	32
19	-70.7107	70.7107	18
20	-84.8528	84.8528	3.92
21	-25	0	48
22	-50	0	42
23	-75	0	32
24	-100	0	18
25	-120	0	3.92
26	-17.6777	-17.6777	48
27	-35.3553	-35.3553	42
28	-53.033	-53.033	32
29	-70.7107	-70.7107	18
30	-84.8528	-84.8528	3.92
31	0	-25	48
32	0	-50	42
33	0	-75	32
34	0	-100	18
35	0	-120	3.92
36	17.6777	-17.6777	48
37	35.3553	-35.3553	42
38	53.033	-53.033	32
39	70.7107	-70.7107	18
40	84.8528	-84.8528	3.92

These points are fed to CMM to measure on the mould. Figure 5.11 shows the points to be measure by CMM on mould.

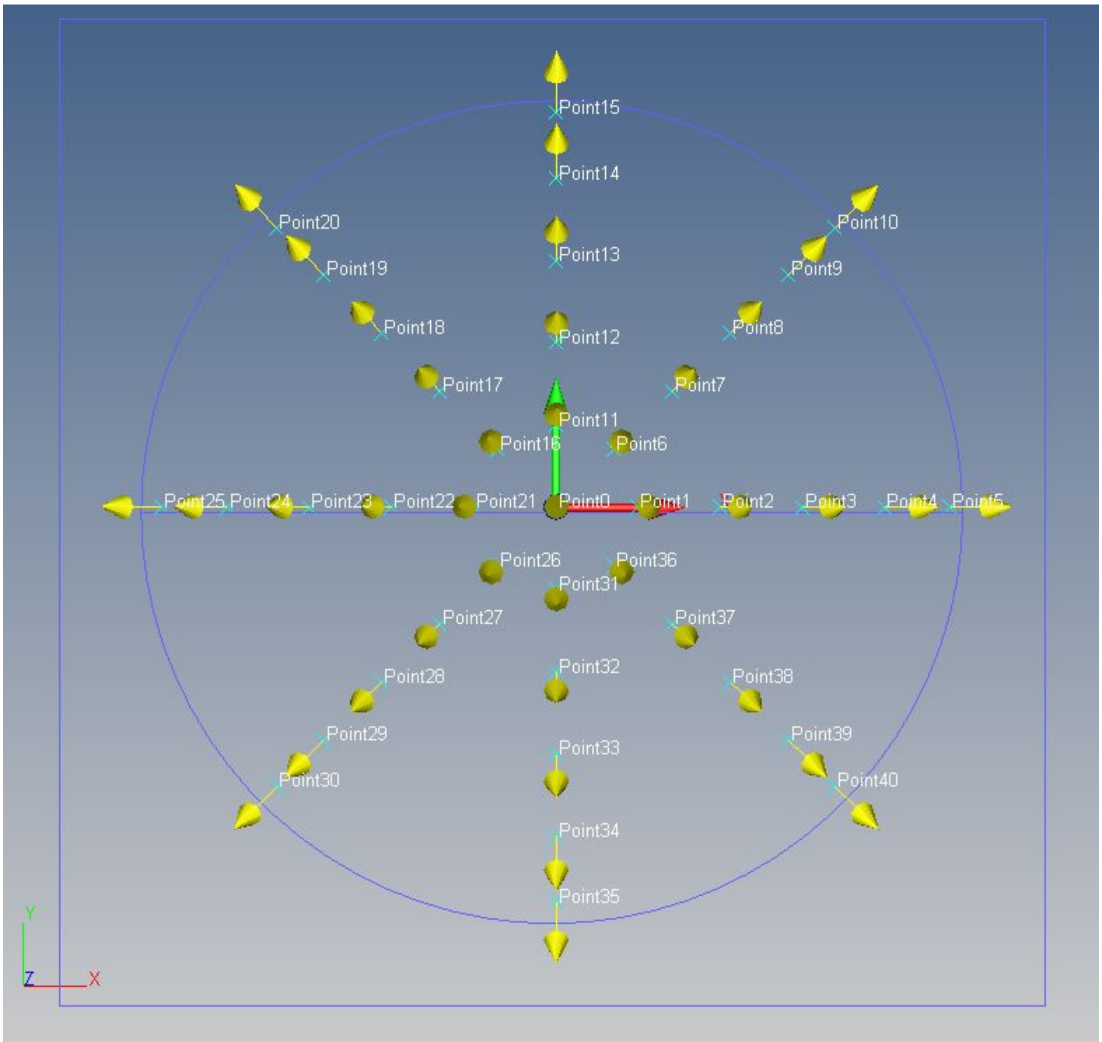

Figure 5.11: Points Measured by CMM on mould

Table 5.2 shows the measured points coordinates on mould.

Table 5.2: Measured Points Coordinates on Mould (mm)

Point No.	X	Y	Z
0	0.0002	0.0002	50.0236
1	24.9967	-0.0002	47.9803
2	49.9905	-0.0003	41.9710
3	74.9880	-0.0002	31.9754
4	99.9894	-0.0002	17.9836
5	119.9924	-0.0001	3.9102
6	17.6739	17.6738	47.9684
7	35.3793	35.3795	42.1030
8	53.2058	53.2064	32.4993
9	70.9426	70.9436	18.5067
10	84.9064	84.9066	4.0178
11	-0.0002	24.9947	47.9690
12	-0.0004	49.9814	41.9435
13	-0.0005	74.9707	31.9400
14	-0.0005	99.9590	17.9365
15	-0.0005	119.9496	3.8548
16	-17.6749	17.6745	47.9737
17	-35.3797	35.3816	42.1115
18	-53.1996	53.2083	32.5046
19	-70.9392	70.9480	18.5138
20	-84.9029	84.9046	4.0137
21	-24.9982	-0.0001	47.9879
22	-49.9941	-0.0002	41.9810
23	-74.9939	-0.0001	31.9871
24	-99.9989	0	17.9983
25	-120.0095	0.0001	3.9325
26	-17.6775	-17.6775	47.9980
27	-35.3887	-35.3884	42.1523
28	-53.2217	-53.2206	32.5660
29	-70.9811	-70.9798	18.6043
30	-84.9586	-84.9582	4.1164
31	0	-25.0001	48.0007
32	0.0001	-50.0024	42.0079
33	0.0002	-75.0112	32.0236
34	0.0004	-100.0329	18.0520
35	0.0005	-120.0502	3.9858
36	17.6773	-17.6774	-47.9967
37	35.3897	-35.3872	42.1470
38	53.2262	-53.2165	32.5563
39	70.9784	-70.9684	18.5814
40	84.9504	-84.9473	4.0971

Table 5.3: Measured Points on Reflector (mm)

Point No.	X	Y	Z
0	0.0002	0.0002	0
1	24.9965	0	48.0019
2	49.9995	0	42.0219
3	75.0001	0	32.0425
4	100.045	0	18.094
5	120.1055	0	4.081
6	17.6794	17.9777	48.0383
7	35.389	35.389	42.1724
8	53.1968	53.1968	32.506
9	70.9233	70.9233	18.4934
10	84.8845	84.8845	4.0021
11	0	24.9988	48.0164
12	0	50	42.034
13	0	75.027	32.0799
14	0	100.027	18.0893
15	0	120.0962	4.0688
16	-17.6777	17.1677	48.0232
17	-35.4026	35.4026	42.2328
18	-53.2751	53.2751	32.7368
19	-71.078	71.078	18.8353
20	-85.1715	85.1715	4.5304
21	-24.9986	0	48.0146
22	-50.0071	0	42.0459
23	-75.0407	0	32.1085
24	-100.0765	0	18.1432
25	-120.1875	0	4.1877
26	-17.6798	-17.6748	47.9979
27	-35.3812	-35.3812	42.1381
28	-53.1891	-53.1891	32.4835
29	-70.8955	-70.8955	18.432
30	-84.824	-84.824	3.8906
31	0	-24.9989	48.0165
32	0	-49.991	41.9953
33	0	-74.9974	32.0182
34	0	-100.0131	18.044
35	0	-119.9726	3.9079
36	17.678	-17.678	48.0263
37	35.3995	-35.3955	42.2188
38	53.2477	-53.2477	32.6561
39	71.0404	-71.0404	18.7521
40	85.125	-85.2542	4.205

The spring-in of the reflector is calulated by finding the difference between measured coordinates of mould and reflector. This can be called as deviation as shown in Table

5.4.

Table 5.4: Deviation in Measured Points from Original (mm)

Point No.	X	Y	Z	Magnitude of Deviation
0	0	0	0	0
1	0.0002	-0.0002	-0.0216	0.021601852
2	-0.009	-0.0003	-0.0509	0.051690425
3	-0.0121	-0.0002	-0.0671	0.068182549
4	-0.0556	-0.0002	-0.1104	0.123610517
5	-0.1131	-0.0001	-0.1708	0.2048518
6	-0.0055	-0.3039	-0.0699	0.311883744
7	-0.0097	-0.0095	-0.0694	0.070715628
8	0.009	0.0096	-0.0067	0.014766516
9	0.0193	0.0203	0.0133	0.03100758
10	0.0219	0.0221	0.0157	0.034849821
11	-0.0002	-0.0041	-0.0474	0.047577411
12	-0.0004	-0.0186	-0.0905	0.092392478
13	-0.0005	-0.0563	-0.1399	0.150804343
14	-0.0005	-0.068	-0.1528	0.167248587
15	-0.0005	-0.1466	-0.214	0.25939894
16	0.0028	0.5068	-0.0495	0.509219334
17	0.0229	-0.021	-0.1213	0.125216213
18	0.0755	-0.0668	-0.2322	0.253138954
19	0.1388	-0.13	-0.3215	0.373534055
20	0.2686	-0.2669	-0.5167	0.640593834
21	0.0004	-0.0001	-0.0267	0.026703183
22	0.013	-0.0002	-0.0649	0.066189501
23	0.0468	-0.0001	-0.1214	0.130108455
24	0.0776	0	-0.1449	0.164370831
25	0.178	0.0001	-0.2552	0.311144741
26	0.0023	-0.0027	1E-04	0.003548239
27	-0.0075	-0.0072	0.0142	0.017599148
28	-0.0326	-0.0315	0.0825	0.094134266
29	-0.0856	-0.0843	0.1723	0.210050327
30	-0.1346	-0.1342	0.2258	0.295148166
31	0	-0.0012	-0.0158	0.015845504
32	0.0001	-0.0114	0.0126	0.016992057
33	0.0002	-0.0138	0.0054	0.014820256
34	0.0004	-0.0198	0.008	0.021358839
35	0.0005	-0.0776	0.0779	0.109956446
36	-0.0007	0.0006	-96.023	0.029614355
37	-0.0098	0.0083	-0.0718	0.072939495
38	-0.0215	0.0312	-0.0998	0.106750785
39	-0.062	0.072	-0.1707	0.195362458
40	-0.1746	0.3069	-1079	0.369208857

Chapter 6

Study of Curing Process on Dimensional Stability of L-Shape Component

Experiments were performed to study the effect of engraving on the manufactured L-shape Carbon Fibre Reinforced Polymer (CFRP) component.

6.1 Laser Engraving on Mould Material

Laser engraving is performed on two different location of aluminium mould. The engraving is shown in Figure 6.1 and 6.2

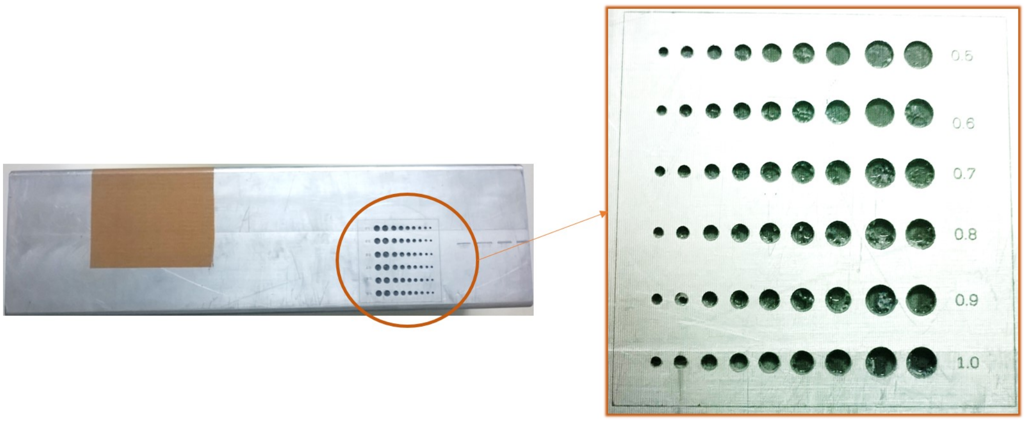

Figure 6.1: Laser Marking on Mould at First Location

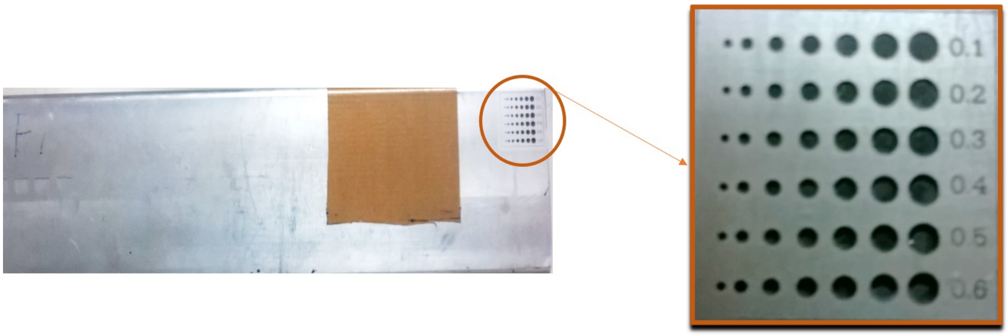

Figure 6.2: Laser Marking on Mould at Second Location

From Figures 6.1 and 6.2 it can be seen that different diameter holes with varying depth are engraved. In Figure 6.1 diameter varies from 1 mm, 1.25 mm, 1.5 mm, 1.75 mm, 2 mm, 2.25 mm, 2.5mm, 2.75mm and 3mm with the depth varying from 0.5 mm, 0.6 mm, 0.7 mm, 0.8 mm, 0.9 mm and 1 mm. Similar kind of engraving has been performed on second location as shown in Figure 6.2. It has diameter sizes 0.5 mm, 1 mm, 1.25 mm, 1.5 mm, 1.75 mm, 2 mm with depth varying from 0.1 mm, 0.2 mm, 0.3 mm, 0.4 mm, 0.5 mm and 0.6 mm.

6.2 Experimental Procedure for Curing of L-shape Composite Part

Prepreg layers are cut into desired shape as shown in Figure 6.3. These prepreg layers will be laid onto the mould for conducting experiment. Release agent and PTFE release film is applied on mould to check its impression on composite part which is to be manufactrured.

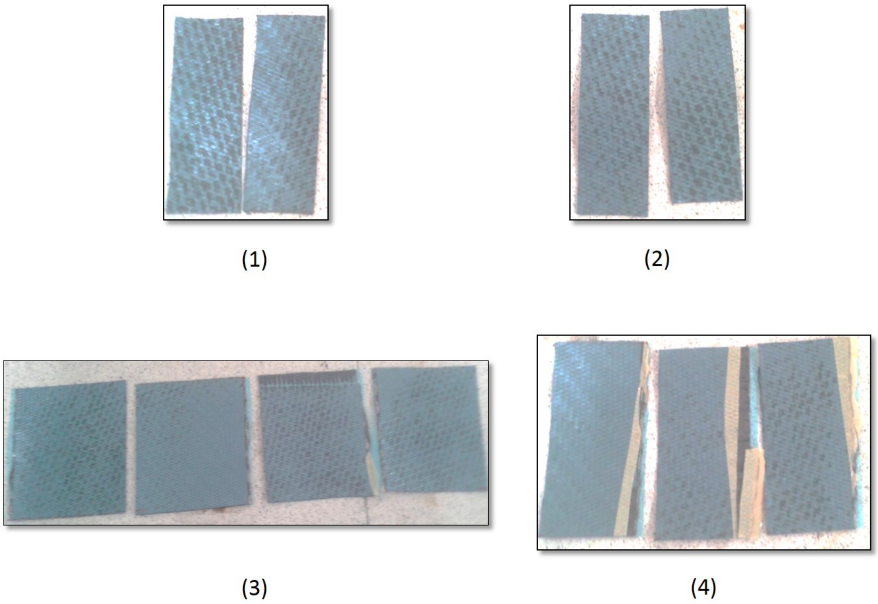

Figure 6.3: cutting prepregs

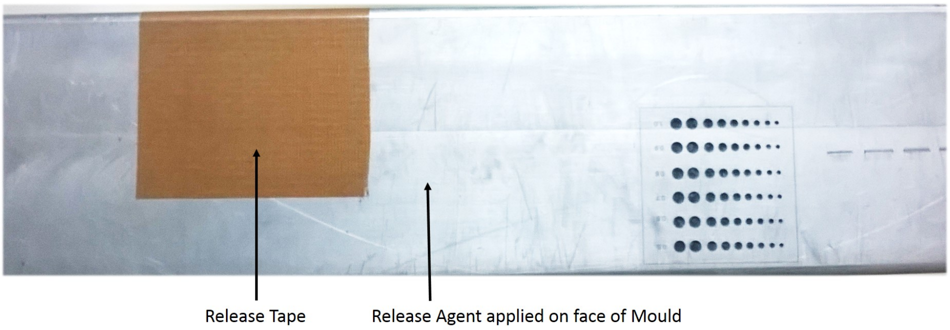

Figure 6.4: Release Tape & Release Agent on Mould

6.2.1 Layup of Prepreg on Mould

Different layers of twill prepregs are laid on 4 locations (1), (2), (3) and (4) as shown in Figure 6.5. The description of each as follows,
(1) In this region, on one of the face laser marking is done and the size of marking is shown in Figure 6.2. The tool surface beneath is treated with release agent to avoid sticking of prepregs during curing process. Two layers of prepregs are laid on this location.Using this configuration effect of laser engraving is studied.
(2) In this region, over the mould release tape is applied. Two prepreg layers are then laid on it. In this configuration effect of release tape on composite part surface is studied.
(3) In this region surface of mould is treated with release agent and three layer of prepreg are laid. In this configuration effect of release agent on composite part surface is studied.

(4) In this region, on one of the face laser marking is done and the size of marking is shown in Figure 6.1. The mould surface beneath is treated with release agent. Three layers of prepregs are laid on this location. Using this configuration effect of engraving is studied.

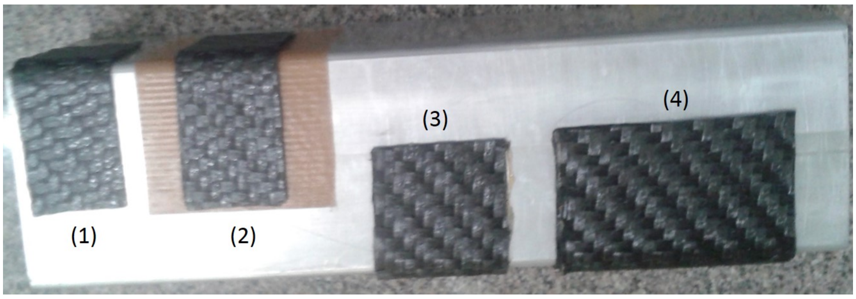

Figure 6.5: Prepreg Layup

After the prepreg layup on mould, vacuum bagging of the mould was performed. Peel ply and breather cloth is laid inside the bag for soaking the extra resin bleeded duirng the curing process in the oven.

Figure 6.6: Vacuum Bagging and Curing Process

The whole assembly kept in the oven for curing.The temprature of 160^0C is set in the oven and kept for four hours in the oven to complete the curing process. After that assembly is taken out from oven and kept it for cooling upto room temperature.

6.3 Demouding process

Consolidation material has been removed and composite parts are recovered from the aluminium mould as shown in Figure 6.7.

Figure 6.7: CFRP L-shape Cured Parts

6.4 Results

The results obtained are as follows,

1. The impressions on composite have been successfully obtained due to engraving at both the locations as shown in Figure 6.8. Figure 6.8 (a) shows the results of engraving at first location and (b) shows the results at second location.

2. Different surface finish have been obtained with release agent and release film as shown in Figure 6.9 (a) and (b) respectively. Composite part which is laid on release tape have some waviness on its interacting surface and on the other hand composite part laid on the surface treated with release agent has smoother surface.

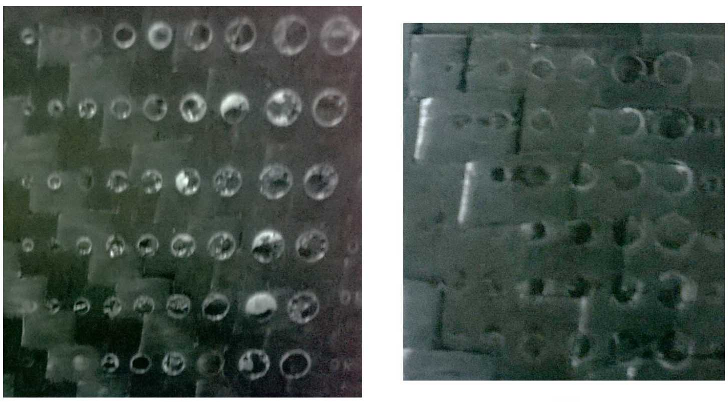

(a) (b)

Figure 6.8: Engraving Impressions on Manufactured Composite Parts

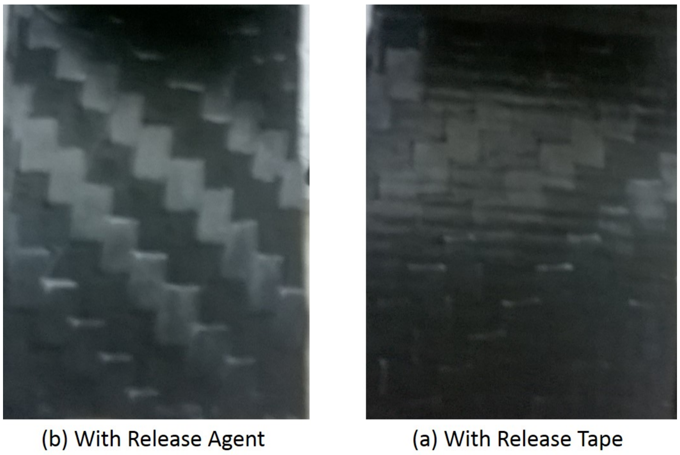

Figure 6.9: Surface Conditions of Manufactured Composites with Release Agent and Release Tape

Chapter 7

Process Modelling

Inefficiency of traditional trial and error approach for tool compensation for minimization of Process induced deformation leads one use process simulation. These process simulation can be used for the prediction of post cure deformation in resin based compsoites of any size and shape. A typical curing process simulation can be performed by incorporating the material models in the Finite Element Analysis (FEA) in the form of codes. Some of these material models includes thermochemical model, resin flow model and stress-deformation models. This chapter reviews major developments in the modelling of autoclave processing.

7.1 Modelling Approach

The material has various parallel mechanisms taking place at a time. These parallel mechanisms makes the problem complex. This complex problem can be bifurcated into various components. This modelling approch can be called as integrated sub-model approach which was first applied by Loos and Springer [25]. Using this approach, a very complex problem is tackled by dividing it into a series of simpler problems, each of which may be examined more or less independently. As illustrated in Figure 7.1 , a model for composites processing may thus be divided into sub-models for such phenomena as heat transfer and resin cure (a 'thermochemical model'), flow of the matrix resin (a 'flow model'), residual stress and deformation (a 'stress model'). A complete process cycle may be divided into a large number of small 'time steps' during each of which one or more of the program sub-models is solved to update predictions for the modelled parameters. FEM can be used in each sub-model to solve the governing equations. The sub-model approach can be explained in a form of flow chart as shown in Figure 7.1.

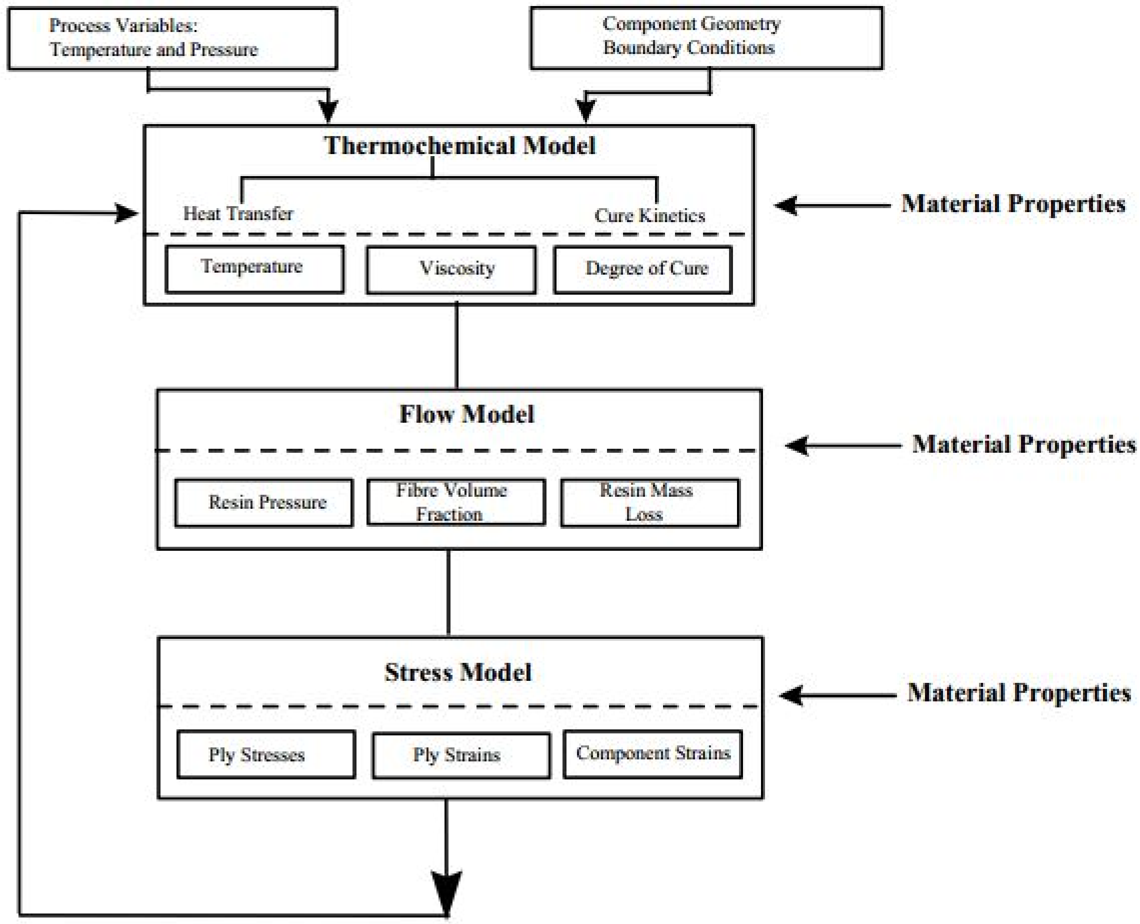

Figure 7.1: Flow Chart Illustrating Sub-Model Approach Applied to a Problem of Composites Processing Modelling [12]

Generally, for composite manufacturing, the process can be divided into three independent sub-models: heat transfer and cure kinetics, flow and compaction, and stress development as shown in Figure 7.1. The material property models as well as the process variables are the external inputs of the sub-analyses. The coupling of the sub-model is ensured by using the output of one sub-model as input for the following sub-model.

7.2 Thermochemical Models

The thermochemical model analyse essentially the heat transfer from the surrounding air to tool and composite part layup assembly. Further, the heat generated from within the part due the exothermic chemical reaction that takes place in the curing resin is also considered. This thermochemical analysis can be used to predict lag in the temperature between the air temperature and the part or tool temperature, temperature gradient within the part, as well as the temperature rise (due to the exothermic reaction) wherein the part temperature exceeds the surrounding air temperature. This analysis requires the orthotropic material properties for the composite part such as, resin thermal conductivity, specific heat capacity, resin heat of reaction etc. The material properties are updated at every solution step to account for the progression of cure and subsequent change in thermal properties.

Thermochemical models generally consist of a combination of 'sub-models' for heat transfer and resin reaction kinetics. In most analyses, these sub-models are treated as 'uncoupled' during individual timesteps of the transient solution [28]. Thus[28], cure reaction and heat generation rates are assumed constant during the time step. This approximation is quite good if time steps are small and allows a more flexible, simpler and less time-consuming computational approach than a more rigorous 'coupled' analysis.

7.2.1 Heat Transfer Modelling

The governing equation of the heat transfer sub-model is the transient Fourier anisotropic heat conduction equation, with a heat generation term from the exothermic resin cure reaction

$$\partial(\rho C_p T)/\partial t = \nabla(k\nabla T) + \dot{Q} \tag{7.1}$$

Where,
ρ =Composite Density.
C_p =Specific Heat.
k =Anisotropic thermal conductivity.
$\dot{Q}$=Resin reaction heat generation rate during the exothermic chemical reaction.
The parameters given in Equation (7.1) (ρ, C_p, k) can be calculated from the fiber volume fraction (V_f), and from the measured data such as properties of resin and fiber material. $\dot{Q}$is related to resin cure kinetics as follws,

$$\dot{Q} = \rho H_T \frac{\partial\alpha}{\partial t} with \frac{\partial\alpha}{\partial t} = f(\alpha, T) \tag{7.2}$$

the cure rate can be described by various cure kinetics model.
Initial conditions are then applied to the temperature and the degree-of-cure
At t=0, T=T_0, and $\alpha = \alpha_0$
Different boundary conditions such as convective, adiabatic or prescribed temperaure can be applied at the external surface of the system,

$$k\frac{\partial T_s}{\partial x} + h(Ts - T(t)) = 0 \tag{7.3}$$

where $T_s$and $\frac{\partial T_s}{\partial x}$are the temperature and the normal derivative of the temperature at the external surface,h is the convective heat transfer coefficient and $T(t)$ is the cure cycle applied during the process.

An incremental finite element method is then employed to solve the heat transfer equation with the applied initial and boundary conditions. Thus, the heat transfer analysis computes the variation of degree-of-cure in the laminate and the change of temperature in the laminate and the mould using the material properties and the process cure cycle.

7.2.2 Resin Cure Kinetic Modelling

The second major component of composites thermochemical models is the sub-model for resin reaction kinetics. The cure process for a thermosetting resin is a very complex, involving a series of chemical reactions which ultimately result in the conversion of low molecular weight monomers into a highly cross-linked macromolecular structure.

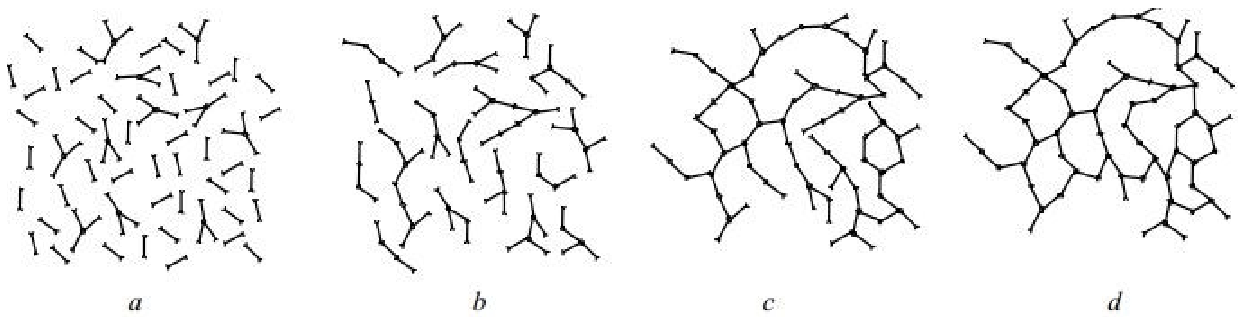

Figure 7.2: Cross-linking of Polymers During Curing [12]

The description of Fig. 3.2 is as follows,
a) Prepolymer and curing agent prior to cure,
b) Curing started and molecular size increasing,
c) Gelation achieved making continuous network,
d) Fully cured polymer

Heat transfer and Cure rate equations are interdependent with each other due to dependence of the rate of resin cure on its temperature and the exothermic nature of the reaction. The extent of chemical reaction is represented by measure of degree of cure of polymer which is denoted by symbol α .
Degree of cure α can be defined as,

$$\alpha = \frac{1}{H_R}\int_0^1 (\frac{dq}{dt})dt \tag{7.4}$$

where,
$\frac{dq}{dt}$= heat generation rate in resin,

H_R= total amount of heat evolved during complete reaction,

α can be determined by conducting experiments by using differential scanning calorimeter (DSC)

The heat generation can be defined from

$$Q = \frac{d\alpha}{dt}(1 - V_f)\rho_r H_R \tag{7.5}$$

where,

$\frac{d\alpha}{dt}$ =cure rate,

ρ_r=resin density

Most cure models employ Arrhenius type equations, with the rate of reaction expressed as some function of degree of cure and temperature. Commonly used semi-empirical expression for autocatalytic amine-cured epoxy system as per Scott [26] as follows

$$\frac{d\alpha}{dt} = \left(K_1 + K_2\alpha^m\right)(1 - \alpha)^n \tag{7.6}$$

and

$$K_i = A_i exp\left(-\Delta E_i/RT\right) \tag{7.7}$$

where,

ΔE_i= Activation energies,

R = Universal Gas constant,

A_i, m, n= Experimentally determined constants for a given material.

Empirical expression for material do not experience autocatalyzation as follows,

$$\frac{d\alpha}{dt} = K_1 (1 - \alpha)^n \tag{7.8}$$

and expression for mechanistic model

$$\frac{d\alpha}{dt} = K_1 (1 - \alpha)^l + K_2\alpha^m (1 - \alpha)^n \tag{7.9}$$

In virtually all practical cases, whether models are mechanistic, semi-empirical or empirical, equation constants and activation energies must be arrived at experimentally. These constants are most often determined using isothermal and/or dynamic DSC measurements and various curve-fitting techniques.

7.2.3 Flow and Compaction Modelling

As discussed in Hubert [27], in the autoclave process flow of the matrix resin is induced to remove excess resin from the laminate, promote bonding between plies, and collapse any voids within the laminate. This flow process may also play an important role in the development of residual stress and deformation. Even in flat laminates, non-uniform resin distribution through the part thickness may develop due to an imperfect compaction process. This will result in variations in not only local material strength, but also in thermal and resin cure shrinkage strains. These non-uniform strains can lead to the development of residual stress and component warpage.

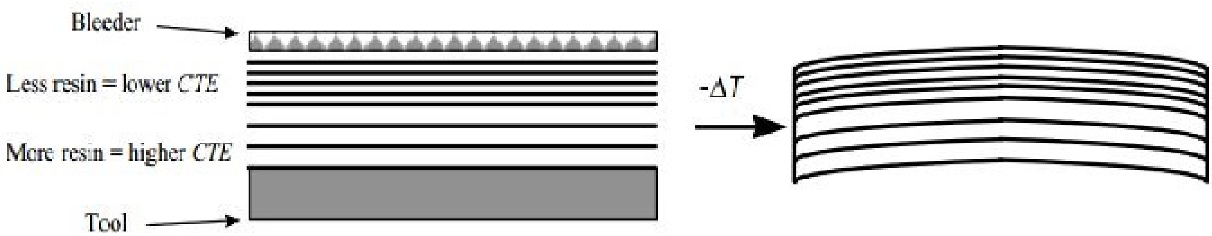

Figure 7.3: Warpage of a Initially Flat Laminate Due to Flow-Induced Uneven Resin Distribution [12]

When using increasingly-common ‘no-bleed’ resin systems, resin distribution problems due to imperfect compaction are of less concern. However, even with these material systems, uneven resin flow may be induced by pressure gradients that develop in curved or tapered sections and at laminate edges. As demonstrated by Hubert [27] and illustrated in Figure 7.4, this may result in variations in local part thickness as well as resin pooling’, both sources of process-induced stress and warpage.

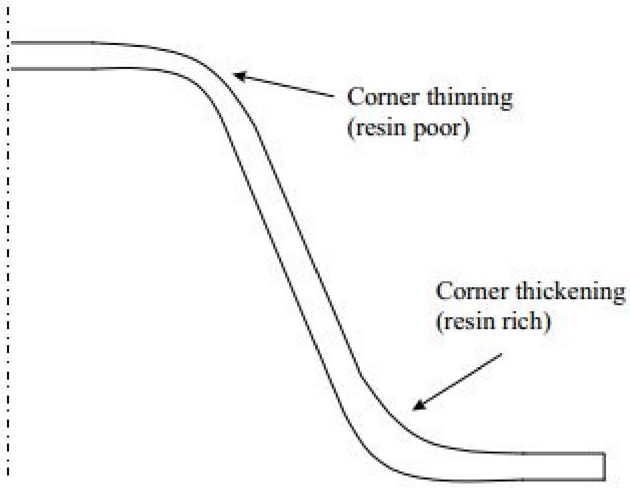

Figure 7.4: . Illustration of a Part Cross-Section Showing Resin Rich and Resin Poor Regions Caused by Uneven Resin Flow [27]

Another important consequence of resin flow, completely separate from the issue of stress or warpage, is its effect on component thickness. For even a moderately thick component, only a small relative amount of resin movement is required to induce several thousandths of an inch change in component dimensions. In some cases, this level of variation may cause problems when joining components even more severe than those caused by warpage (warped components can often be simply forced-to-fit). The typical autoclave process as discussed in section 1.10.1 uses the cure cycle which is shown in Figure 7.5.

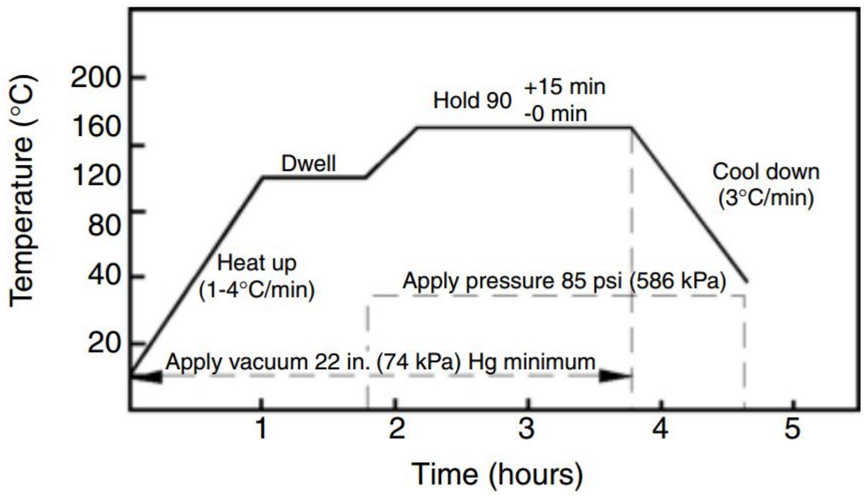

Figure 7.5: Curing Cycle Example for Autoclave Process

Heat supplied during autoclave process is to start the curing process because thermoset polymers requires some energy to initiate the chemical reaction. The pressure given during the curing in autoclave to escavate the excess resin from uncured composite laminate. In the presence of temperature and pressure, resin flows normal to the plane of laminate, parallel to the laminate, or some other combination of the two. The amount of resin flow in these directions depends on the width-to-thickness ratio of the part, edge constraints, and bleeder arrangements. The prepreg motion is shown in Figure 3.6 during resin flows in only normal direction. First the top layer starts moving and then it starts to squeez excess resin from the first and second prepreg layers, as shown in the Figure 3.7. In the next phase, the first and second layers move toward the third prepreg layer which removes excess resin between the second and third layers. This phenomena also occurs for other layers.

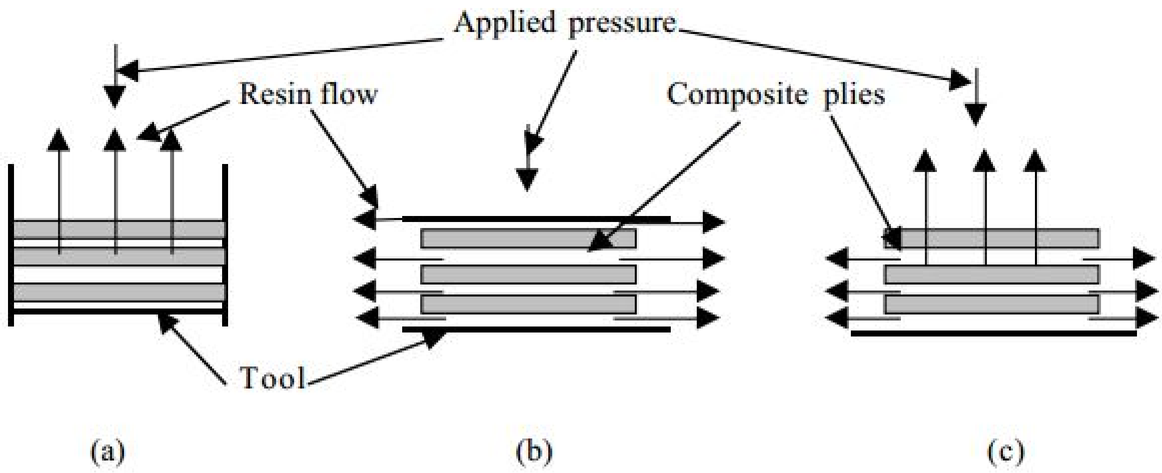

Figure 7.6: Resin Flow Description For Three Cases During Autoclave Process: (a) Flow Normal to the Plies, (b) Flow Parallel to the Plies, and (c) Flow in Both Directions. [1]

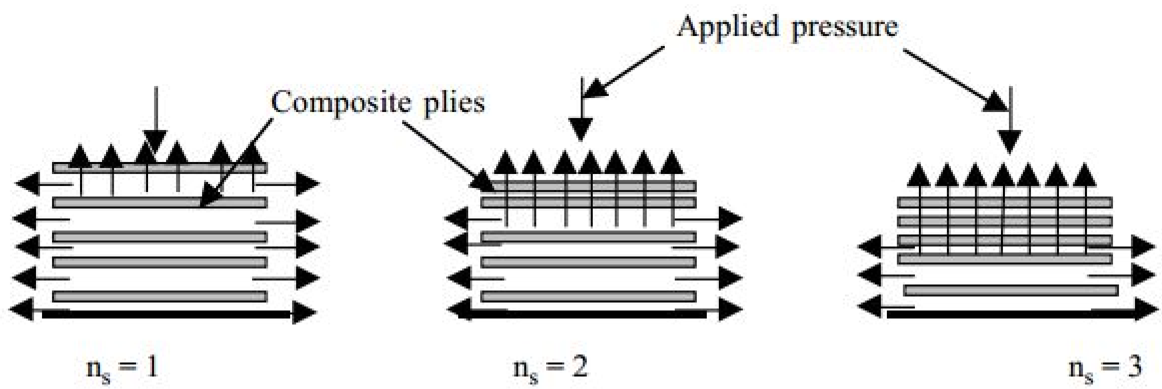

Figure 7.7: Resin Flow Motion for Both Normal and Parallel to the Tool Plate Directions.[1]

Uniform ply movement will be there if resin flow is only in parallel direction. Springer and Loos [25] developed models to represent these three modes of resin flow with the assumption that fibers do not touch each other.

In this analysis, both the behaviour of the composite constituent, the resin and the reinforcement have to be considered. The general approach to model the resin flow through the fibre reinforcement is to consider it as flow through a porous media using Darcy's law.

$$\overrightarrow{V} = -\frac{\widetilde{K}}{\mu}\nabla P \tag{7.10}$$

where $\overrightarrow{V}$ is the Darcy velocity vector, μ is the resin viscosity, $\widetilde{K}$ is the permeability tensor of prepreg and ∇P is the pressure gradient. The resin viscosity is the function is a function of the degree of cure and temperature. The Darcy velocity vector is related to the resin velocity vector $\overrightarrow{v}$ as follows,

$$\overrightarrow{V} = \Phi\vec{v} \tag{7.11}$$

where ϕ is the fiber bed porosity.

7.2.4 Stress and Deformation Models

Few analysis have been done for stress and deformation, other than final cool down stage. In Bogetti and Gillespie [28] and White and Hahn [9] no examination of residual stress was performed for entire cure cycle.

Stresses Development

The governing equations of the stress analysis are based on the classical laminated plate theory. Considering the laminate as a two-dimensional orthotropic material, the compliance relationship in the ply orientation can be written as follows

$$[\varepsilon_{ij}]_{(l,t)} = [S_{ij}]\,[\sigma_{ij}]_{(l,t)} \tag{7.12}$$

where the subscript "l" and "t" refer to the longitudinal and transverse directions, $[\varepsilon_{xyz}]$and $[\sigma_{xyz}]$are the laminate strains and stresses in the material directions. $[S]$is the compliance matrix expressed as follows,

$$[S_{ij}] = \begin{pmatrix} \frac{1}{E_t} & \frac{-\nu_{tl}}{E_t} & 0 \\ \frac{-\nu_{tl}}{E_l} & \frac{1}{E_t} & 0 \\ 0 & 0 & \frac{1}{G_{lt}} \end{pmatrix} \tag{7.13}$$

where "E_l"and "E_t"are the longitudinal and transverse moduli, "ν_{lt}"and "ν_{tl}"are the Poisson's ratio and "G_{lt}"is the shear modulus.

Types of Residual Stresses

Two types of stresses are generally characterized in composite residual stress analyses which are micro-mechanical stresses and macro-mechanical stresses. Micromechanical stresses are usually defined as those stresses that develop between the fibre and matrix as a result of such things as differences in thermal expansion strains, resin shrinkage during cure, and matrix swelling during moisture absorption. Due to the locally complex fibre and matrix arrangement within a ply, micromechanical stresses are highly variable even on a ply scale and difficult to evaluate. Thus the local effects of these stresses are difficult to assess directly, although they may be reflected in a reduction in composite ply strength. Fortunately, the moments induced by micromechanical stresses are generally very small and self-equilibrating over only a few laminae. Thus variations in micromechanical stress are generally not important in large-scale deformation. Macromechanical stresses originate on the larger scale of the ply and laminate. These stresses are the source of large scale dimensional changes, including warpage, as well as such problems as delamination and matrix cracking. Macromechanical stresses are generally calculated based on the assumption that individual plies can be treated as anisotropic (or transversely isotropic), but homogeneous layers. These stresses are thus usually assumed to vary continuously within each ply although they may be discontinuous between plies. Macromechanical stresses are effectively the 'weighted average' of the discontinuous local micromechanical stresses. A schematic representation of the relationship between microscopic, macroscopic, and overall laminate stress is shown in Figure 7.8 .

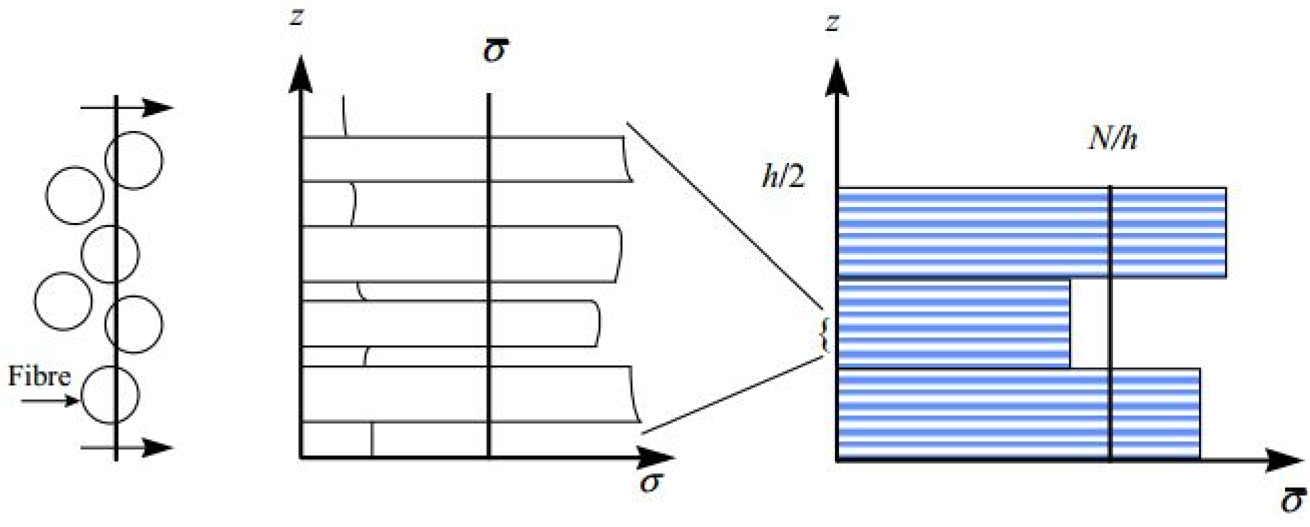

Figure 7.8: Micromechanical Stresses in Fibre and Resin [12]

Macromechanical stresses are easy to determine than micromechanical stresses and are more useful for prepdiction of laminate deformation.

Sources of Residual Stress and Deformation

Different processes leads to development of residual stress and deformation during autoclave process. A very simple way of categorizing and analyzing these processes is to distinguish individual residual stress and deformation 'sources' and 'mechanisms'. The stress source may be defined as the driving force for residual stress generation and mechnism can be the combination of these stress sources with behaviour of the used material.
Five main sources has been identified [12]

- Thermal strains,
- Resin cure shrinkage strains,
- Gradients in component temperature and resin degree of cure,
- Resin pressure gradients (resulting in resin flow),
- Tooling mechanical constraints.

Description of major sources as follows,

Thermal Strains

Due to increase in temperature during autoclave curing leads to thermal strains. Their is development of residual stresses due to mechanisms propagated by thermal strains which are as follows,

1. Anisotropic ply thermal strains

This is one of the major source of residual deformation in composite materials. . Thermal strains of prepreg plies are highly anisotropic. The majority of residual stress analyses are based on the assumption that this is the only source of process-induced stress and deformation [29]. In these analyses, stress is generally assumed to develop only during the cool-down process as the component temperature is decreased to room temperature from some assumed temperature. By using symmetric layup residual stress can be reduced. For curved sections, however, differences in strains in the through-thickness and in-plane directions will result in a change in part shape. This phenomenon, illustrated in Figure 7.9, is known as 'spring back'.

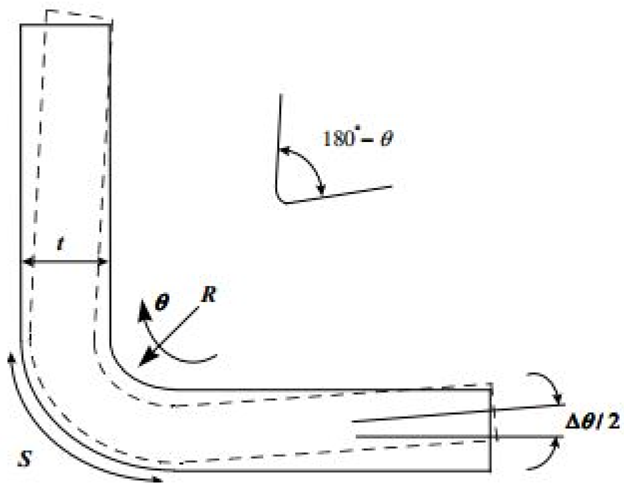

Figure 7.9: Thermal Strain Anisotropy-Induced Springback [12]

For the simple geometry shown in Figure 7.9, the magnitude of included angle change for a symmetric layup can be calculated using the following equation from Nelson and Cairns [36],

$$\Delta\theta = \theta \left[\frac{(CTE_\theta - CTE_R)\,\Delta T}{1 + CTE_R \Delta T} \right] \tag{7.14}$$

where,
$\Delta\theta$ =change in included angle,
θ= Original angle,
$CTE_\theta$and CTE_R= laminate thermal expansion coefficients in the circumferential and radial directions,
ΔT= Temperature Change
2. Thermal strain mismatch
Strain mismatch along with resin modulus of part and tool between components of the composite structure in also an important sources. This stress source has not been examined in previous autoclave processing models since none have included multiple types of materials in model stress calculations.

Resin Cure Shrinkage Strains

Cure shrinkage can be defined as reduction in volume and increase in density due to polymerization of thermosetting resin. Cure shrinkage results from the conversion of the weak van der Waals bonds between resin monomers into strong covalent bonds as a complex network structure is formed [30]. The much smaller interatomic spacing in covalent bonds compared to van der Waals bonds results in a decrease in overall resin volume as cure progresses. Transverse direction strain are much larger than strains in fiber direction. The effect of cure shrinkage on residual stress will be very similar to that of a decrease in part temperature and may be analysed in much the same way. Stress-free temperature is illustrated in Figure 7.10. Resin cure shrinkage will increase a component's stress-free temperature.

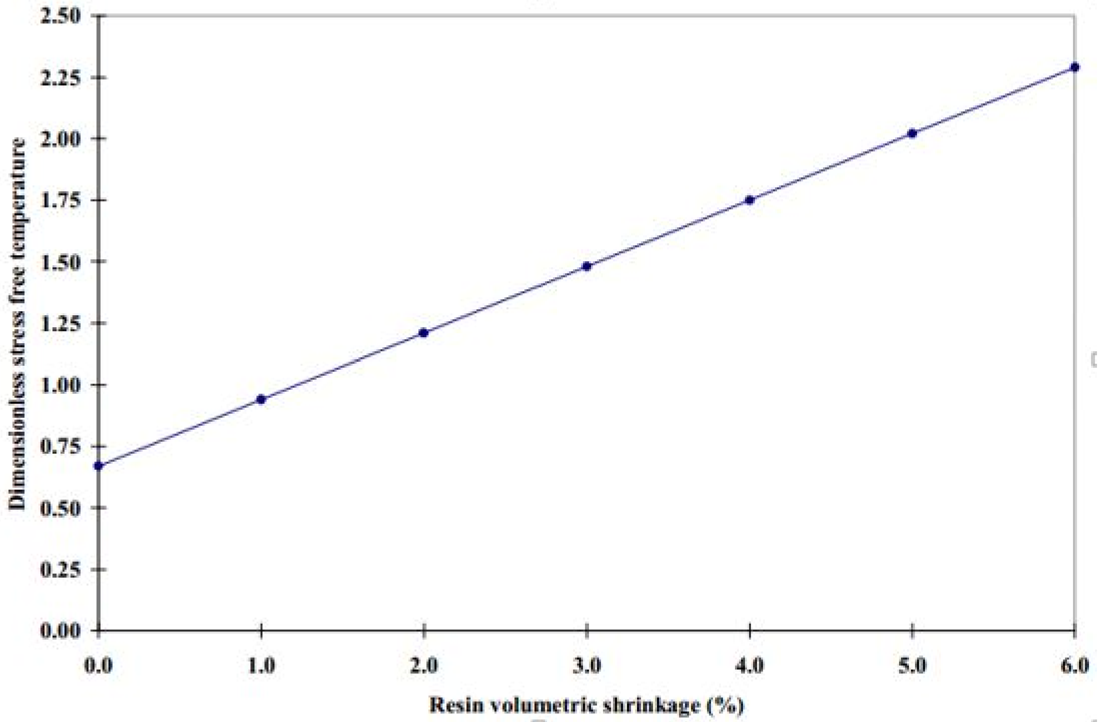

Figure 7.10: Predicted Influence of Resin Cure Shrinkage on Dimensionless Stress Free Temperature [12]

Process Tooling

The tools used affects components stress development in two ways one is by influencing the component internal temperature and other is mechanical constrains and loads applied at interface. Their can be through thickness variation due to different cooling and heating rates at tool and bag side. There are also normal and shear loads at tool-part interface.The Shear loads can be due difference in thermal expansions. These interface stresses are the source of inducing warpage. Loads normal to the tool/part interface are induced by such things as tooling restraint of component warpage. As shown in Figure 7.11 [12], the forces required to constrain warpage during the initial 'heat-up' phase of the process cycle will be small since the part is relatively compliant at this point in the process. By 'cool-down', however, the component is much stiffer and the tooling must exert much greater loads to prevent it from deforming. At the end of processing, therefore, a net normal load exists between the tool and part. Once the tooling is removed, component warpage results. If the component had been allowed to deform freely during both heat-up and cool-down, little warpage would have resulted (in the absence of cure shrinkage strains). No previous autoclave processing models have included analyses of tooling mechanical constraints.

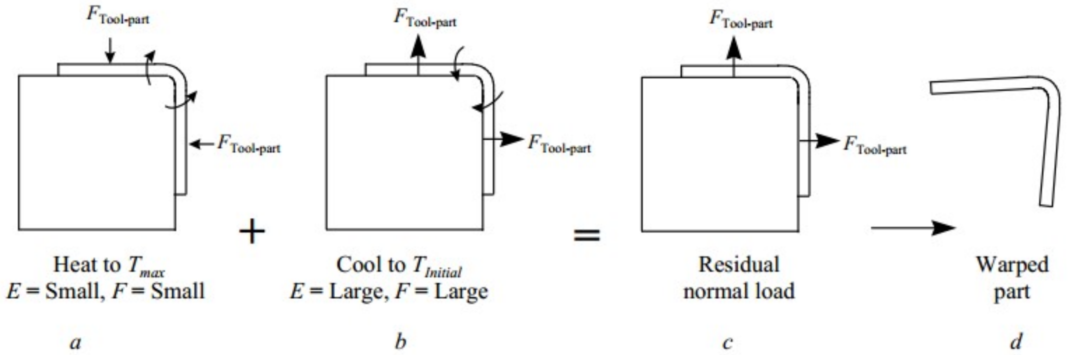

Figure 7.11: Contribution of Tooling Normal Loads to Process-Induced Deformation

Stages of process induced deformation are as follows,

a) Part heated to maximum temperature, tries to increase internal angle. Since part modulus is low, minimal force is required to maintain shape,

b) Part cooled to initial temperature, tries to decrease angle. Since modulus is now high, tooling loads are large,

c) Residual normal loads exist after reaching initial temperature,

d) Part is removed from tool. Relief of tooling loads results in springback.

7.2.5 Resin Mechanical Behaviour During Processing

One of the primary objectives of processing thermosetting composite materials is to transform the matrix resin from a low molecular weight semi-solid material to a highly-crosslinked macromolecular structure. As the resin undergoes this transition its effective elastic modulus increases by several orders of magnitude. Understanding and accurately modelling resin behaviour during processing is critical to understanding the development of residual stress and the roles played by the identified stress sources. Resin mechanical behaviour during processing includes study of stages of property development and stress generation stage.

Due to increase in temperature, resin conversion from semisolid to viscous form. As curing process progresses resin viscosity increases rapidly. It is convenient to divide the continuum of resin mechanical property development during processing into 3 stages as follows,

I. Purely viscous behaviour. During this stage, the low molecular weight resin is unable to support shear loads and thus develops no internal stress

II. Viscoelastic behaviour. After resin gelation, resin behaviour will be highly viscoelastic. Any stresses generated during this stage will decay to some degree.
III. Elastic behaviour. At this stage, the resin will undergo vitrification and mechanical response will become effectively elastic. The time at which this transition occurs depends on the process cycle and the development of resin Tg (glass transition temperature) with the progression of cure.
All these stages are shown in Figure 7.12 ,

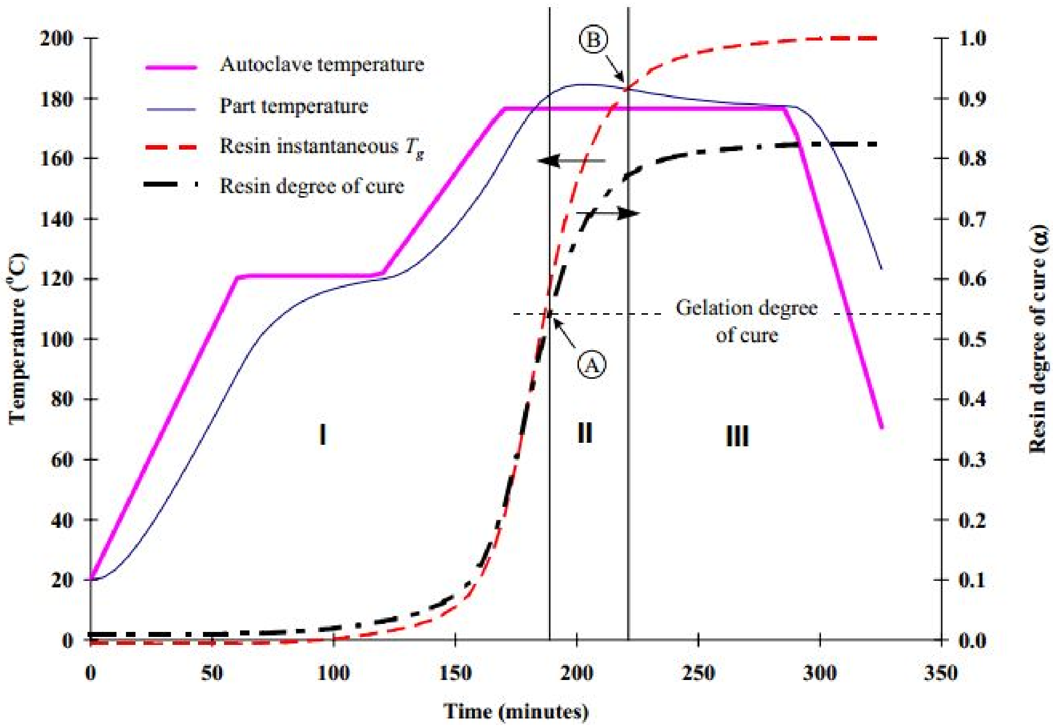

Figure 7.12: Stages in Resin Property Development for a Resin with a Glass Transition Temperature Greater than the Maximum Curing Temperature. [12]

7.3 Compro Component Architecture (CCA)

It is an add-on used along with Abaqus software used for conducting curing process simulation for shape and size of layered composite laminate. It is a subroutine allowing the interface between the material properties and the Abaqus finite element solver This add-on includes all the above process models discussed which are used as per defined prepreg system. This is a proprietary item of Convergent Manufacturing Technologies, Canada. Along with the add-on some commonly used composite prepreg properties are readily available in the software. To add the property of any other prepreg system any of the xml extension file can be modified by changing the values of constants written in the file. These constants can be obtained by characterizing the prepreg material.

7.3.1 CCA Model Documentation

The documentation contains [32] the details of models used for performing calculations. These models include which are as follows,

- Cure Kinetics in the composite part
- Cure Shrinkage
- Modulus Development
- Density
- Conductivity
- CTE
- Lumped Specific Heat Capacity
- Lumped CTE
- Lumped Density
- Umped Conductivity
- Permeability
- Poisson's Ratio
- Specific Heat
- Viscosity
- Fiber Bed Compaction

In these models, equations are mentioned along with its references. Out of different equations available required equations are used according to prepreg system used during analysis.

7.3.2 Compro Plug-in for Abaqus CAE

The Compro plug-in for Abaqus CAE is a graphical user interface that automates many commonly performed steps and guides the user in setting up the model using best practices. The Compro plug-in makes many changes to the input files when a job is submitted. These changes allow for, for example, a single model to be set up while up to three analyses are actually run.

7.3.3 Analysis workflow

The typical workflow for setting up a process simulation includes using built-in Abaqus CAE features along with automations performed by the Compro plug-in is shown in Figure 7.13 [32].

Workflow Step	Primary User Interface
1. Create the part and tool geometry	ABAQUS CAE
2. Add materials	**COMPRO plug-in**
3. Create and assign sections	ABAQUS CAE
4. Assign material orientations	ABAQUS CAE
5. Create the assembly	ABAQUS CAE
6. Define the analysis steps	**COMPRO plug-in**
7. Assign initial and boundary conditions	ABAQUS CAE
8. Mesh the geometry	ABAQUS CAE
9. Run the job	**COMPRO plug-in**
10. Post-process the results	ABAQUS CAE / **COMPRO plug-in**

Figure 7.13: Workflow of Curing Simulation

7.3.4 Modules in Compro

There are three modules in Compro plug-in which are as follows,

Thermo-Chemical Module

In this module thermo-chemical analysis takes place [33], task of this simulation is modeling the temperature distribution and history throughout a composite part and tool assembly during the cure cycle. This analysis considers heat transfer from surrounding autoclave or oven air to the part and tool as well as heat generation from within the part due to an exothermic cure reaction. A thermochemical analysis can be used to predict a temperature lag as shown in Figure 3.17 between the air temperature and the part or tool temperature, a temperature gradient within the part, and a temperature overshoot (exotherm) where the part temperature exceeds the air temperature due to the internal heat generation.

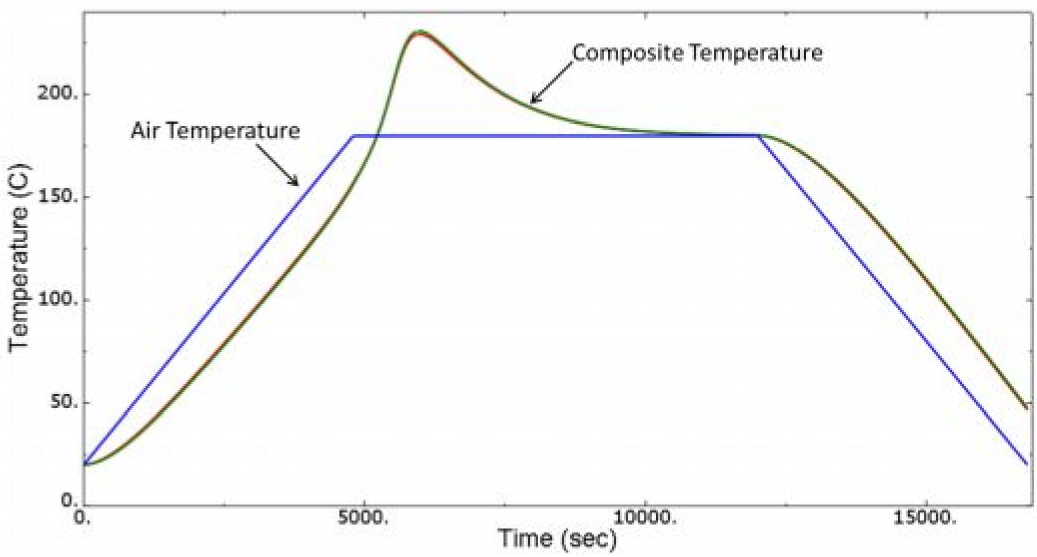

Figure 7.14: Thermo-chemical Analysis Prediction of Thermal Lag and Exotherm

Flow-Compaction Module

In flow-compaction analysis [33], the analyst is generally interested in modeling the migration and relative distribution of resin within the fiberbed of the composite. This resin migration may result in non-uniform fiber volume fractions and/or thickness variations. A flow-compaction analysis in process simulations considers the migration (or flow) of resin relative to an elastic, porous fiberbed. The curing composite material is idealized as a void free fibre bed fully saturated with a curing resin. The resin flow is governed by Darcy's law. The fibres are considered incompressible and the resin is considered as an incompressible newtonian fluid. The fiberbed stiffness and permeability are a function of the volume fraction. A flow-compaction analysis can be used to predict the distribution of fiber and resin volume fractions within the composite, the pressure load developed in the resin, or the change in laminate thickness in various regions of the composite. This type of analysis requires orthotropic material properties for the composite part. The material properties are updated at each solution step to account for the progression of cure and the change in volume fraction.

Stress-Deformation Module

A stress-deformation analysis [33]can be used to predict process induced deformations such as spring-in or warpage as well as residual stresses in the part due to self-constraints. These predictions can be used to define tool geometric compensations or to complement structural analysis. This type of analysis requires orthotropic material properties for the composite part. In Abaqus, the composite layup can be

defined directly. The material properties are updated at each solution step to account for the progression of cure and the subsequent change in thermo-mechanical properties.
All the three modules are shown in Figure 7.15.

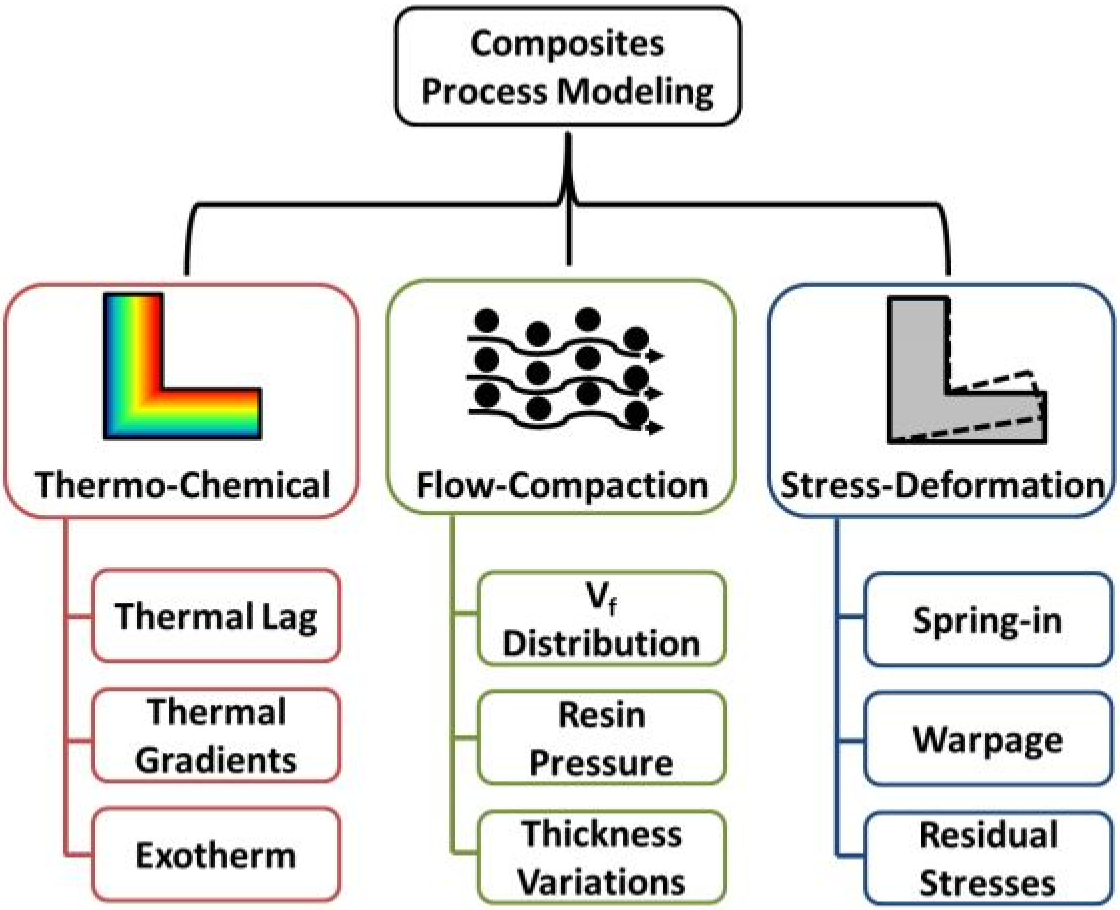

Figure 7.15: Modules in COMPRO[33]

7.3.5 Process Parameters

There are number of process parameters effecting warpage and spring-in of composite laminates. These parameters can be classified by extrinsic and intrinsic factors. Intrinsic factors can be anisotropic thermal expansion and resin cure shrinkage, and examples of extrinsic factors are Stacking sequence, part and tool geometry, cure cycle, types of tool material used, tool surface condition, and tool heat treatment.
Using the extrinsic parameters Design of experiment can be performed for getting the optimum number of experiments to be conducted. The parameters which we have to consider are layup sequence, tool material, cure cycles.

- Tool material: On the basis of Coefficient of thermal expansion mould material has been selected. According to the literature survey the mould material having least C.T.E. should be used. Out of the available materials four mould materials are selected which are Stainless Steel AISI 430, Graphite EDM Grade, Cast Iron Grade 30, Invar 36.

- Cure Cycles: There are two types of cure cycles single hold and double hold cycle. In single hold cycle there is single dwell for some duration and in double hold there are two dwell periods.
- Layup: For different layup sequence it is observed that different magnitude of warpage is noticed. The reason for this phenomena is change in mechanical properties according to stacking sequence of prepregs. By taking different layup sequence the results are obtained. These results will help us to draw the conclusion regarding effect of layup sequence on warpage or spring-in on curved laminates.

Chapter 8

Curing Process Simulation of L-shape 2D Laminate

Some sample runs are performed on L-shaped 2D laminate. The purpose of conducting the sample run is to validate our results with the results available in literature. This will ensure us that the methodology adopted is correct or not. And using this methodology laminates of any shape can be analysed. For carrying out the simulation Abaqus 14.1 [34] is used along with Compro plug-in.

8.1 Methodology

General Steps for performing Curing Process Simulation

1. Create the part and tool geometry in Abaqus Modeler.
2. Create sets and surfaces for the part.
3. Create sets and surfaces for the tool.
4. Assign materials and sections using Compro Plug-in for both tool and part.
5. Create an assembly of Tool and part and assign tool part interaction properties.
6. Assign Initial Conditions, Boundary Conditions and Loads.
7. Mesh the geometry.

Thermochemical Analysis Model Setup

1. Define an analysis step as Thermo-Chemical using Compro plug-in.
2. Assign heat transfer boundary conditions to tool and part.
3. Run the analysis using Compro plug-in. Check the status of analysis in Jobs.
4. Analyse and plot the required results.

Flow-Compaction Analysis Model Setup

1. Define the Flow-compaction analysis step using Compro plug-in.
2. Assign resin pressure boundary condition and pressure loads.
3. Run the analysis using Compro plug-in.
4. Analyse and plot the results.

Stress-Deformation analysis

1. Create the stress-deformation step using Compro plug-in
2. Deactivate the tool elements at tool removal step and the tool-part interaction.
3. Modify boundary conditions for the part at tool removal step.
4. Run the analysis using Compro plug-in.
5. Analyse and plot the results.

8.2 Sample Problem

8.2.1 Problem Statement

To determine the spring-in in L-shaped angle laminate. Consider prepreg system as Hexcel AS4/8552 and tool material as Aluminum 6061. Layup sequence of laminate is $[0/90]_{6s}$. Total thickness of laminate is 4.8 mm.

8.2.2 Solution

Modelling of the problem is performed in Abaqus along with Compro plug-in. Modelling and solution are as follows,

Modelling, Assembly and Boundary Conditions Modelling of part and tool are done in Abaqus. In the abaqus modeller, L-shape part and aluminium tool are created.

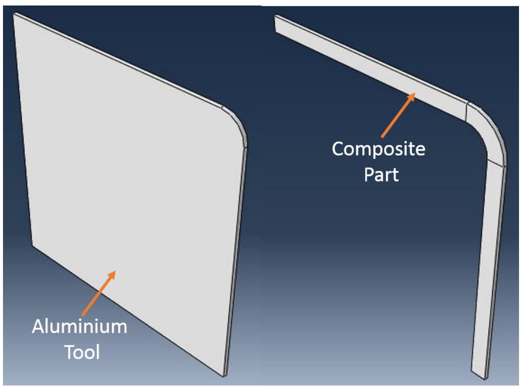

Figure 8.1: Part and Tool Geometry

Once the parts are created, respective material are assigned i.e., AS4/8552 prepreg system to compsite laminate and Aluminium 6061 to tool material. The stacking sequence is defined in solid, composite section. Only solid sections can be used for process modelling of composites since shell sections do not adequately represent the through thickness behaviour of the real composite. Tooling should generally be assigned solid homogenous sections. Material orientation is also assigned to different portion of the composite part. While assigning orientation 3-direction is kept in stacking direction and 1-direction is kept in 0^o fiber direction. For any curved portion in the part, cylindrical coordinate system is used with 3-direction as 0^o fiber direction and 1-direction as stacking direction. The material orientation on different portion of the composite part is shown in Figure 8.2, 8.3 and 8.4. The stacking direction is kept along the thickness and 0^ofiber direction is along direction-1.

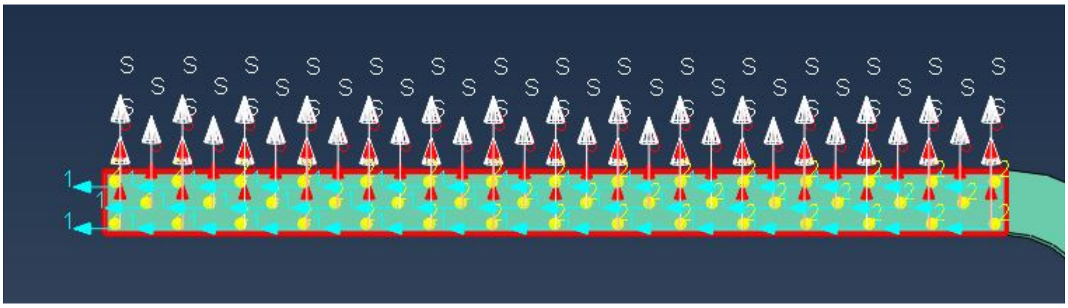

Figure 8.2: Material Orientation Assignment on Left Flange

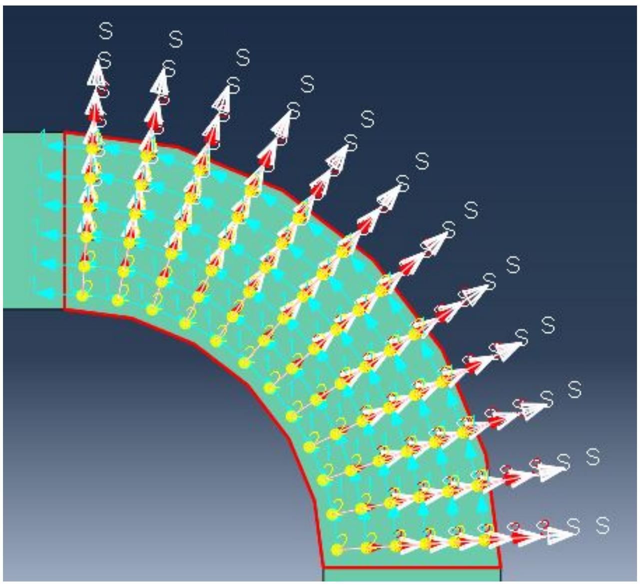

Figure 8.3: Material Orientation Assignment on Corner Portion

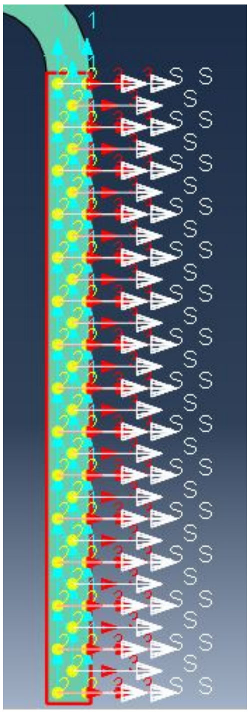

Figure 8.4: Material Orientation Assignment on Right Flange

In the actual practice laminate is laid on the tool before carrying out the autoclave curing. In abaqus this task can be accomplished by making assembly of both the parts as shown in Figure 8.5. The tool-part interaction properties can be given by defining coefficient of friction as 0.15 and shear stress limit between composite and aluminium tool interface as 40000 N/mm^2 .

After this Initial boundary conditions are assigned which are initial temperature and displacement boundary conditions to the respective surfaces. Now the meshing is done on both tool and composite laminate. For meshing 3D stress, quadratic (C3D20) element is used. It is a 20 noded element. This is a brick elements that include full integration, quadratic displacement have been shown to best capture the through thickness shrinkage strains during composite process modeling. The composite part and tool is meshed with 420 and 527 elements respecctively. The meshed parts are shown in Figure 8.6. Since for different module different element is used but compro solver has the capability to change the element type according to the type of analysis. The aspect ratio of elements should be as shown in Figure 4.2 [32]

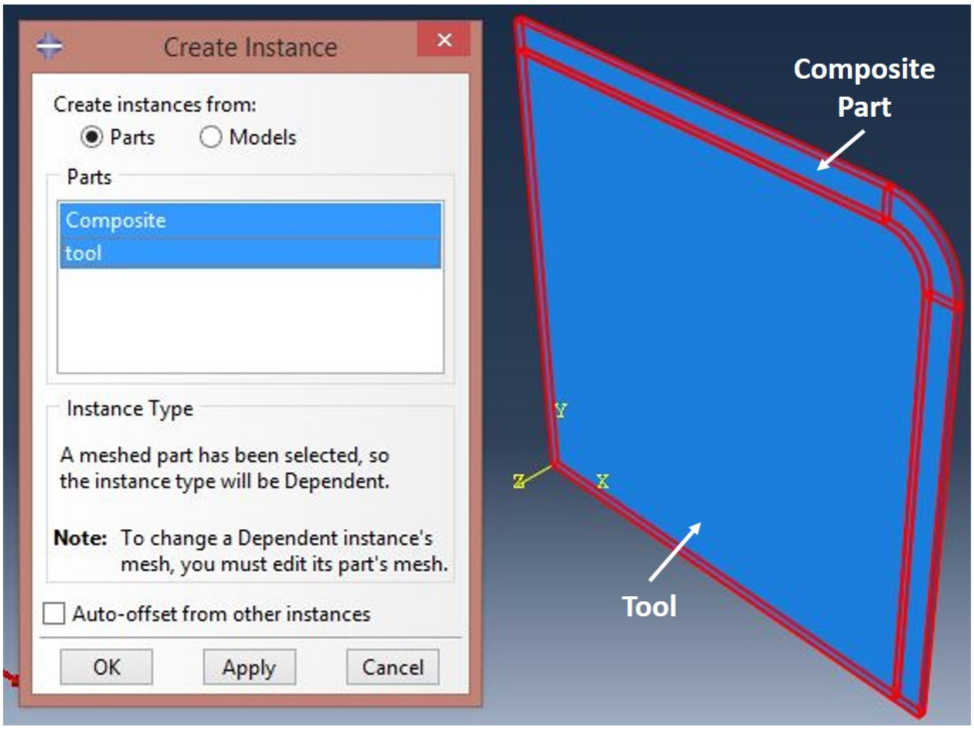

Figure 8.5: Assembly of Tool and Composite Part

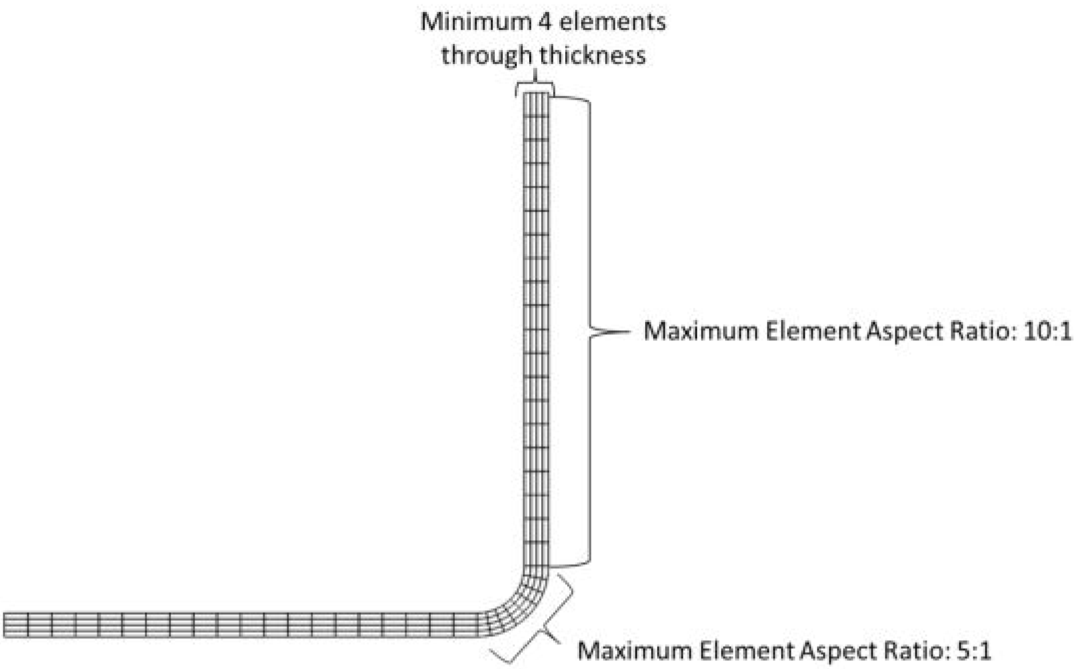

Figure 8.6: Element Aspect Ratio

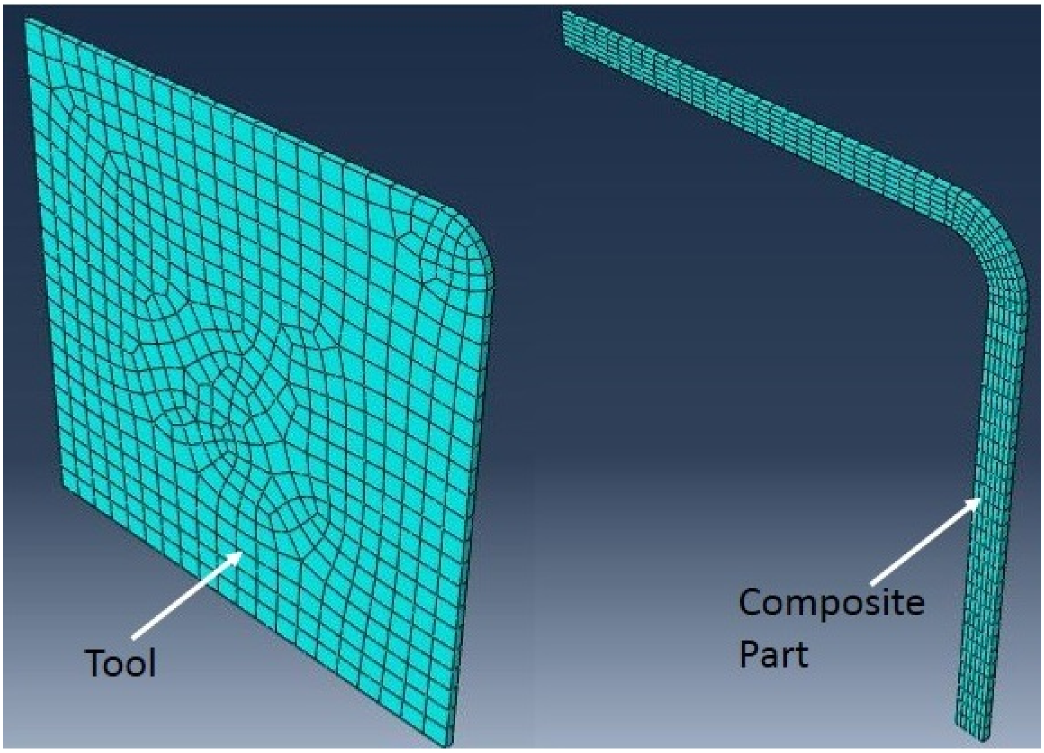

Figure 8.7: Meshed Tool and Composite Part

In the meshed composite part there are 6 element layers across the thickness which is shown in Figure 4.6. A single layer of element contains $[0/90]_s$ layup. All 6 elements stack makes the layup as $[0/90]_{6s}$ as shown in Figure 4.7.

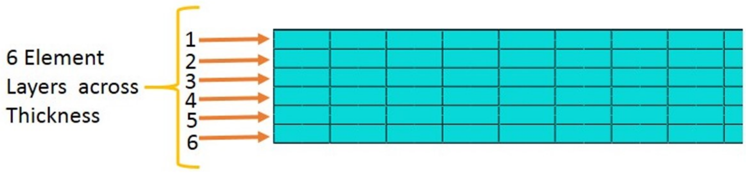

Figure 8.8: No. of Element Layers Across Thickness

Mechanical-displacement boundary conditions are applied for constraining the composite and tool in space and at the same time expansion or contraction of the tool and part should be allowed during the whole process cycle. This is accomplished by assigning the respective boundary condition to the surfaces of composite part and tool as shown in Figure 4.9.

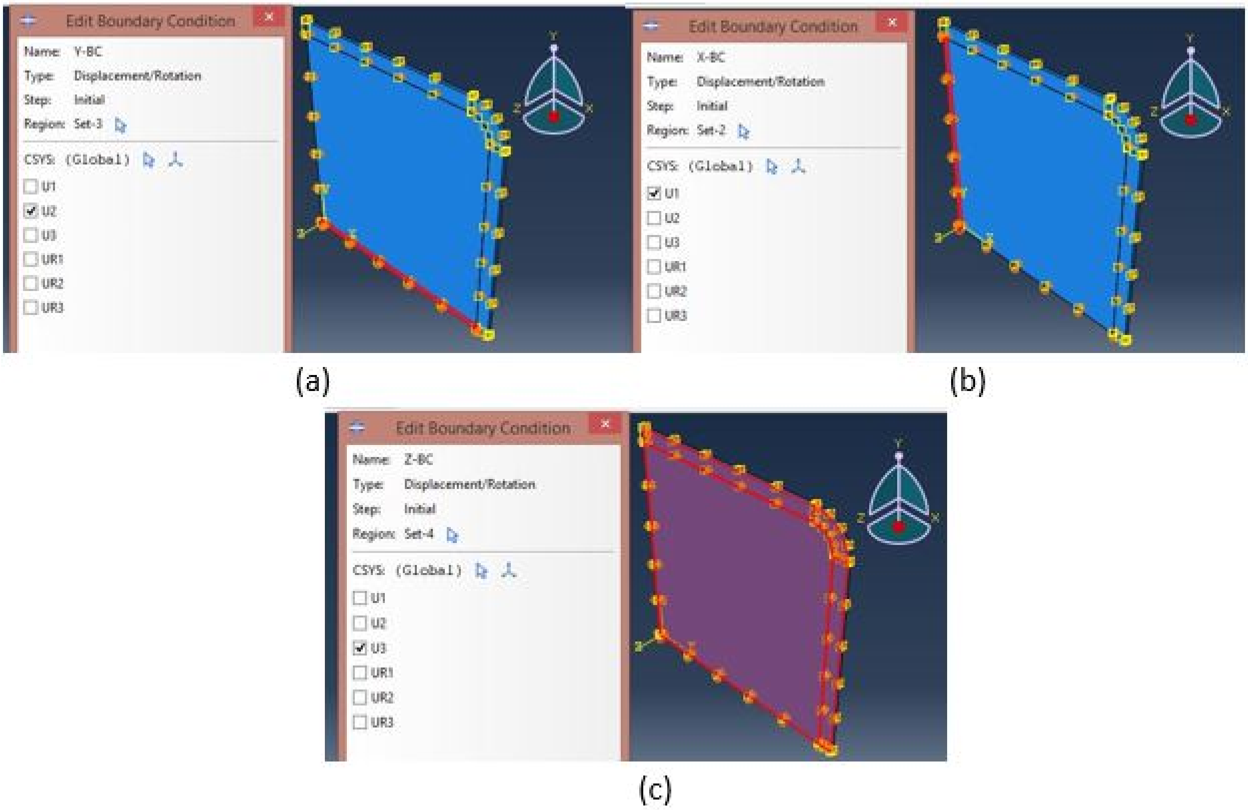

Figure 8.9: Boundary Constraint in (a) Y-direction (b) X-direction and (c) Z-direction

Thermochemical Analysis

For the thermo-chemical analysis, convective heat transfer boundary conditions are applied to the top and bottom surfaces of assembly while the edges are assumed to be adiabatic (no heat transfer). This will demonstrate the thermal lag of the composite material and the tool material relative to the applied temperature cycle due to heat transfer conditions. In addition, due to internal heat generation during cure, a temperature overshoot is shown. The results of the analysis will also act as input to subsequent stress-deformation. First of all thermo-chemical Step must be defined using Compro plug-in. For AS4/8552 prepreg system single hold curing cycle is recommended which is shown on figure. Its total curing cycle time is 24000 sec.

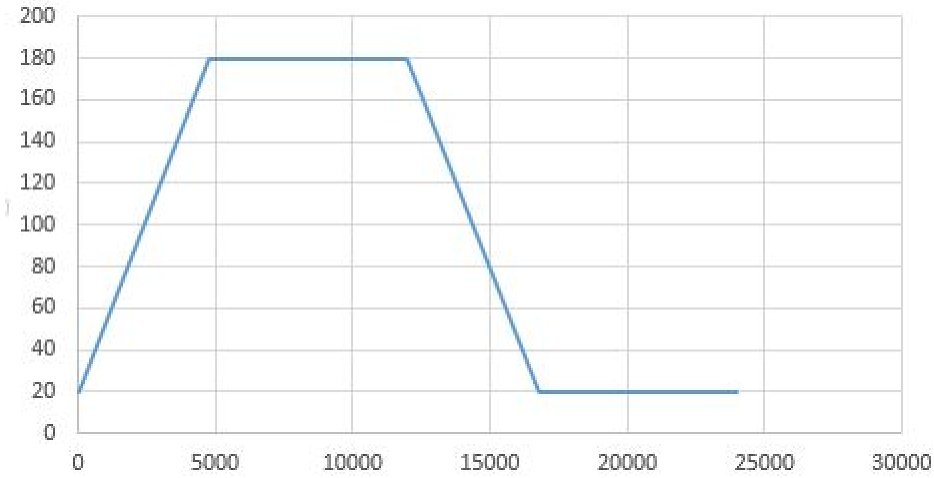

Figure 8.10: Single Hold Curing Cycle

In this analysis heat transfer coefficients (HTC) at top and bottom surface of assembly are defined, along with this cure cycle is also defined in the form of table of time and temperature amplitudes. Here top HTC is kept as 80 W/mK and bottom HTC is 20 W/mK.

Thermochemical Results:

Temperature gradient in the laminate for any step of analysis can be visualised. Temperature profile for step time 24000 sec is shown in Fig. 4.11.

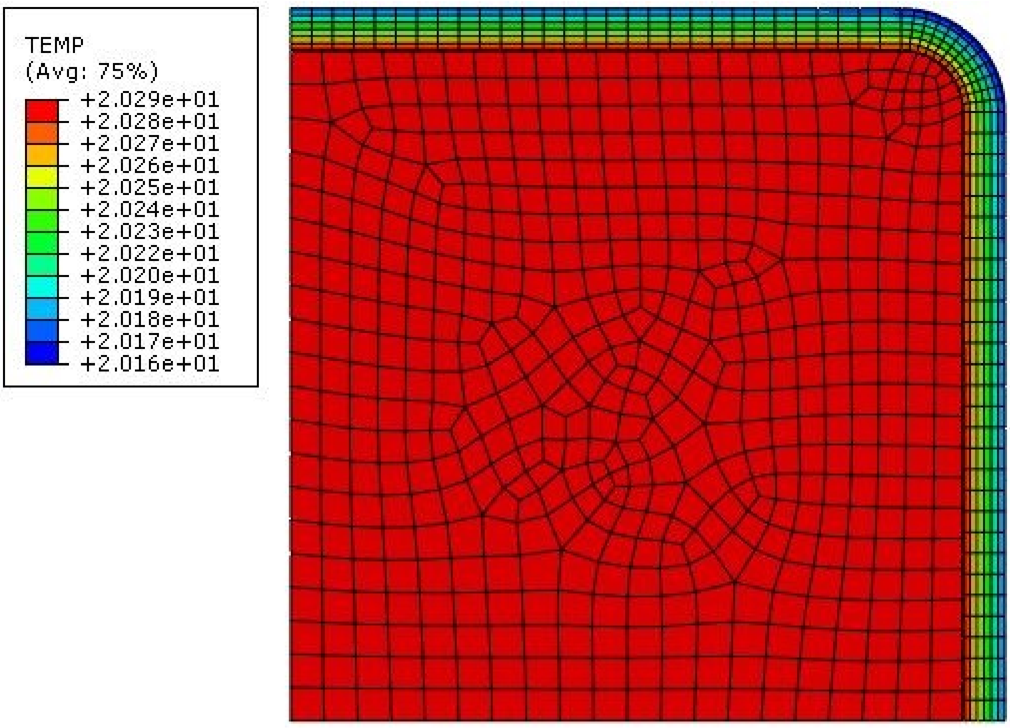

Figure 8.11: Temperature Contour

From the temperature contours it is confirm that there is a thermal gradient through the thickness of the part and tool. By changing the frame the direction of heat transfer and the interaction between the composite and the tool during heating vs. cooling segments of the air temperature cycle can be visualized.
Maximum and minimum temperature and degree of cure development can be plotted using Compro plug-in which is shown in Figure 4.12 and 4.13 respectively. From the plot the average maximum and minimum temperature curves can be obtained. The maximum and minimum temperature of a composite part shows that there is gradient exist in a part. The temperature gradient can also arise a gradient in DOC of a component which is shown in Figure. 10. In the Figure maximum (green curve) and minimum DOC (red curve) can be seen. This gradient depends on the thickness of laminate. More gradient in DOC will be there if component has greater thickness.

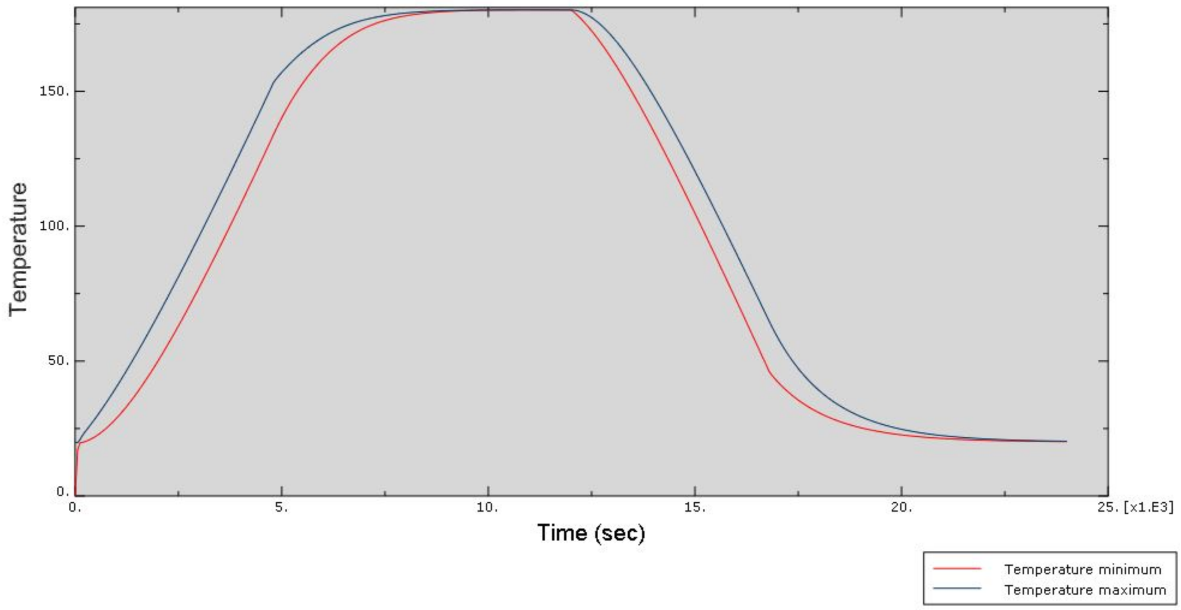

Figure 8.12: Temperature vs. Time plot

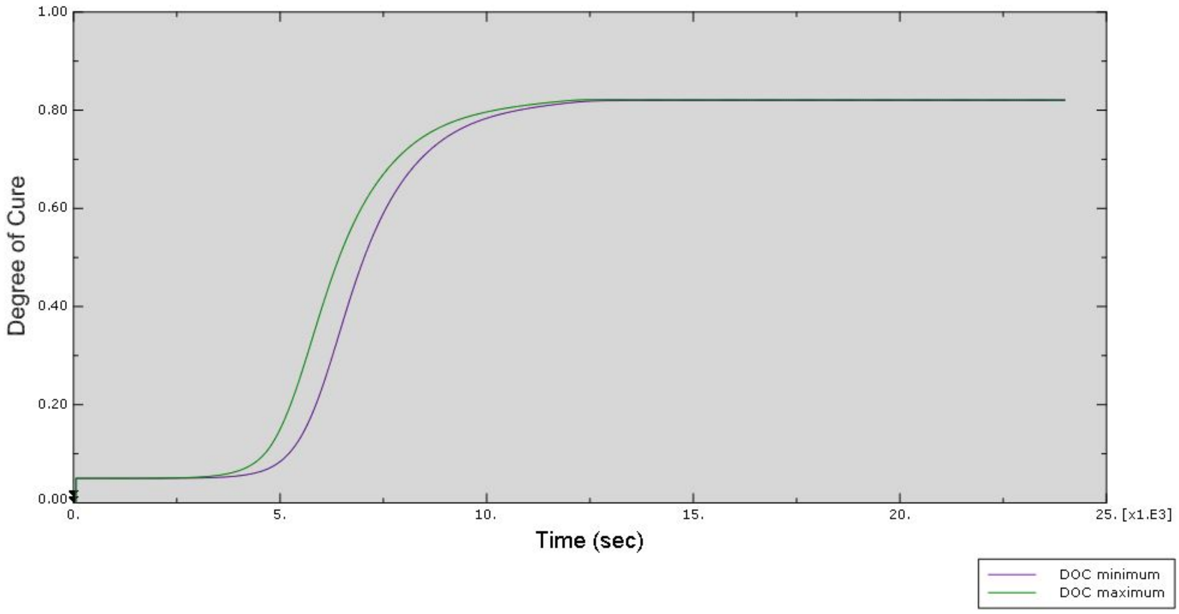

Figure 8.13: Degree of Cure vs. Time plot

Stress-Deformation Analysis

In stress-deformation analysis, displacement boundary conditions are applied to the corner. At the end of the analysis, the part is removed from the tool and allowed to deform freely. The final deformed shape shows typical "spring-in" of curved composite laminates. This analysis also use temperatures history from the thermo-chemical analysis results. It is observed that maximum stresses are induced in the corner portion of the composite part as shown in Figure 4.14. These stresses got released after tool removal from the assembly and composite part results into Spring-in as shwon in Figure 4.15. The spring-in shown in Figure 8.15 is sixteen times magnified than actual.

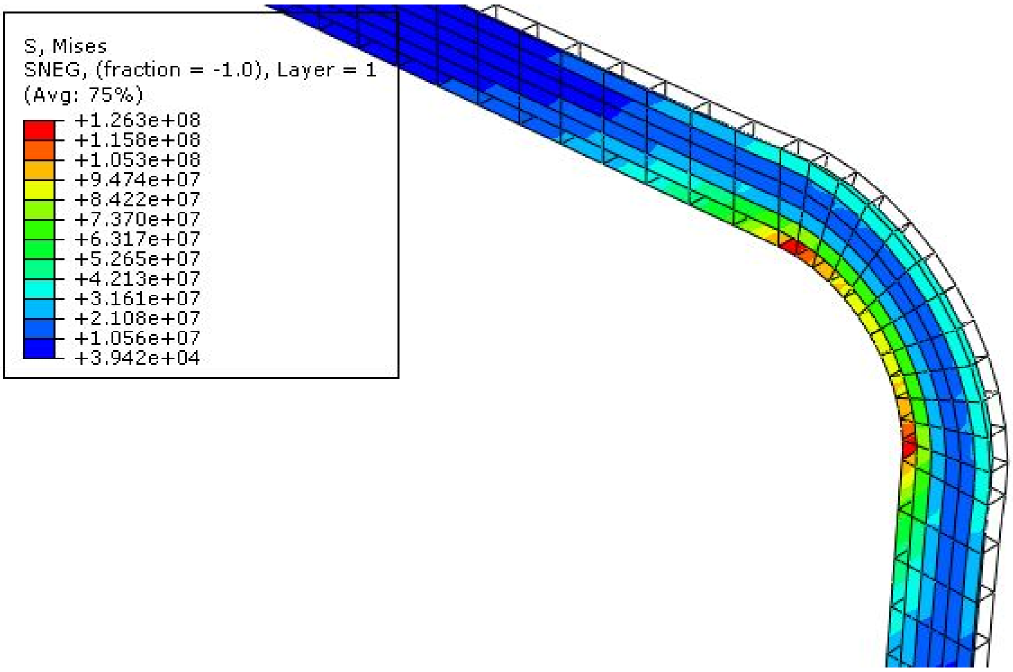

Figure 8.14: Residual Stresses Induced during Process at the Corner

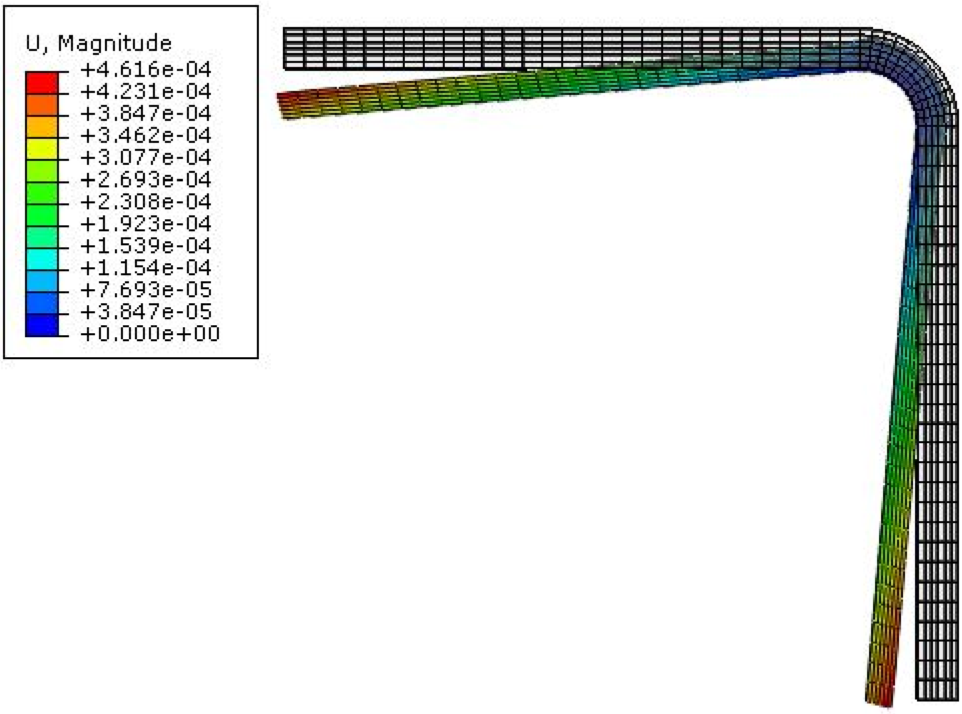

Figure 8.15: Deformed Shape of Laminate

Using the value of maximum deflection of part, spring-in is predicted as 0.66^o. The prediction is in good agreement with available literature[15].

Chapter 9

Curing Process Simulation of Paraboloid Reflector

The curing process of CFRP reflector is simulated using Abaqus along with Compro plugin. Different combination of parameters are analysed. Considering mould material, prepreg material and curing cycle as the contant parameters. For all the analysis, prepreg system AS4/8552 and SS as the mould material is used. Double hold curing curing cycle is also considered as the constant parameters. Layup sequence and thickness are considered as the varying parameters. The table 9.1 shows the number of analysis conducted using different parameters. Thermochemical and stress deformation analysis are conduted using Compro.

Table 9.1: Number of Analysis conducted

S. No.	Layup Sequence	Thickness
1	$[0]_{10}$	2
2	[0/45/-45/90]	0.8
3	$[0/90]_s$	0.8
4	$[0]_4$	0.8
5	$[0/90/0/90/0]_s$	2
6	$[0/45/-45/90/0]_s$	2
7	$[0]_8$	1.6
8	$[0/90/90/0]_s$	1.6

9.1 Methodology

Same methodology is followed as discussed in section 4.1 for carrying out the simulation of curing process of Carbon Fiber Reinforced Polymer (CFRP) paraboloid reflector.

9.2 Geometry

Mould and reflector geometries will be used while carrying the simulation. These are modelled using Creo 3.0 and then imported in Abaqus for carrying out the further modelling of the problem . The paraboloid profile is made using the Equation (9.1).

$$y = .0032x^2 \tag{9.1}$$

9.2.1 Mould

A male mould is used for conducting curing process simulation. The mould is partioned along two planes A and B passing through the center of the model which is shown in Figure 9.1. The partition is intentionally kept to assign the required boundary conditions in the following modelling steps.

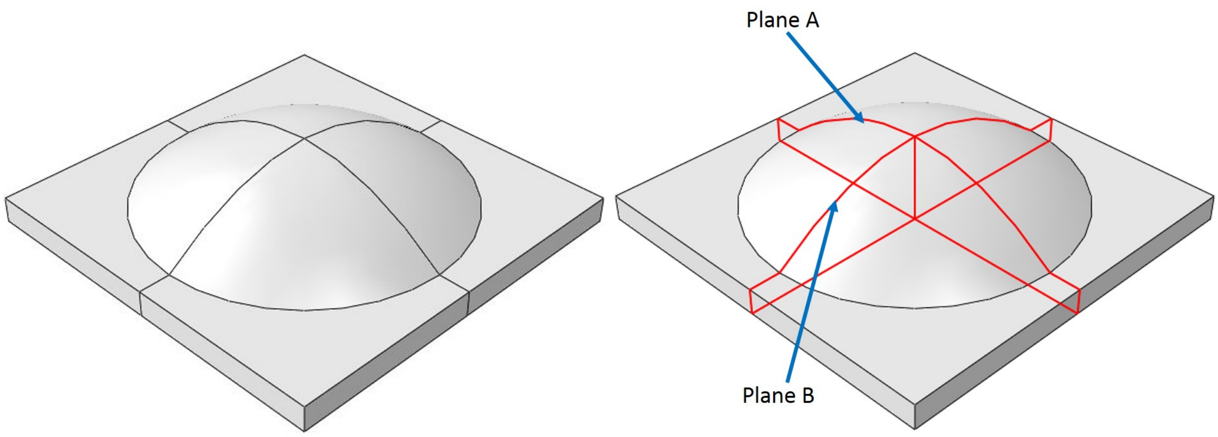

Figure 9.1: Partitioning of Mould

9.2.2 Reflector

A paraboloid reflector is modelled using Equation (1). The partitioning of the reflector is performed in Abaqus modeller. Total Eight partiotions are created in the reflector as shown in Figure 9.2 across planes C, D, E and F.

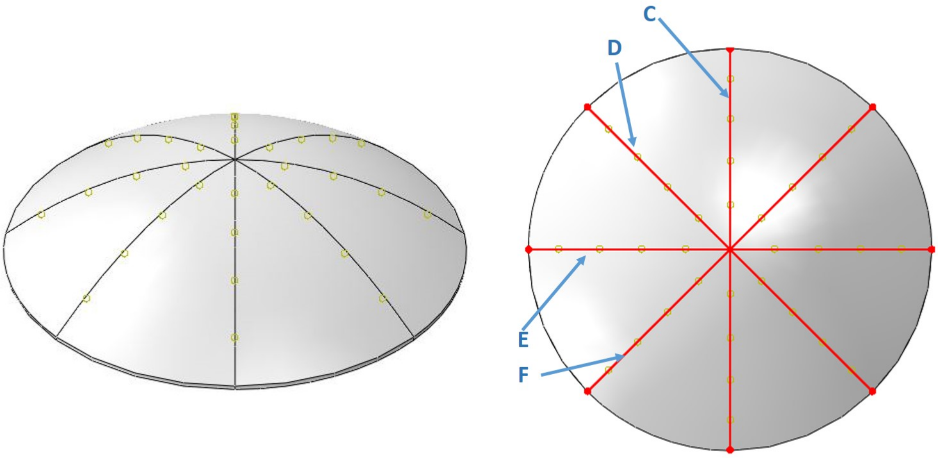

Figure 9.2: Partitioned Reflector

Lower edges are also partitioned. Each edge is partitioned in 5 parts as shown in Figure 9.3. The red spot specify the partitioned vertices.

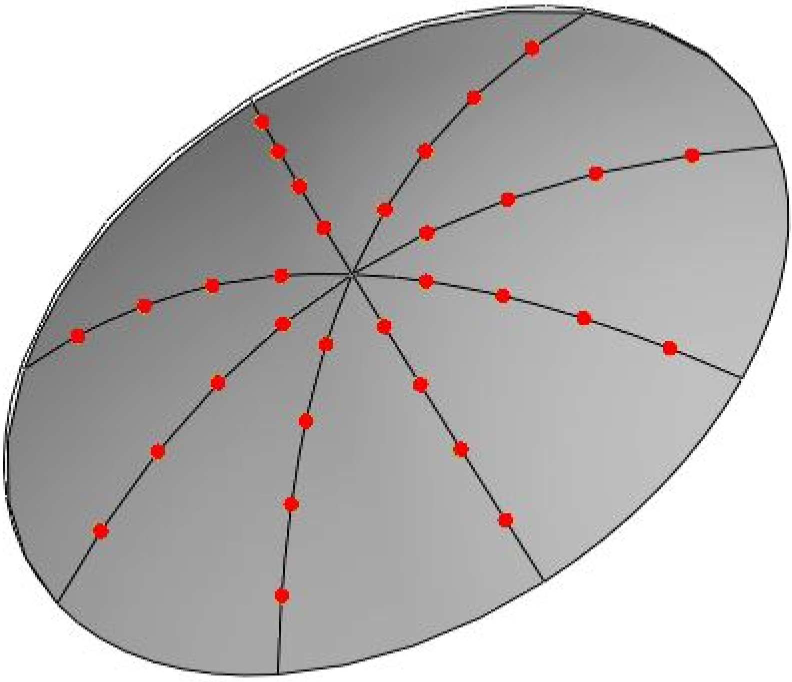

Figure 9.3: Lower edge Partitions

The partion of edges are made at radius 25, 50, 75 and 100 mm. The purpose of these partitions is, a node will get created at these junctions after meshing of the component, and after the completion of the analysis deformed coordinates can be obtained at these locations. The thickness of reflector should be modelled according to number of layer of prepreg laid on the mould and thickness of each layer should be known. For example if 4 layers are considered for the analysis and each having

0.2 mm thickness then it is required to make the CAD model of reflector of 0.8 mm thickness.

9.3 Meshing

Meshing of mould and reflector is performed in Abaqus using 3D Stress, quadratic C3D20 element. It is a 20 noded element. This is a brick elements that include full integration, quadratic displacement have been shown to best capture the through thickness shrinkage strains during composite process modeling. Mould has been meshed with 776 elements. The meshed mould (a) and Reflector (b) is shown in Figure 9.4

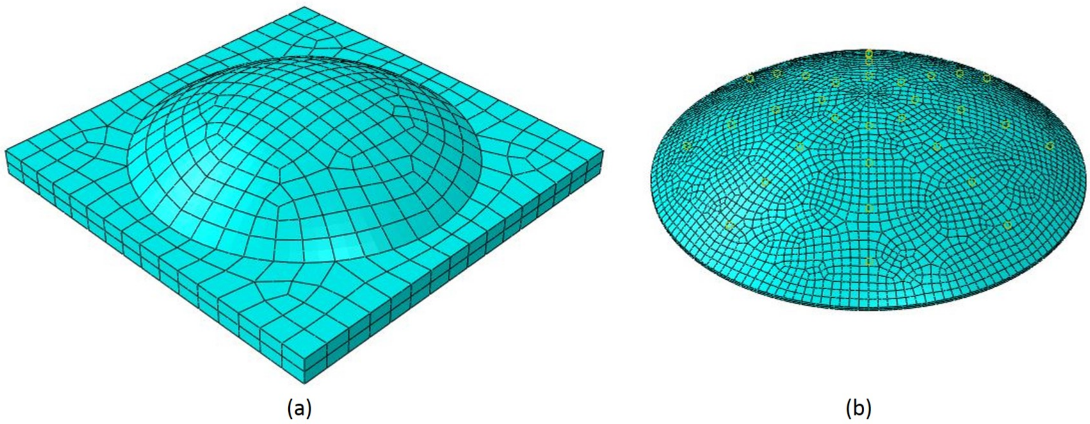

Figure 9.4: Meshed Mould and Reflector

9.3.1 Meshing of Reflectors

For the simulation, reflectors of different thickness is used according to the layup sequence. Since a single layer of mesh element in reflector contains the layup defined in Composite Section in Abaqus. So the number of element layers across the thickness should be decided according to the layup considered for the simulation. From the table 9.1 it can be observed that their are eight different layups considered during simulations. Considering $[0]_{10}$layup. In this case the reflector is meshed with two layers of elements across thickness as shown in Figure 9.5. One layer of element will contain five zero degree fiber layers ($[0]_5$) and other also contains the same number of layers. Total number of layers makes it to ten zero degree fiber layers in the reflector. Similarly other layups are defined in the reflector for other cases.

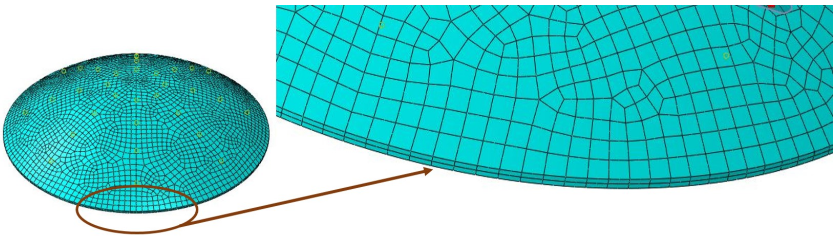

Figure 9.5: Meshed layers of Element on Reflector

9.4 Material Property Assignment in Abaqus

In the Abaqus, mould is assigned a stainless steel material and reflector is assigned a AS4/8552 prepreg system. These both materials are added in Abaqus using Compro as shown in Figure 9.6

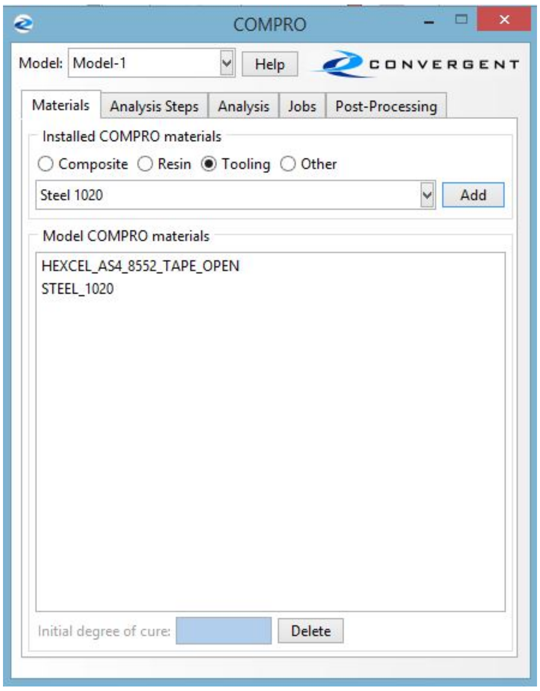

Figure 9.6: Materials Added in Abaqus using Compro

9.5 Material Orientation Assignment to Reflector

Prepregs stacking direction and Zero degree fiber direction should be assigned to the reflector for carrying out the solution using Compro solver. Compro need these reference direction to carry the solution. This task is accomplished by assigning the material orientation to the reflcetor in Abaqus. Figure 9.7 shows the assigned orientation to reflector where “N-3” shows the layer stacking direction (director normal to upper or lower surface of reflector) and “P-1” shows the zero degree fiber direction.

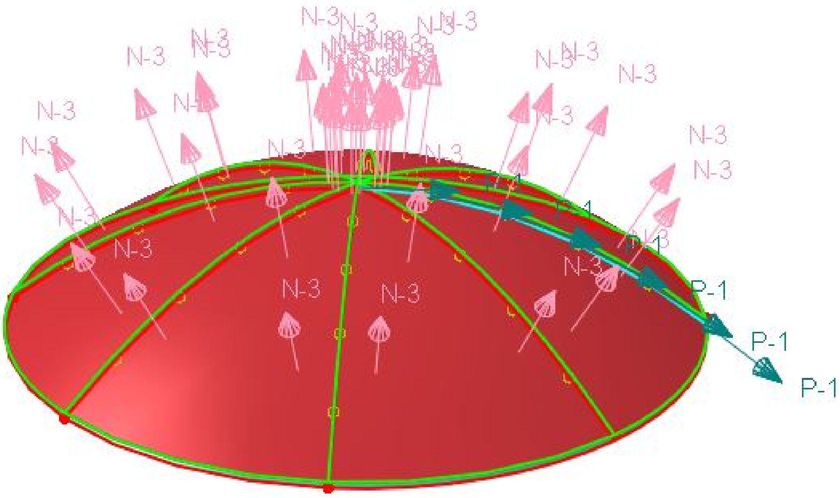

Figure 9.7: Orientation assigned to Reflector

9.6 Assembly of Mould and Reflector

Assembly of mould and reflector is performed in Abaqus by creating individual instances in assembly module as shown in Figure 9.8.

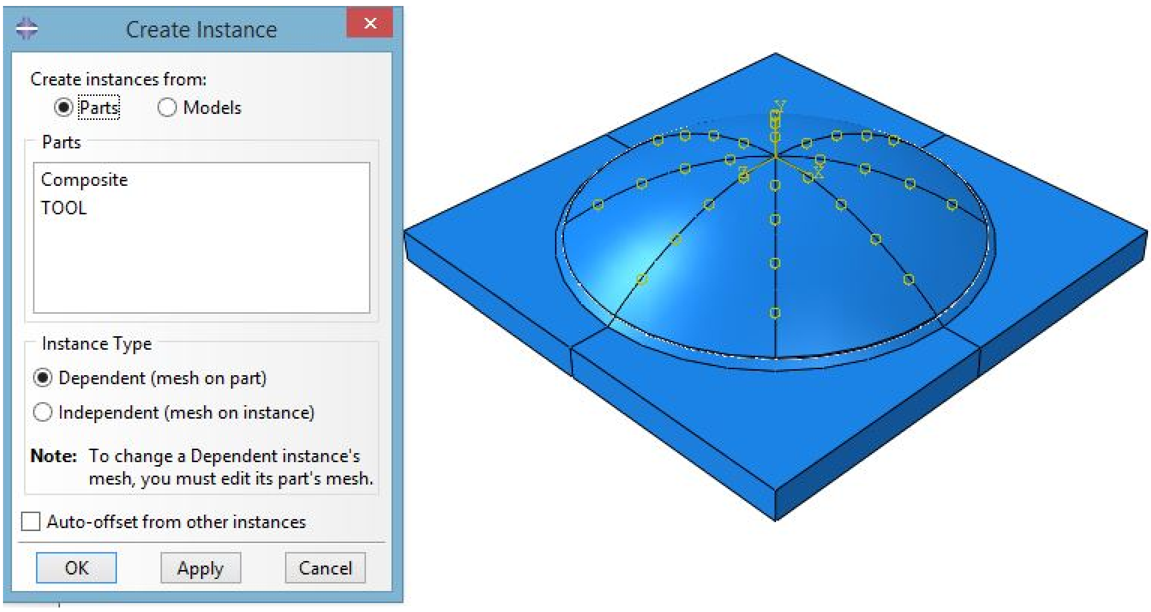

Figure 9.8: Instances of Mould and Reflector

9.7 Mould and Reflector Surface Interaction Properties

Frictional properties are assigned to the interaction surfaces of mould and reflector. In this master surface is selected as mould top surface as shown in Figure 9.9 (a) and slave surface is selected as reflector's bottom surface as shown in Figure 5.10 (b).

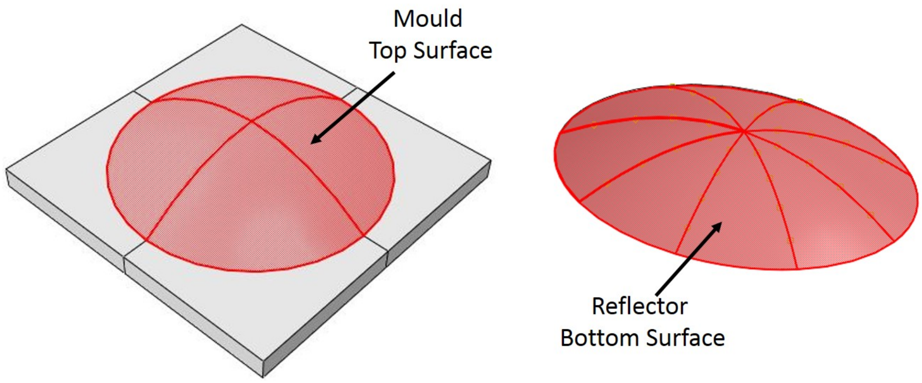

Figure 9.9: Interaction Surfaces of Mould and Reflector

Frictional properties are assigned to interaction. For all the simulations conducted, coefficient of friction (μ) is taken as 0.15 and maximum limiting shear stress is considered as 140000 N/mm^2.

9.8 Predefined Field and Boundary Condtions applied on the Assembly

The assembly of Mould and Reflector is assigned an Initial temperature of 20^oC. Mechanical boundary constrains are also defined for both mould and reflector such that along with their free expansion during the cycle they should be constrained in space in X, Y and Z directions . X, Y and Z boundary contraints are given to the mould and reflector as shown in Figures 9.10, 9.11 and 9.12.

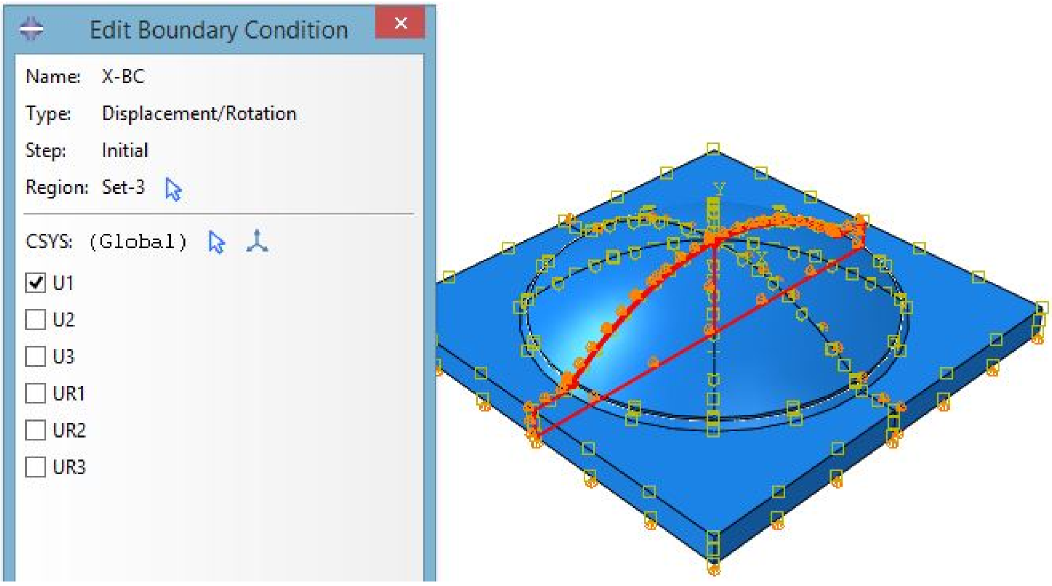

Figure 9.10: X direction Boundary Constraint

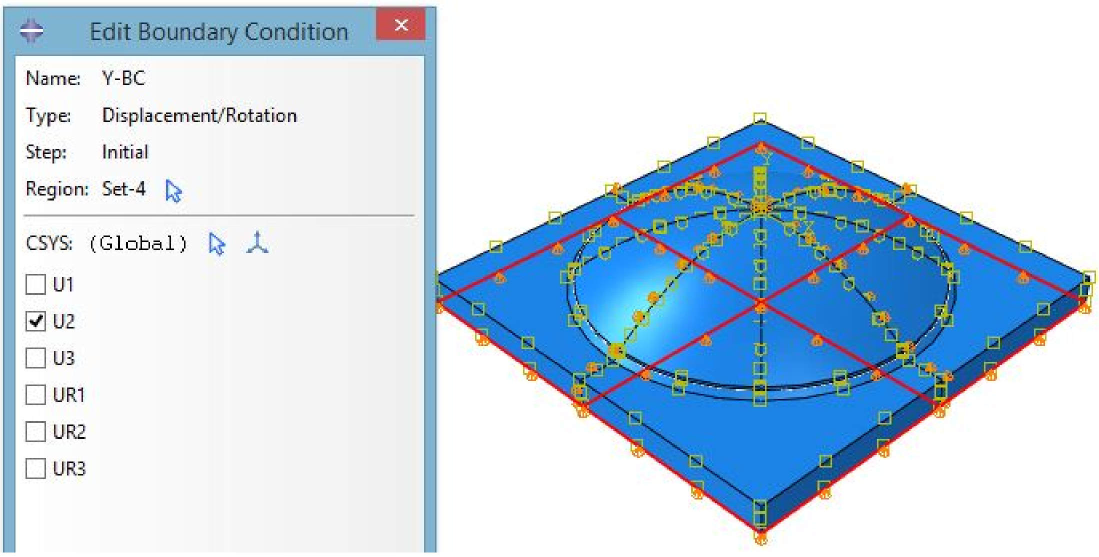

Figure 9.11: Y direction Boundary Constraint

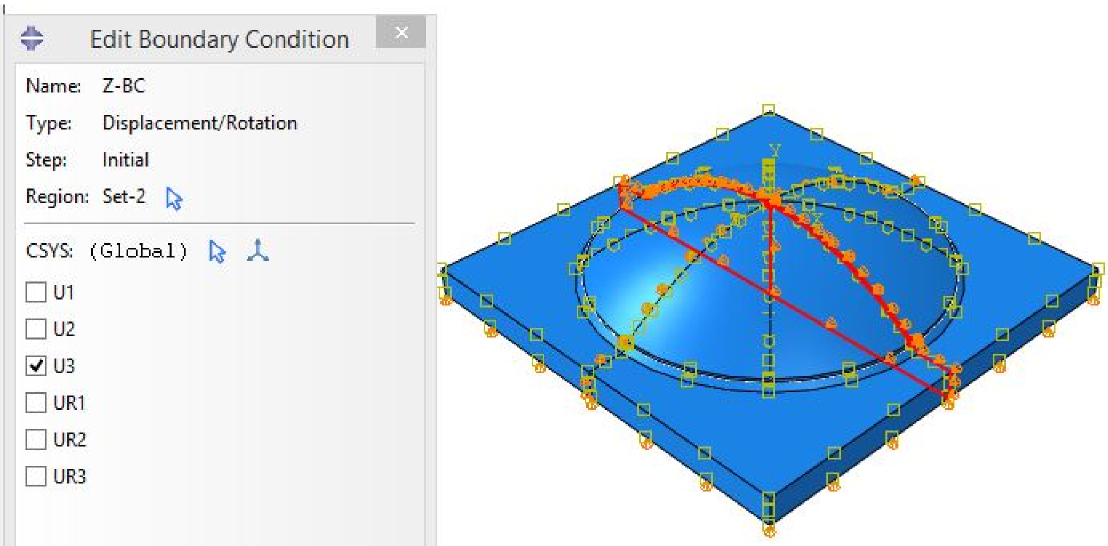

Figure 9.12: Z direction Boundary Constraint

9.9 Thermochemical Analysis

For conducting thermochemical analysis, a step should be defined using Compro as shown in Figure 9.13

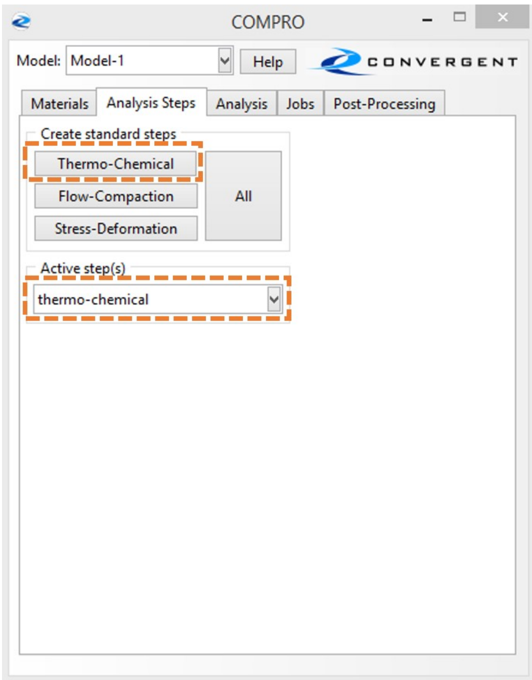

Figure 9.13: Defining Thermochemical Step using COMPRO

After defining the step, HTC and curing cycle is defined. For all the cases of simulation, double hold curing cycle is assigned as shown in Figure 9.14. The total cycle is of 24000 second with two holds. First hold is at temperature 110^oC for 3600 sec and second hold is at 180^oC for 2700 sec. HTC of $80W/m^2K$ is also applied on surfaces of reflector and mould as shown in Figure 9.15.

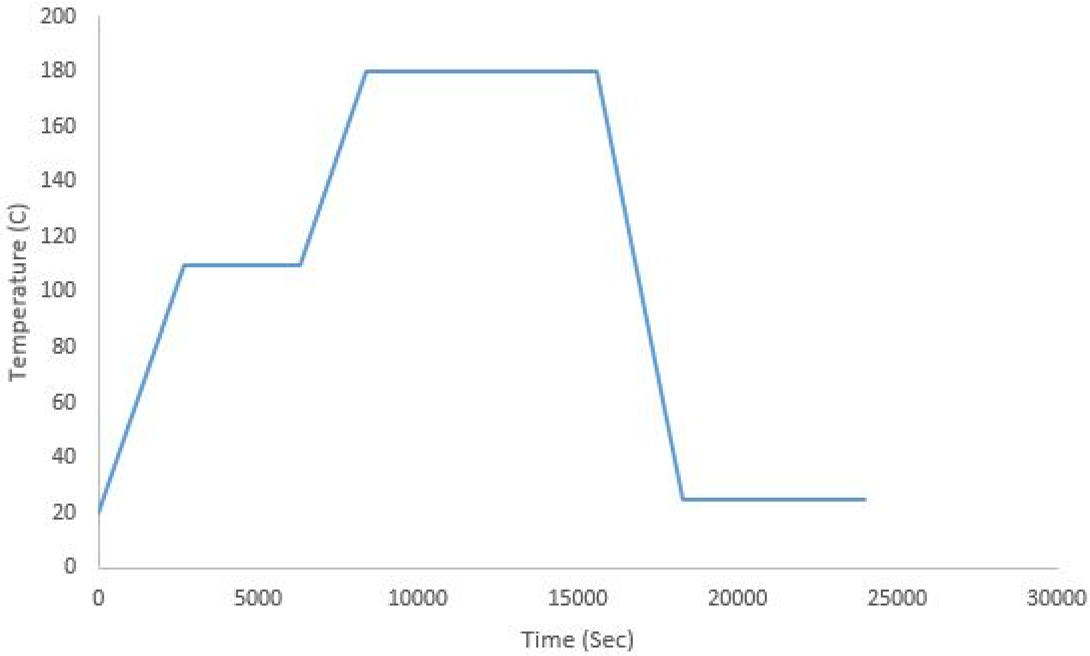

Figure 9.14: Double Hold Curing Cycle

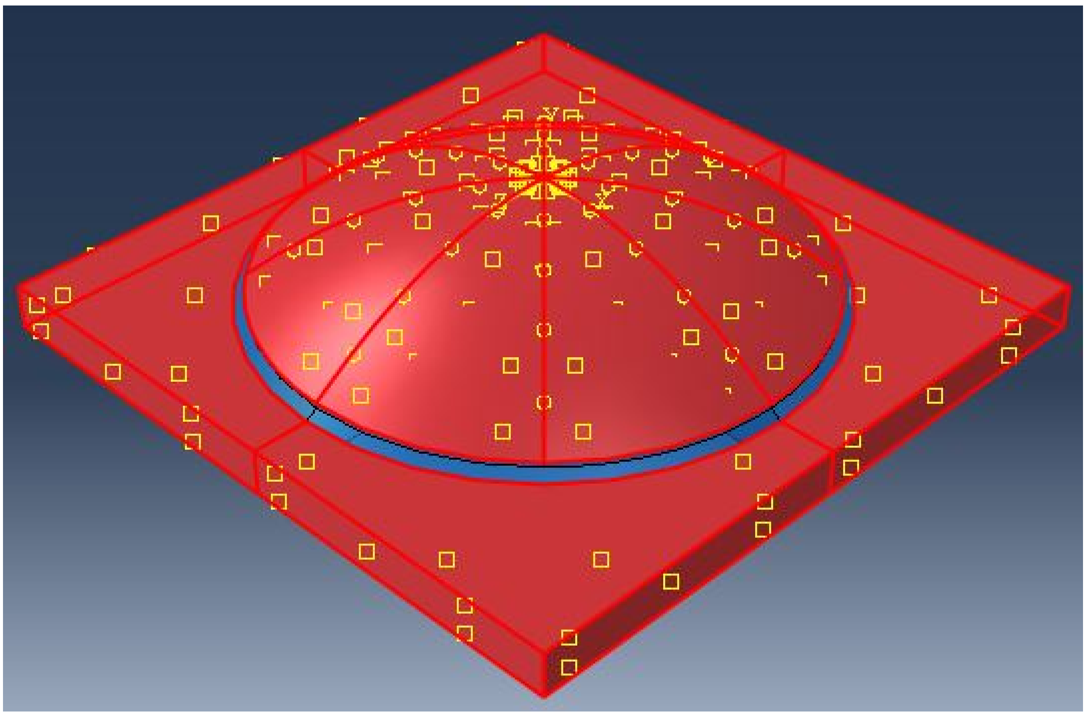

Figure 9.15: Surfaces on which HTC is Assigned

9.9.1 Thermochemical Results

After completion of thermochemical analysis, temperature profile and degree of cure plot can be obtained. Using these plot one can find the gradient in temperature and degree of cure during the cycle. In Abaqus output of this analysis is formed as thermo-chemical-compro.odb file and this file can be opened to see the analysis results. Temperature for simulation with layup $[0]_{10}$ can be visualized for different time steps. Figure 9.16 shows the temperature of the assembly at time step 20040 sec.

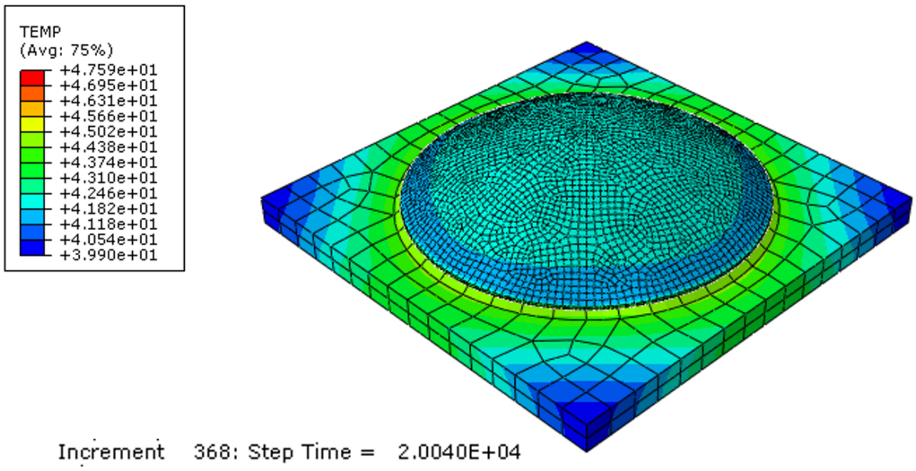

Figure 9.16: Temperature

Temperature and degree of Cure profiles is shown in Figure 9.17 and Figure 9.18 respectively.

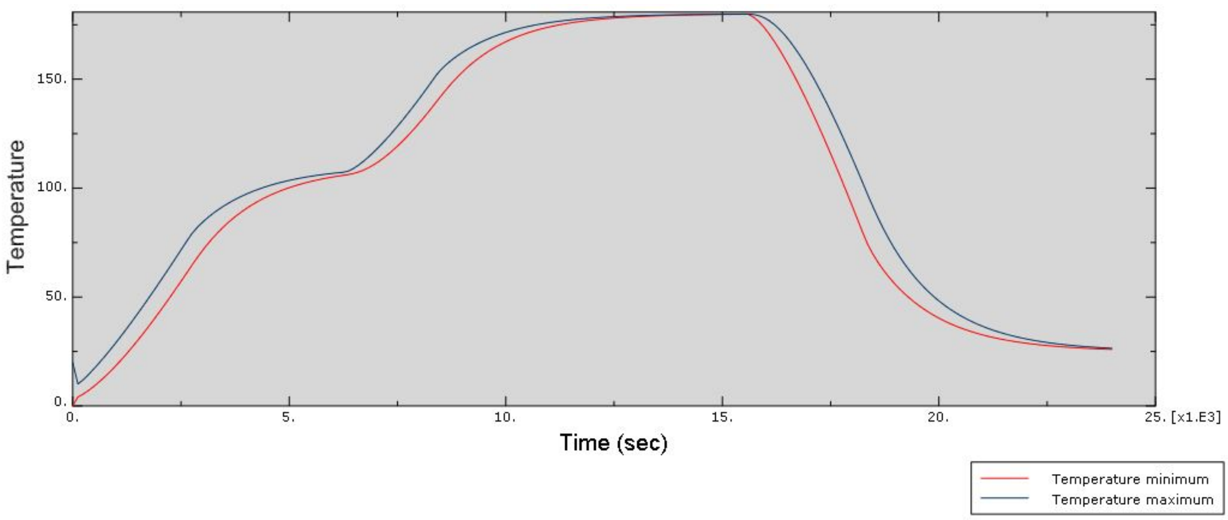

Figure 9.17: Temperature Profile

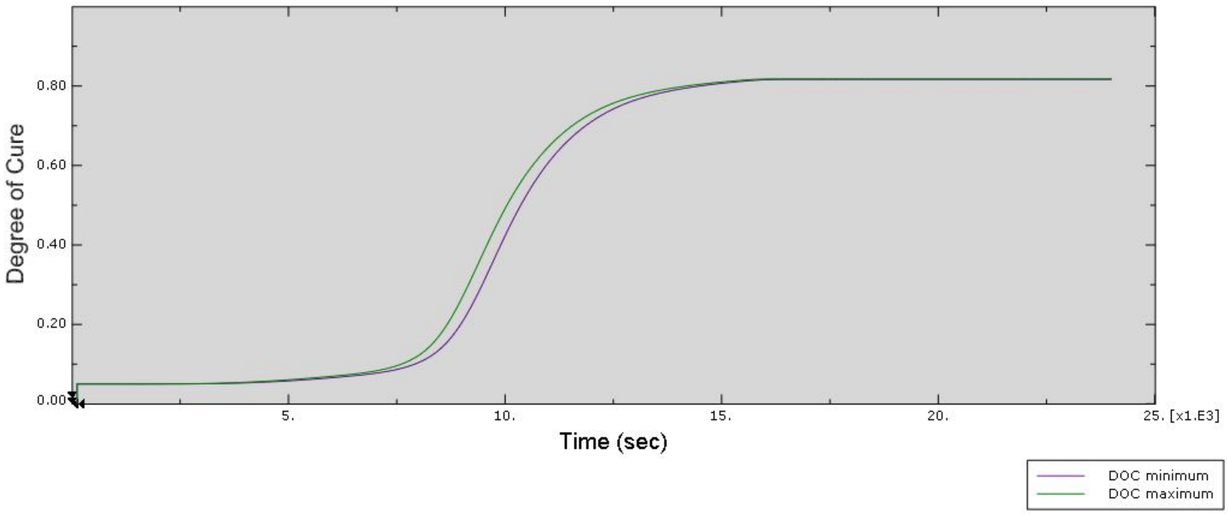

Figure 9.18: Degree of Cure Profile

9.10 Stress Deformation Analysis

For carrying stress deformation analysis, “step-stress-deformation” and “step-tool-removal” are added using Compro. For obtaining the deformed shape of reflector, a step of demoulding of the reflector from the mould should be defined. To perform this task, in the step-tool-removal, mould is deactivated using model change command in interaction module as shown in Figure 5.19.

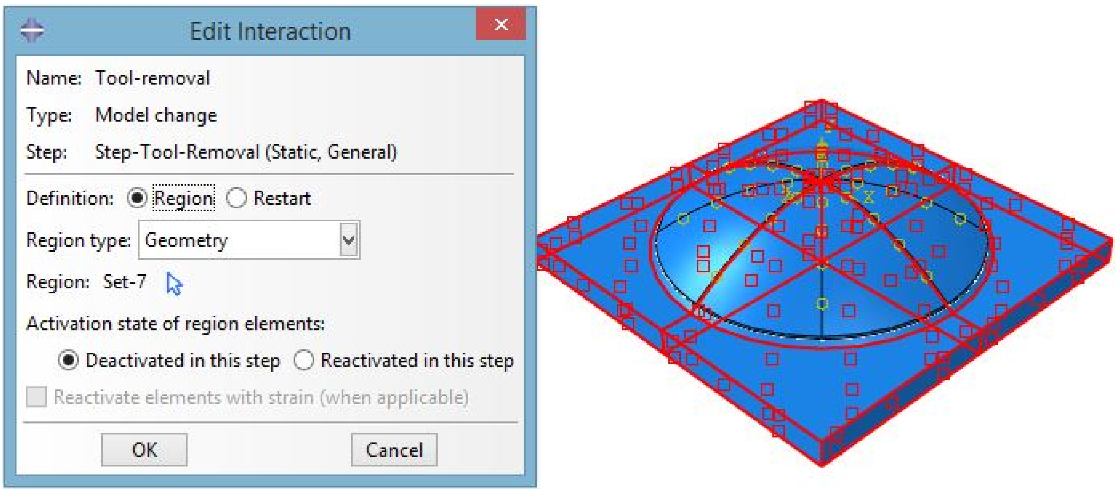

Figure 9.19: Deactivation of Mould

A boundary condition is also applied on the reflector such that reflector is constrained in space and is able to deform uniformly during step-tool-removal. The deformation in the reflector occurs due to relaxation of residual stresses generated during curing process. The central edge of reflector as shown in Figure 9.20.

9.10.1 Stress Deformation Analysis Results

From the stress deformation analysis, residual stress and deformed shape can be obtained. The generation of residual stress can be visualised by changing the step time. Residual stress in reflector at step time 24000 is shown in Figure 9.20.

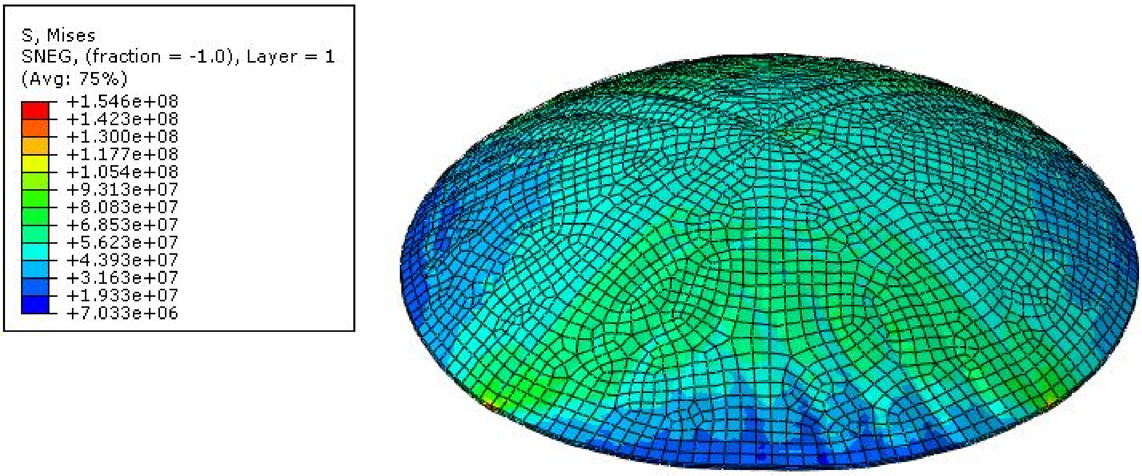

Figure 9.20: Residual Stresses in Reflector

Deformed shape after demoulding is shown in Figure 9.21.

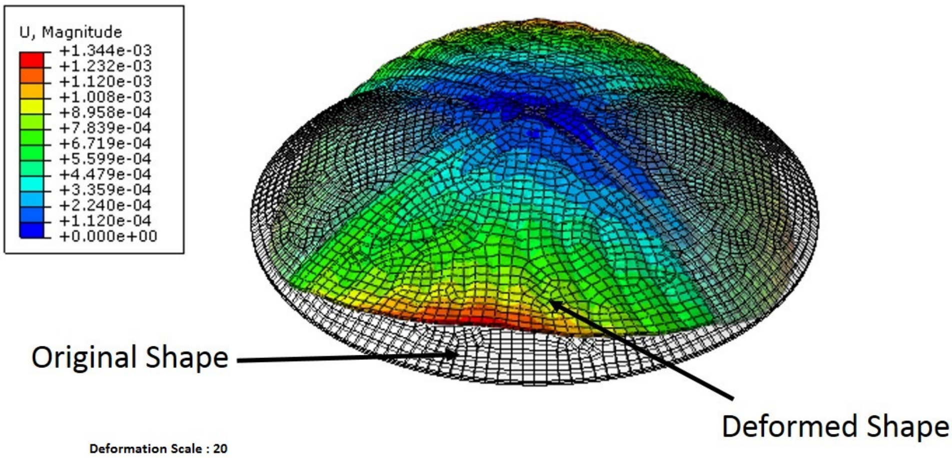

Figure 9.21: Original and Deformed Shape of Reflector

9.11 Measurement of Deformed Coordinates of Reflector

The mesurement of deformation of reflector is performed by obtaining original and deformed coordinates at 4 different locations as shown in Figure 9.22. There are eight simulations carried out in sequence as shown in Table 9.1. The original coordinates remain same for all analysis carried out as shown in Table 9.2.

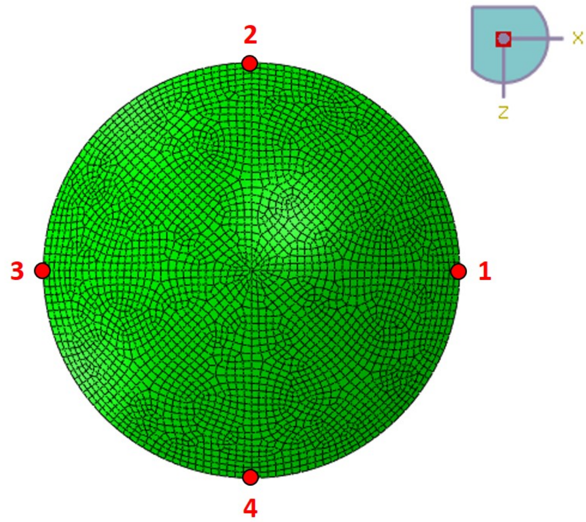

Figure 9.22: Points Specified on Reflector

Table 9.2: Original Coordinates of Reflector (mm)

Point No.	X	Y	Z
1	120	-46.08	0
2	0	-46.08	-120
3	-120	-46.08	0
4	0	-46.08	120

The deformed coordinates of the reflector for all analysis are shown in Table 9.3

Table 9.3: Deformed Coordinates of Points specified on Reflector (mm)

S. No.	Points	X	Y	Z
1	1	119.31	-47.4148	0.236796
	2	0.249174	-44.2962	-120.089
	3	-119.348	-47.3216	-0.237753
	4	-0.224347	-44.3059	120.115
2	1	119.31	-47.4148	0.236796
	2	0.249174	-44.2962	-120.089
	3	-119.348	-47.3216	-0.237753
	4	-0.224347	-44.3059	120.115
3	1	119.31	-47.4148	-0.466378
	2	-0.454	-44.2962	-120.089
	3	-119.348	-47.3216	0.465421
	4	0.478827	-44.3059	120.115
4	1	119.31	-47.4148	0.229948
	2	0.242326	-44.2962	-120.089
	3	-119.348	-47.3216	-0.230907
	4	-0.217499	-44.3059	120.114
5	1	119.647	-45.9382	0.233717
	2	0.430345	-45.9588	-119.676
	3	-119.729	-45.6152	-0.225017
	4	-0.440399	-45.6523	119.775
6	1	119.647	-45.9382	0.183407
	2	0.380036	-45.9588	-119.676
	3	-119.729	-45.6152	-0.174708
	4	-0.39009	-45.6523	119.775
7	1	119.498	-47.0323	-0.376975
	2	-0.359197	-43.0897	-119.82
	3	-119.53	-46.9579	0.377709
	4	0.395686	-44.6494	119.829
8	1	119.499	-47.0324	-0.214865
	2	-0.197796	-44.6572	-119.847
	3	-119.53	-46.9577	0.215325
	4	0.233307	-44.6512	119.831

The spring back of the reflector for all the analysis carried out can be determined by calculating the deviation. The deviation is defined as the difference of original and deformed coordinates of the reflector. Once the deviation coordinates are determined, magnitude of deviation on all points of reflector are calculated for all the cases as shown in Table 9.4.

Table 9.4: Mangnitude of Deviation for All Points on Reflector (mm)

		Points			
S. No.	Layup Sequence	1	2	3	4
1	$[0]_{10}$	1.521138845	1.8033167	1.42239272	1.791922818
2	[0/45/-45/90]	0.758949007	0.295451939	0.715711933	0.303243052
3	$[0/90]_s$	1.57330845	1.842818342	1.477596449	1.841176555
4	$[0]_4$	1.520087867	1.802383236	1.421264438	1.791014412
5	$[0/90/0/90/0]_s$	0.446474945	0.552143332	0.583191813	0.653837571
6	$[0/45/\text{-}45/90/0]_s$	0.422320219	0.513899602	0.565688011	0.621065615
7	$[0]_8$	1.140609241	1.447189198	1.0650223	1.494130105
8	$[0/90/90/0]_s$	1.09737584	1.44460794	1.01863740	1.45755363

From the Table 9.4, it is observed that the least deviation is coming for the analysis having [0/45/-45/90] and [0/45/-45/90/0] layups. These both layups contain prepregs in four different orientations, during the curing process there will be a resistance for the contraction of the compposite from four directions which results into the least springback. It is also observed that as the thickness of laminate is increasing from 0.8 mm to 2 mm, the magnitude of deviation get decreased.

Chapter 10

Conclusion and Future Scope

10.1 Conclusion

The numerical and experimental study has been carried out for determination of springback deformation for CFRP L-shape components and parabolic reflector. The material for the moulds and grade of the prepreg are selected. Three mould materials are selected i.e, Cast Iron grade 30, Graphite EDM grade and Stainless Steel 430. Selection of the mould materials are performed on the basis of their CTE and manufacturability. Hinpreg A45/HCU 200 prepreg system is a carbon fiber/epoxy based prepregs which is selected for carrying the experiments. On the basis of CAD model of mould, manufacturing of procured mould materials is conducted using VMC to obtain the desired shape.

Experimental work for manufacturing of CFRP parabolid reflector has been conduted. For the experiments stainless steel mould is used. The curing process is performed using hot air oven. Coordinates of some specified points on manufactured mould and reflector have been measured using CMM. To measure the springback deformation of the parabolid reflector, deviation in coordinates is calculated. Using this methodology springback of any paraboloid shape reflector can be measured.

Effect of curing process is studied on dimensional stability of L-shape component. An experiment is carried for manufacturing of L-shape component using rectangular cross section aluminium mould. Laser engraving is done on two surface of mould to study its effect on manufactured L-shape component. Total four prepreg layups are laid on the mould, some portion of mould is treated with release agent and other with release film. L-shape component manufactured with release agent have better surface finish than the component manufactured on release film. The Ra value obtained with release agent is 1.019 μm and with release film is 1.528 μm. The engraving effect is also observed on the manufactured composite parts.

Curing process simualtion for prediction of spring-in of L-shape part is carried out using Abaqus and Compro. AS4/8552 as prepreg system and Aluminium as mould material is used during the analysis. After conducting thermochemical and stress deformation analysis results of curing process are obtained. The predicted spring in value is with good agreement with available literature. A parametric study for curing process of CFRP reflector is conducted by considering layup sequence and thickness as variable parameters and AS4/8552 as prepreg system and Steel as mould material as constant parameters. It is observed that springback deformation is least for layup sequence $[0/45/-45/90/0]_s$. It is also observed that thick component experiences lesser springback deformation than thin component.

10.2 Future Scope

1. The study of effect of various parameters related to mould, curing process and prepreg for parabolic reflector needs to be carried out. Such a study needs to be undertaken using experimental and numerical approach.

References

[1] Sanjay K. Mazumdar, “Composite Manufacturing”, CRC Press.

[2] Autar K. Kaw, “Mechanics of Composite Material”, CRC Taylor & Francis.

[3] https://en.wikipedia.org/wiki/Reflector_%28antenna%29.

[4] http://www.belfastmetcomposites.com/autoclave-commissioned/.

[5] HexPly® Prepreg Technology Manual.

[6] http://www.nuplex.com/composites/processes/resin-transfer-moulding.

[7] Carolyne Albert, Goran Fernlund, “Spring-in and warpage of angled composite laminates”, Composites Science and Technology 62 (2002).

[8] D. Stefaniak, E. Kappel, T. Sprowitz, C. Huhne, “Experimental identification of process parameters inducing warpage of autoclave-processed CFRP parts”, Composites: Part A 43 (2012).

[9] H.T. Hahn and N.J. Pagano, “Curing Stresses in Composite Laminates”, Journal of Composite Materials (1975).

[10] S.R. White and H.T. Hahn, “Process Modeling of Composite Materials: Residual Stress Development during Cure. Part I. Model Formulation” Journal of Composite Materials 1992 26: 2402.

[11] S.R. White and H.T. Hahn, “Process Modeling of Composite Materials: Residual Stress Development during Cure. Part II. Experimental Validation” Journal of Composite Materials 1992 26: 2423.

[12] Andrew A. Johnston, “An integrated model of the development of process-induced deformation in autoclave processing of composite structures”. Phd Thesis, The University of New Brunswick (1992).

[13] Andrew Johnston, Reza Vaziri And Anoush Poursartip, “A Plane Strain Model for Process-Induced Deformation of Laminated Composite Structures”, Journal of Composite Materials, Vol. 35, No. 16/2001.

[14] G.Fernlund, N.Rahman, R.Courdji, M.Bresslauer, A. Poursartip, K. Nelson, "Experimental and numerical study of the effect of cure cycle, tool surface, geometry and layup on the dimensional fidelity of autoclave-processed composite parts", Composite: Part A 33 (2002)

[15] Goran Fernlund and Anoush Poursartip, "The Effect of Tooling Material, Cure Cycle, and Tool Surface Finish on Spring-In of Autoclave Processed Curved Composite Parts".

[16] G. Fernlund, A. Osooly, A. Poursartip, R. Vaziri, R. Courdji, K. Nelson, P. George, L. Hendrickson, J. Griffith, "Finite element based prediction of process-induced deformation of autoclaved composite structures using 2D process analysis and 3D structural analysis", Composite Structures 62 (2003).

[17] Graham Twigg, Anoush Poursartip, Goran Fernlund, "An experimental method for quantifying tool–part shear interaction during composites processing", Composites Science and Technology 63 (2003).

[18] Graham Twigg, Anoush Poursartip, Goran Fernlund, "Tool–part interaction in composites processing. Part I: experimental investigation and analytical model", Composites: Part A 35 (2004).

[19] Graham Twigg, Anoush Poursartip, Goran Fernlund, "Tool–part interaction in composites processing. Part II: numerical modelling", Composites: Part A 35 (2004).

[20] Goran Fernlund, "Spring-in of angled sandwich panels", Composites Science and Technology 65 (2005).

[21] Goran Fernlund & Anthony Floyd, "Process Analysis and Tool Compensation for A Complex Composite Panel", American Society for Composites 22nd Annual Technical Conference, Seattle, Sep. 17-20 (2007).

[22] Chensong Dong, "Modeling the Dimensional Variations of Composites Using Effective Coefficients of Thermal Expansion", Journal of Composite Materials, Vol. 43, No. 22 (2009).

[23] V. Kaushik, J. Raghavan, "Experimental study of tool–part interaction during autoclave processing of thermoset polymer composite structures", Composites: Part A 41 (2010).

[24] X. Zeng, J. Raghavan, "Role of tool-part interaction in process-induced warpage of autoclave-manufactured composite structures", Composites: Part A 41 (2010).

[25] Alfred C. Loos and George S. Springer, “Curing of Epoxy Matrix Composites”, Journal of Composite Materials 1983 17: 135.

[26] E.P. Scott, “Determination of Kinetic Parameters Associated with the Curing of Thermoset Resins Using Dielectric and DSC Data”, Composites: Design, Manufacture, and Application, ICCM/VIII, Honolulu (1991).

[27] Pascal Hubert, “Aspects of flow and compaction of laminated composite shapes during cure”, The University of British Columbia (1996).

[28] T.A. Bogetti and J.W. Gillespie Jr., “Process-Induced Stress and Deformation in Thick-Section Thermoset Composite Laminates”, Journal of Composite Materials (1992).

[29] D. Adolf and J.E. Martin, “Calculation of Stresses in Crosslinking Polymers”, Journal of Composite Materials (1996).

[30] A.M. Boriek, J.E. Akin, and C.D. Armeniades, “Setting Stress Distribution in Particle Reinforced Polymer Composites”, Journal of Composite Materials (1988).

[31] Woo Il Lee, Alfred C. Loos, and George S. Springer, “Heat of Reaction, Degree of cure, and Viscosity of Hercules 3501-6 Resin” J. Composite Material, Vol. 16 (1982).

[32] Compro Model Documentation, Release 1.3, Convergent Manufacturing Technologies Inc. (2013).

[33] COMPRO for ABAQUS Modeling Guidelines, , Convergent Manufacturing Technologies Inc. (2014).

[34] Abaqus 14.1 manual.

[35] http://zoltek.com/products/panex-35/prepreg/

[36] R.H. Nelson and D.S. Cairns, “Prediction of Dimensional Changes in Composite Laminates During Cure”, 34th International SAMPE Symposium,1989, pp. 2397-2410.